REPORT NO.
UCB/EERC-79/15
JULY 1979

EARTHQUAKE ENGINEERING RESEARCH CENTER

OPTIMAL DESIGN OF LOCALIZED NONLINEAR SYSTEMS WITH DUAL PERFORMANCE CRITERIA UNDER EARTHQUAKE EXCITATIONS

by

M. A. BHATTI

A report on research sponsored by
the National Science Foundation

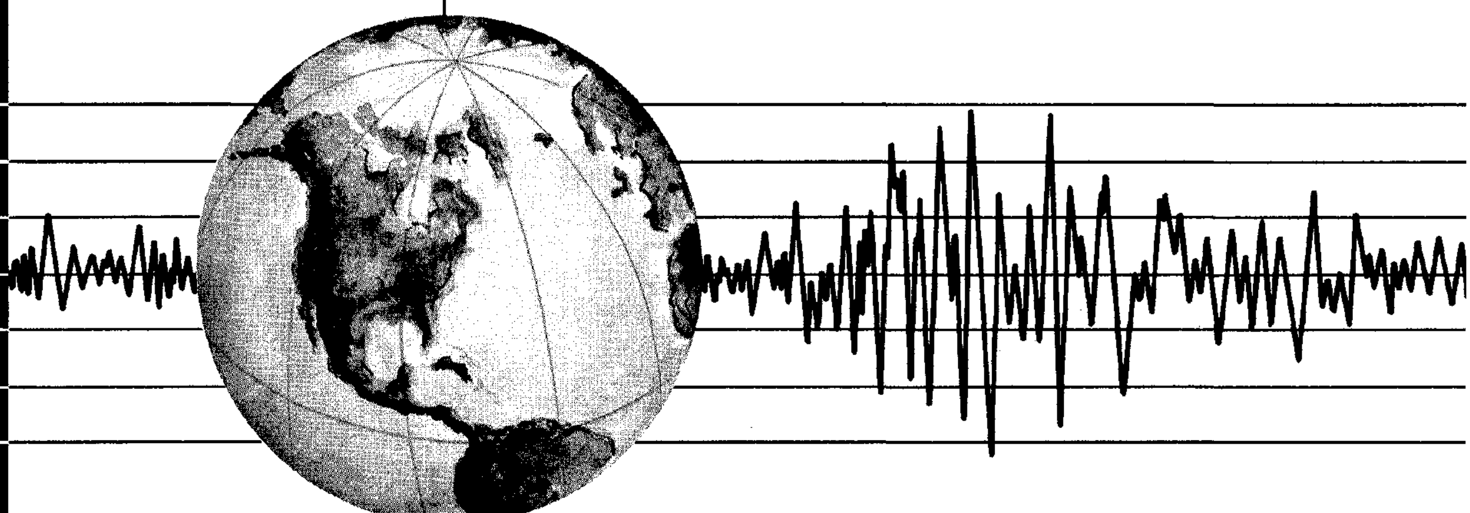

COLLEGE OF ENGINEERING

UNIVERSITY OF CALIFORNIA · Berkeley, California

REPRODUCED BY
NATIONAL TECHNICAL
INFORMATION SERVICE
U.S. DEPARTMENT OF COMMERCE
SPRINGFIELD, VA. 22161

BIBLIOGRAPHIC DATA SHEET	1. Report No. NSF/RA-790395	2.	3. Recipient's Accession No. PB 80 167109
4. Title and Subtitle: Optimal Design of Localized Nonlinear Systems with Dual Performance Criteria Under Earthquake Excitations			5. Report Date: July 1979
			6.
7. Author(s): M.A. Bhatti			8. Performing Organization Rept. No. UCB/EERC-79/15
9. Performing Organization Name and Address: Earthquake Engineering Research Center, University of California, Richmond Field Station, 47th and Hoffman Blvd., Richmond, California 94804			10. Project/Task/Work Unit No.
			11. Contract/Grant No. ENV76-04264
12. Sponsoring Organization Name and Address: National Science Foundation, 1800 G Street, N.W., Washington, D.C. 20550			13. Type of Report & Period Covered
			14.

15. Supplementary Notes

16. Abstracts

This report presents a formulation for earthquake-resistant design of localized nonlinear systems. Based upon the current design criteria, two levels of performance constraints are imposed as follows. For small earthquakes which occur frequently, the structure is constrained to remain elastic with no structural damage. For a large earthquake, the structure can undergo inelastic deformations at known locations of nonlinearities, with limited damage.

The problem is formulated as a min-max problem, and a general strategy to transcribe it to the canonical form of a nonlinear programming problem is given. An algorithm of the feasible directions type is given to solve the resulting nonlinear programming problem.

The general techniques are applied to the design of nonlinear energy-absorbing devices, which are part of an earthquake isolation system for many types of buildings. Several design problems with different performance criteria are considered and the results compared to see the effect of these different criteria. Comparison is also made with results reported earlier with only one level of constraints. The results clearly show the effectiveness of the present approach with dual performance criteria over the conventional single criterion approach.

17c. COSATI Field/Group

18. Availability Statement	19. Security Class (This Report) UNCLASSIFIED	21. No. of Pages 110
Release unlimited	20. Security Class (This Page) UNCLASSIFIED	22. Price

OPTIMAL DESIGN OF LOCALIZED NONLINEAR SYSTEMS WITH DUAL PERFORMANCE CRITERIA UNDER EARTHQUAKE EXCITATIONS

by

M. A. Bhatti

Prepared under the sponsorship of the
National Science Foundation
Grant ENV76-04264

Report No. UCB/EERC-79/15
Earthquake Engineering Research Center
College of Engineering
University of California
Berkeley, California 94720

July 1979

ABSTRACT

This report presents a formulation for earthquake-resistant design of localized nonlinear systems. Based upon the current design criteria, two levels of performance constraints are imposed as follows. For small earthquakes which occur frequently, the structure is constrained to remain elastic with no structural damage. For a large earthquake, the structure can undergo inelastic deformations at known locations of nonlinearities, with limited damage.

The problem is formulated as a min-max problem, and a general strategy to transcribe it to the canonical form of a nonlinear programming problem is given. An algorithm of the feasible directions type is given to solve the resulting nonlinear programming problem.

The general techniques are applied to the design of nonlinear energy-absorbing devices, which are part of an earthquake isolation system for many types of buildings. Several design problems with different performance criteria are considered and the results compared to see the effect of these different criteria. Comparison is also made with results reported earlier with only one level of constraints. The results clearly show the effectiveness of the present approach with dual performance criteria over the conventional single criterion approach.

ACKNOWLEDGMENTS

The work reported here was carried out during the course of study for a Ph.D. degree in Civil Engineering at the University of California, Berkeley. The research was sponsored by a grant from the National Science Foundation. This support is gratefully acknowledged.

The author wishes to express his deep appreciation to Professors K. S. Pister and E. Polak for their supervision of the work and continuous assistance throughout his graduate program. Sincere appreciation is expressed to Professor J. M. Kelly, whose work on energy-absorbing devices to mitigate earthquake-induced structural damage brought this problem to the author's attention.

The author gratefully acknowledges the support of the staff at the Earthquake Engineering Research Center at the Richmond Field Station for their continuous help and assistance throughout the course of this work. Special thanks are due to Aileen Donovan and S. Joy Svihra for keeping the author up-to-date on the current literature in the field and B. Bolt for editing the manuscript.

Assistance in typing the manuscript on the UNIX system by Linda Calvin and Mary Carol is gratefully acknowledged.

TABLE OF CONTENTS

1. INTRODUCTION

A well-established philosophy [1] for design of earthquake-resistant structural systems is to:

(i) prevent any damage from minor earthquakes which may occur frequently during the service life of the structure;

(ii) prevent damage to main structural components from moderate earthquakes;

(iii) prevent major structural damage and collapse of the structure from a major earthquake which may rarely occur.

The present design practice is to proportion the structure to resist minor and moderate earthquakes without any significant structural damage. Moreover, the behavior is idealized as linear elastic, and response spectra types of analyses are used to compute the structural response. The safety of the structure from a major earthquake is taken care of either implicitly through the use of building codes or explicitly by performing an elaborate nonlinear dynamic analysis of the structure. Several design cycles might be necessary before achieving an acceptable design.

Several attempts have been made to automate the design of structural systems using optimization techniques. An exhaustive literature survey of the field appears in references [2,3]. In most of the earlier work optimal design was sought by satisfying only one of the design criteria. Recently, Walker [4] attempted to automate the design of earthquake-resistant multi-story steel building frames by considering explicitly the dual design criteria mentioned above. The frame was designed to remain elastic when subjected to a moderate earthquake, with a specified amount of ductility to withstand a major earthquake without collapse. The analysis was simplified by introducing a number of assumptions which make generalization of the process difficult. In the present study, a more general approach is followed, and both levels of constraints are satisfied explicitly by monitoring the response to moderate and major earthquakes during the optimization process.

1.1 Objectives and Limitations of the Study

The main objective of the present study is to obtain the optimal design of earthquake-resistant structural systems satisfying two levels of design criteria. At the first level, the structure is designed to remain elastic when subjected to minor and moderate earthquakes. The earthquake input is modeled using a design response spectrum. The response is computed using modal superposition. At the second level, the structure is expected to undergo inelastic deformations within the prescribed limits when subjected to a major earthquake. This requires a dynamic response analysis of a nonlinear system. Fortunately, in many practical situations, the significant inelastic deformations induced in the structure by an earthquake are confined to a relatively small portion of the structure. Examples of such systems are buildings with a "soft" first story, equipment mounted on flexible supports, and structures with earthquake isolation devices. Such systems are characterized by the fact that the inelastic behavior is confined to known locations in the system. Generally speaking, the nonlinear behavior occurs in that portion of the system which is more flexible than the rest, either by intentional design or by prevailing circumstances. The dynamic response analysis of such localized nonlinear structures is considerably simplified, as will be explained later. Therefore, the present study considers only systems with localized nonlinearities.

An actual ground motion record is used as input for the nonlinear system. In the absence of any suitable method for characterization of earthquake excitations for nonlinear systems, the probabilistic nature of the design problem is taken into account by carrying out a series of analyses for different earthquake inputs and comparing the structural response to these earthquakes for the structure designed from a single record. This procedure gives at least an indirect indication of the sensitivity of the optimal design to the selection of input earthquake ground motion.

The optimization problem is solved by an algorithm of the feasible directions type which is capable of handling time-dependent constraints. In order to achieve computational efficiency for the class of design problems associated with earthquake-resistant design, a number of modifications to the basic algorithm is required.

The objectives of the present research are summarized as follows:

(i) to formulate the problem of designing earthquake-resistant localized nonlinear structures, satisfying dual design criteria, as an optimization problem suitable for the application of nonlinear programming techniques;

(ii) to develop an efficient response analysis procedure for structures with localized nonlinearities;

(iii) to apply the method of feasible directions to obtain the optimal design, making use of the special nature of the design problem to achieve computational efficiency;

(iv) to apply the general techniques to the optimal design of an earthquake isolation system, consisting of natural rubber bearings and mild steel energy-absorbing devices, for a three-story steel frame.

1.2 Outline of the Report

A class of optimal design problems for structural systems with two levels of performance constraint under earthquake excitations is formulated in Section 2. A technique to transcribe the optimal design problem to the canonical form of nonlinear programming problem is given and major computational tasks are identified. Section 3 contains a brief description of the response analysis of a linear system using an earthquake response spectrum. Equations for sensitivity analysis of a linear system are derived in this section also. A mathematical model for the hysteretic behavior of nonlinear elements is described in Section 4 as well as an algorithm, based upon the Newmark and Runge-Kutta methods, for the solution of equations of motion of the localized nonlinear system. A technique for sensitivity analysis of a nonlinear system is introduced. Section 5 presents an algorithm of the feasible directions type for the solution of the nonlinear programming problem with time-dependent constraints. Details about the computational aspects of the algorithm are included. Section 6 describes the application of the general techniques presented in Sections 2, 3, 4, and 5 to the optimal design of an earthquake isolation system for a three-story steel frame. Some general remarks about the present study are included in Section 7, which also gives some suggestions for future research in this area.

2. FORMULATION OF AN OPTIMAL DESIGN PROBLEM FOR STRUCTURAL SYSTEMS SUBJECTED TO EARTHQUAKES

This section formulates a class of optimal design problems for structural systems subjected to earthquake ground excitations. A general strategy to transcribe the optimal design problem to the canonical form of a nonlinear programming problem is presented. The section is concluded by identifying the major computational tasks to be performed to achieve the optimal solution of the problem.

2.1 Optimal Design Problem

As pointed out earlier, the current design philosophy for structural systems to resist earthquakes is that the structure should be sufficiently rigid to have small deformations when subjected to small earthquakes, but should be ductile enough to withstand large inelastic deformations in order to resist large earthquakes. This design philosophy suggests at least two levels of performance constraints on the system; namely, one on the response to small earthquakes and the other on the response to large earthquakes. The objective of the design problem is to achieve the most "efficient" structural system which satisfies the above criteria. A number of objective functions has been considered in the literature. For example, Ray et al [5] considered weight of the structure as an objective while Walker [4] considered life-time cost of the structure, which includes the present construction cost plus future damage and repair costs, as an objective. In this study, the objective function is simply taken to be some function of the structural response. This approach includes previous work as special cases and can easily be made explicit to treat particular design problems for which the manner in which the design objective depends on structural response is specified. Thus, a class of optimal design problems for structural systems subjected to earthquakes can be written in the form:

$$\min_{\mathbf{z}} \max_{t \in T} [F\{\mathbf{R}^l(\mathbf{z},t),\ \mathbf{R}^s(\mathbf{z},t)\}]$$

such that

$$\begin{aligned} \max_{t \in T} \mathbf{G}^l(\mathbf{R}^l(\mathbf{z},t)) &\leqq \delta_1^l \\ \max_{t \in T} \mathbf{G}^s(\mathbf{R}^s(\mathbf{z},t)) &\leqq \delta_1^s \qquad (2.1.1) \\ \mathbf{H}(\mathbf{z}) &\leqq \delta_2, \end{aligned}$$

where

$\mathbf{R}^l, \mathbf{R}^s : \mathbb{R}^P \times \mathbb{R} \to \mathbb{R}^Q \times \mathbb{R}$ *is* some function of structural response. The superscripts l and s refer to response when subjected to a large and a small earthquake respectively;

$T = [t_0, t_f]$ is the interval in which significant earthquake ground motion occurs;

$\mathbf{z} \in \mathbb{R}^P$ *is* the design parameter vector;

P is the total number of design parameters;

$F : \mathbb{R}^Q \times \mathbb{R} \to \mathbb{R}$ is some function of structural response, which is to be minimized;

Q is the number of structural response functions;

$\mathbf{G} : \mathbb{R}^Q \times \mathbb{R} \to \mathbb{R}^M$ are time-dependent inequality constraints (functional constraints);

M is number of functional inequality constraints;

$\mathbf{H} : \mathbb{R}^P \to \mathbb{R}^L$ are conventional inequality constraints;

L is number of conventional inequality constraints;

$\delta_1 \in \mathbb{R}^M, \delta_2, \in \mathbb{R}^L$ are prescribed constraint bounds.

As an example, consider the following problem: a multi-story shear frame is constrained to remain elastic when subjected to a small earthquake but the bottom floor is permitted to sustain inelastic deformation when subjected to a large earthquake. The design objective is to minimize the maximum acceleration of the top floor with the bottom floor displacement less than a certain allowable value. The design variables are the story stiffnesses. In this case the function F is chosen as the square of the top floor acceleration when subjected to a large earthquake, while $\mathbf{G}^l$ is equal to the square of the bottom floor displacement, with δ_1^l being its maximum allowable value. The function $\mathbf{G}^s$ is the shear in the bottom floor when subjected to a small earthquake and δ_1^s is the corresponding yield force. The function $\mathbf{H}$ represents positivity constraints on the story stiffnesses.

2.2 Transcription of the Optimal Design Problem to the Canonical Form of a Nonlinear Programming Problem

The optimal design problem formulated in Equation (2.1.1) is not directly suitable for application of nonlinear programming techniques. An appropriate canonical form of the nonlinear programming problem can be expressed as [6,7]:

$$\min_{\mathbf{z}} \; \{f^o(\mathbf{z})\}$$

such that

$$\begin{aligned} \max_{t \in T} \varphi^j(\mathbf{z},t) &\leqq 0 \qquad j=1,\ldots,M \\ g^j(\mathbf{z}) &\leqq 0 \qquad j=1,\ldots,L \end{aligned} \tag{2.2.1}$$

where

$$\begin{aligned} \varphi^j : \mathbb{R}^P \times \mathbb{R} \to \mathbb{R} &= \textit{functional inequality constraints}; \\ \mathbf{z} \in \mathbb{R}^P &= \textit{design parameter vector}; \\ f^o : \mathbb{R}^P \to \mathbb{R} &= \textit{objective function}; \\ g^j : \mathbb{R}^P \to \mathbb{R} &= \textit{conventional inequality constraints}. \end{aligned}$$

The optimal design problem (2.1.1) can be transcribed to canonical form (2.2.1) by augmenting the parameter vector $\mathbf{z}$ by a dummy cost parameter z_{P+1}. The dummy cost parameter is an upper bound to the objective function to be minimized, that is,

$$z_{P+1} \geqq \max_{t \in T} \left[F\left(\mathbf{R}^l(\mathbf{z},t),\ \mathbf{R}^s(\mathbf{z},t)\right) \right].$$

Thus, the minimization of z_{P+1} will imply the minimization of the actual objective function. The optimal design problem can then be written as:

$$\min_{\mathbf{z}}\ z_{P+1}$$

such that

$$\begin{aligned} \max_{t \in T} \left[F\{\mathbf{R}^l(\mathbf{z},t),\mathbf{R}^s(\mathbf{z},t)\} \right] - z_{P+1} &\leqq 0 \\ \max_{t \in T} \mathbf{G}^l\{\mathbf{R}^l(\mathbf{z},t)\} - \delta_1^l &\leqq 0 \\ \max_{t \in T} \mathbf{G}^s\{\mathbf{R}^s(\mathbf{z},t)\} - \delta_1^s &\leqq 0 \\ \mathbf{H}(\mathbf{z}) - \delta_2 &\leqq 0. \end{aligned} \tag{2.2.2}$$

Equation (2.2.2) is in canonical form with:

$$\begin{aligned} f^{\circ}(\mathbf{z}) &= z_{P+1} \\ \varphi^1(\mathbf{z},t) &= F\{\mathbf{R}^l(\mathbf{z},t),\mathbf{R}^s(\mathbf{z},t)\} - z_{P+1} \\ \varphi^j(\mathbf{z},t) &= G_j^l\{\mathbf{R}^l(\mathbf{z},t) - \delta_{1j}^l \quad j=2,\ldots,J_l \\ \varphi^j(\mathbf{z},t) &= G_j^s\{\mathbf{R}^s(\mathbf{z},t)\} - \delta_{1j}^s \quad j=J_l,\ldots,M \\ g^j(\mathbf{z},t) &= H_j(\mathbf{z}) - \delta_{2j} \quad j=1,2,\ldots,L. \end{aligned} \tag{2.2.3}$$

2.3 Major Computational Tasks

The optimal design problem formulated in Equation (2.2.2) is suitable for application of nonlinear programming techniques for its solution. These techniques start out with a given point in the design space and make iterative improvements on it until an optimum is reached. At each design iteration, the objective and constraint functions are evaluated at least once. Moreover, if a gradient type of nonlinear programming technique, such as the method of feasible directions used in this study, is employed, it will require computation of the gradients of objective and constraint functions at each iteration as well.

Since the functions F and $\mathbf{G}$ involve structural response quantities, their evaluation requires dynamic response analysis of the structural system. Separate dynamic analyses are needed for large and small earthquakes. The gradients of functions F and $\mathbf{G}$ involve the gradients of the response quantities with respect to the design parameters. Computation of these gradients is known as sensitivity analysis.

In accordance with the assumed underlying earthquake-resistant design philosophy, the structure is to remain elastic when subjected to a small earthquake but can go into the inelastic range when subjected to a large earthquake. Thus, for a small earthquake linear response analysis methods can be employed, while a large earthquake will require nonlinear response analysis. The major computational tasks can now be summarized as follows.

1. Earthquake response analysis of a linear structure. A response spectrum approach is used, an outline of which is found in Section 3.

2. Sensitivity analysis of a linear structure. The procedure is given in Section 3.

3. Earthquake response analysis of a nonlinear structure. In this study only systems with localized nonlinearities are considered. A step-by-step numerical integration scheme is used for response computation, as explained in Section 4.

4. Sensitivity analysis of a nonlinear system. This procedure is outlined in Section 4.

5. Solution of the optimization problem with time-dependent constraints. Section 5 describes an algorithm by which this is accomplished.

3. EARTHQUAKE RESPONSE ANALYSIS OF LINEAR SYSTEMS

This section gives a brief description of the response analysis of a linear system using an earthquake response spectrum. A design response spectrum based upon analyses of thirty-three past earthquake accelerograms is described. Equations for sensitivity analysis of a linear system are derived. Further details about the response spectrum analysis procedure and sensitivity analysis can be found in references [8,5].

3.1 Response Spectrum Analysis of Linear Systems

The equations of motion for an N degree-of-freedom linear system can be written as (see reference [8]):

$$\mathbf{M}\,\ddot{\mathbf{u}}(t) + \mathbf{C}\,\dot{\mathbf{u}}(t) + \mathbf{K}\,\mathbf{u}(t) = -\mathbf{M}\,\mathbf{r}\,\ddot{u}_g(t) \qquad (3.1.1)$$

where

$t \in T = [t_0, t_f]$ = time interval of interest;

$\mathbf{M} \in \mathbb{R}^N \times \mathbb{R}^N$ = mass matrix;

$\mathbf{C} \in \mathbb{R}^N \times \mathbb{R}^N$ = damping matrix;

$\mathbf{K} \in \mathbb{R}^N \times \mathbb{R}^N$ = stiffness matrix;

$\mathbf{u}, \dot{\mathbf{u}}, \ddot{\mathbf{u}} \in \mathbb{R}^N$ = displacement, velocity and acceleration vectors of structural response;

$\mathbf{r} \in \mathbb{R}^N$ = earthquake influence coefficient vector. This vector represents displacements at nodal degrees-of-freedom resulting from a unit support displacement. For example, $\mathbf{r}^T = (1,1,\ldots,1)$ for an N story shear frame (with one degree-of-freedom at each story) subjected to horizontal ground motion;

$\ddot{u}_g(t) \in \mathbb{R}$ = ground acceleration time history.

Equation (3.1.1) can be uncoupled by introducing the transformation:

$$\mathbf{u}(t) = \sum_{i=1}^{N} \varphi_i \, Y_i(t) \tag{3.1.2}$$

where

$\varphi_i \in \mathbb{R}^N$ is the i^{th} mode shape or eigenvector of the system obtained from solving the eigenvalue problem;

$$\mathbf{K}\,\varphi_i = \lambda_i\,\mathbf{M}\,\varphi_i \qquad i=1,...,N \tag{3.1.3}$$

where λ_i is the i^{th} eigenvalue.

$Y_i(t) \in \mathbb{R}$ is the i^{th} generalized coordinate.

Substituting Equation (3.1.2) in Equation (3.1.1) and using the orthogonality property of the mode shapes, the uncoupled equations of motion are:

$$M_i^{*}\,\ddot{Y}_i(t) + C_i^{*}\,\dot{Y}_i(t) + K_i^{*}\,Y_i(t) = P_i^{*}(t) \tag{3.1.4}$$

where

$$\begin{aligned} K_i^{*} &= \varphi_i^T\,\mathbf{K}\,\varphi_i \\ M_i^{*} &= \varphi_i^T\,\mathbf{M}\,\varphi_i \\ C_i^{*} &= \varphi_i^T\,\mathbf{C}\,\varphi_i \\ P_i^{*}(t) &= -\varphi_i^T\,\mathbf{M}\,\mathbf{r}\,\ddot{u}_g(t) \end{aligned}$$

Note that it is assumed that the mode shapes are orthogonal with respect to the damping matrix, i.e. $\varphi_i^T\,\mathbf{C}\,\varphi_j = 0$ for all i$\neq$ j.

The solution of Equation (3.1.4) is given by:

$$Y_i(t) = -\frac{L_i^{*}}{M_i^{*}\,\omega_i^D}\,V(t) \tag{3.1.5}$$

where

$L_i^{*} = \varphi_i^T\,\mathbf{M}\,\mathbf{r}$ is the modal participation factor;

$\omega_i^D = \omega_i\sqrt{1-\xi_i^2}$ is the damped natural frequency of the i^{th} mode; where ω_i, ξ_i are the natural frequency and the critical damping ratio in the i^{th} mode, respectively.

V(t) is the earthquake response integral defined as:

$$V(t) = \int_0^t \ddot{u}_g(\tau) \exp[-\xi_i \, \omega_i(t-\tau)] \sin \omega_i^D(t-\tau) d\tau. \tag{3.1.6}$$

The pseudo-velocity response spectrum for $\ddot{u}_g(t)$ is defined as:

$$S_{v,i}(\xi_i, \omega_i) = \max_t |V(t)|. \tag{3.1.7}$$

Therefore, the maximum value of the i^{th} generalized coordinate is given by:

$$Y_{i,max} = \max_t |Y_i(t)| = \frac{L_i^*}{M_i^* \, \omega_i^D} S_{v,i}(\xi_i, \omega_i). \tag{3.1.8}$$

The maximum displacement in the i^{th} mode is then obtained from:

$$\overline{u}_{i,max} = \varphi_i \, Y_{i,max} \qquad i=1,\ldots,N$$

The maximum displacement at the k^{th} degree-of-freedom is approximated by taking the square root of the sum of squares of modal displacements (see reference [8]):

$$u_k^{\max} = \{(\overline{u}_{1,max,k})^2 + (\overline{u}_{2,max,k})^2 + \cdots + (\overline{u}_{N,max,k})^2\}^{\frac{1}{2}}$$

Thus,

$$\max_t \mathbf{u}(t) = [u_1^{\max}, u_2^{\max}, \ldots, u_N^{\max}]^T \tag{3.1.9}$$

The computational procedure is summarized in the following algorithm.

ALGORITHM

DATA: Structural property matrices **M** and **K**.

Number of modes to be used in response computations, NM.

Critical damping ratios in each mode.

STEP 1: Solve the generalized eigenvalue problem.

$$\mathbf{K} \, \varphi_i = \lambda_i \, \mathbf{M} \, \varphi_i \qquad i=1,\ldots,NM$$

STEP 2: Compute the generalized property matrices.

$$M_i^* = \varphi_i^T \, \mathbf{M} \, \varphi_i$$

$$L_i^* = \varphi_i^T \mathbf{M} \mathbf{r} \qquad i=1,\ldots,NM$$

STEP 3: From the pseudo-velocity response spectrum, get $S_{v,i}\ (\xi_i,\omega_i) \quad i=1,\ldots,NM.$

STEP 4: Compute the maximum displacement in each mode as follows:

$$\overline{\mathbf{u}}_i = \varphi_i \, Y_{i,max} \qquad i=1,\ldots,NM$$

where

$$Y_{i,max} = \frac{L_i^*}{M_i^* \omega_i^D} S_{v,i}$$

and

$$\omega_i^D = \omega_i \sqrt{1 - \xi_i^2}$$

STEP 5: The maximum displacements at nodal degrees-of-freedom are estimated by the square root of the sum of squares of modal displacements. Thus,

$$u_{i,max} = \left[\sum_{j=1}^{NM} (\overline{u}_{ij})^2 \right]^{\frac{1}{2}} \qquad i=1,\ldots,N$$

where the matrix $\overline{u} \in \mathbb{R}^N \times \mathbb{R}^{NM}$, is defined as

$$\overline{\mathbf{u}} = [\overline{u}_1, \ldots, \overline{u}_{NM}]^T$$

3.2 Earthquake Response Spectrum

The response analysis procedure given in Section 3.1 requires a pseudo-velocity response spectrum defined in Equations (3.1.6) and (3.1.7) for a particular earthquake. A response spectrum can be generated from a specified earthquake ground motion time history by following procedures given in reference [8].

Since different earthquakes have different response spectra, a number of attempts have been made to generate the so-called design response spectrum by averaging past earthquake response spectra. Blume et al [9] have recommended design response spectrum shapes based on the analyses of thirty-three different accelerograms of past earthquakes. The basic spectrum shape consists of two straight lines followed by an exponential decay curve, as shown in Figure 1. Coordinates of transition points are given for earthquakes with large (50%), small (15.8%) and negligible (2.3%) probabilities of being exceeded and for damping ratios of 0.5, 1, 2, 5, 7 and 10 percent of critical. The design pseudo-velocity response spectrum derived from these recommended shapes can be expressed as:

$$S_v = D(\xi,T)\,\frac{a}{\omega} \tag{3.2.1}$$

where

a = maximum absolute acceleration for which the structure is to be designed;

ω = frequency of the system;

T = $2\pi/\omega$ = period of the system;

ξ = damping ratio.

D is obtained from recommended shape in Figure 1 for a prescribed probability of being exceeded.

3.3 Sensitivity Analysis for Linear Systems

Sensitivity analysis (i.e., computation of the rate of change of response quantities with respect to design parameters) is an integral part of optimization processes that use gradient techniques. For a linear system the response equations can be differentiated to obtain analytical expressions for sensitivity analysis [4]. Expressions for the rate of change of maximum nodal displacements in the structural model represented by Equation (3.1.1) with respect to design parameters are derived below.

Maximum nodal displacements are obtained from the following equation derived in Section 3.1.

$$u_i(\mathbf{z}) = \left[\sum_{j=1}^{NM} (\overline{u}_{ij}(\mathbf{z}))^2\right]^{\frac{1}{2}} \qquad i=1,\ldots,N \tag{3.3.1}$$

where

NM = number of modes to be considered in the analysis

N = total number of degrees of freedom.

$\overline{u}_{ij}$ is the $(i,j)^{th}$ element of the matrix $\overline{\mathbf{u}} \in \mathbb{R}^N \times \mathbb{R}^{NM}$ whose n^{th} column consists of

$$\overline{\mathbf{u}}_n = \varphi_n \, Y_{n,max} \qquad n=1,\ldots,NM \tag{3.3.2}$$

$\varphi_n \in \mathbb{R}^N$ is the n^{th} mode shape and

$$Y_{n,max} = \frac{L_n^*}{M_n^* \omega_n^D} S_{v,n}(\omega_n, \xi_n)$$

where

$$\begin{aligned} \omega_n^D &= \omega_n \sqrt{1-\xi_n^2} \\ &= \sqrt{\lambda_n (1-\xi_n^2)} \end{aligned}$$

Therefore,

$$Y_{n,max} = \frac{L_n^*}{M_n^*} \frac{S_{v,n}\ (\omega_n, \xi_n)}{\sqrt{\lambda_n (1-\xi_n^2)}} \tag{3.3.3}$$

Differentiate Equation (3.3.1) with respect to the design parameter z_l to get

$$\frac{\partial u_i(\mathbf{z})}{\partial z_l} = \frac{1}{2} \left[\sum_{j=1}^{NM} (\overline{u}_{ij})^2 \right]^{-\frac{1}{2}} \left[\sum_{j=1}^{NM} 2\overline{u}_{ij} \ \frac{\partial \overline{u}_{ij}}{\partial z_l} \right]$$

or

$$\frac{\partial u_i(\mathbf{z})}{\partial z_l} = \frac{\sum_{j=1}^{NM} \overline{u}_{ij} \ \frac{\partial \overline{u}_{ij}}{\partial z_l}}{u_i} \tag{3.3.4}$$

$\frac{\partial \overline{u}_{ij}}{\partial z_l}$ in Equation (3.3.4) is computed as follows.

For convenience, define a diagonal matrix $\mathbf{Y}_{\max} \in \mathbb{R}^{NM} \times \mathbb{R}^{NM}$ whose diagonal elements consist of $Y_{n,max}$ n=1,...,NM defined by Equation (3.3.3). Then the matrix $\overline{\mathbf{u}}$ can be written as:

$$\overline{\mathbf{u}} = \Phi \, \mathbf{Y}_{\max} \tag{3.3.5}$$

where $\Phi \in \mathbb{R}^N \times \mathbb{R}^{NM}$ is the modal matrix whose n^{th} column consists of the n^{th}

mode shape of the system.

Differentiating Equation (3.3.5) with respect to z_l gives

$$\frac{\partial \overline{\mathbf{u}}}{\partial z_l} = \frac{\partial \Phi}{\partial z_l}\,\mathbf{Y}_{\max} + \Phi\,\frac{\partial \mathbf{Y}_{\max}}{\partial z_l} \tag{3.3.6}$$

The quantities $\frac{\partial \Phi}{\partial z_l}$ are the derivatives of the eigenvectors. The expressions for computation of these derivatives are given in Appendix A. $\frac{\partial \mathbf{Y}_{\max}}{\partial z_l}$ is a diagonal matrix whose n^{th} diagonal element is obtained by differentiating Equation (3.3.3) as follows:

$$\begin{aligned}\frac{\partial Y_{n,max}}{\partial z_l} &= \frac{\partial}{\partial z_l}\left[\frac{L_n^*}{M_n^*}\,\frac{S_{v,n}}{\sqrt{\lambda_n(1-\xi_n^2)}}\right] \qquad (3.3.7)\\ &= \frac{1}{M_n^*\sqrt{1-\xi_n^2}}\,\frac{\partial L_n^*}{\partial z_l}\,\frac{S_{v,n}}{\sqrt{\lambda_n}} - \frac{L_n^*}{(M_n^*)^2\sqrt{1-\xi_n^2}}\,\frac{\partial M_n^*}{\partial z_l}\,\frac{S_{v,n}}{\sqrt{\lambda_n}}\\ &+ \frac{L_n^*}{M_n^*\sqrt{1-\xi_n^2}}\left(-\frac{1}{2}(\lambda_n)^{-\frac{3}{2}}\right)\frac{\partial \lambda_n}{\partial z_l}\,S_{v,n} + \frac{L_n^*}{M_n^*\sqrt{1-\xi_n^2}}\,\frac{1}{\sqrt{\lambda_n}}\,\frac{\partial S_{v,n}}{\partial z_l}\end{aligned}$$

where

$$\frac{\partial L_n^*}{\partial z_l} = \frac{\partial \varphi_n^T}{\partial z_l}\,\mathbf{M}\,\mathbf{r} \tag{3.3.8}$$

$$\frac{\partial M_n^*}{\partial z_l} = 2\,\frac{\partial \varphi_n^T}{\partial z_l}\,\mathbf{M}\,\varphi_n \tag{3.3.9}$$

and

$$\frac{\partial S_{v,n}}{\partial z_l} = \frac{\partial S_{v,n}}{\partial \lambda_n}\,\frac{\partial \lambda_n}{\partial z_l}. \tag{3.3.10}$$

Computation of $\frac{\partial \lambda_n}{\partial z_l}$ is given in Appendix A.

The derivatives of the pseudo-velocity response spectrum are obtained from the design response spectrum shape given in Section 3.2. The expressions for these derivatives are derived in Appendix B.

Rearrangement of Equation (3.3.7) gives

$$\frac{\partial Y_{n,max}}{\partial z_l} = \frac{1}{M_n^* \sqrt{\lambda_n (1-\xi_n^2)}} \left[S_{v,n} \frac{\partial \varphi_n^T}{\partial z_l} \mathbf{M}\,\mathbf{r} - 2 \frac{L_n^*}{M_n^*} S_{v,n} \frac{\partial \varphi_n^T}{\partial z_l} \mathbf{M}\,\varphi_n \right.$$
$$\left. - \frac{L_n^*}{2\lambda_n} S_{v,n} \frac{\partial \lambda_n}{\partial z_l} + L_n^* \frac{\partial S_{v,n}}{\partial \lambda_n} \frac{\partial \lambda_n}{\partial z_l} \right] \tag{3.3.11}$$

Once Equation (3.3.11) is evaluated for all NM modes to be considered, Equation (3.3.6) can be evaluated and, in turn, used in Equation (3.3.4) to compute the required sensitivity matrix.

4. EARTHQUAKE RESPONSE ANALYSIS OF LOCALIZED NONLINEAR SYSTEMS

In this section a mathematical model describing hysteretic behavior of nonlinear elements is introduced. Equations of motion for a structure with a type of localized nonlinear element are given and an algorithm for numerical solution of these equations is presented, together with a technique for computing sensitivity matrices.

4.1 A Model for Hysteretic Behavior of Nonlinear Elements

A number of models has been employed to specify the force-deformation relationship for inelastic structural elements under cyclic loading. Two of the most common are the bilinear and the Ramberg-Osgood models. The bilinear model exhibits sharp transition from elastic to inelastic states. Kinematic or isotropic hardening rules are used for unloading and reloading. The model fails to represent actual material behavior under cyclic loading and is computationally quite inefficient because it requires one to keep track of all stiffness transition points.

The Ramberg-Osgood model, coupled with Masing's rule for unloading and reloading gives a continuous transition from elastic to inelastic states. Computationally, this is a very difficult model to use because of different equations for different parts of the loop. Matzen and McNiven [10] have pointed out that the model as presented originally is not suitable for random earthquake-type excitations. At least thirteen new rules have been added to make it applicable to this case, making the model even harder to use.

Recently a series of newly-proposed models for cyclic behavior of structural elements has been described [11]. These models are given in the form of differential equations and are sufficiently general to include strain hardening, stiffness degradation, etc. A single set of equations governs initial loading, unloading and reloading (facilitating computation) and the model behaves well in the case of arbitrary excitations.

The particular rate-independent model to be used for nonlinear elements in this study is given by the following equations:

$$\dot{F}(t) = K_0\left[\dot{\delta}(t) - |\dot{\delta}(t)|\left[\frac{F(t)}{F_0} - S\right]^n\right] \qquad (4.1.1)$$

$$S(t) = \alpha\left[\frac{\delta(t)}{\delta_0} - \frac{F(t)}{F_0}\right] \qquad (4.1.2)$$

where

$F(t)$ = generalized force in the nonlinear element;

$\delta(t)$ = generalized deformation of the nonlinear element;

$\dot{\delta}(t)$ = deformation rate of the nonlinear element;

K_0 = F_0/δ_0 ;

F_0 = generalized yield force;

δ_0 = generalized yield deformation;

α = a constant which controls the slope after yielding, $K_y \approx K_0 \dfrac{\alpha}{1+\alpha}$;

n = a material parameter, taken as an odd integer which controls the sharpness of transition from the elastic to the inelastic region. As $n \to \infty$ the model approaches a bilinear model.

The parameters F_0, δ_0, α and n are chosen so that predicted response from the model closely matches experimental response. Typical loops generated by this model under deformation varying sinusoidally in time are shown in Figure 2.

It should be pointed out that the above model is just one of a class of models for inelastic behavior. This particular choice was made for the immediate application of the present work to optimal design of frames with energy-absorbing devices described in Section 6. More complicated models, such as models exhibiting stiffness degradation, etc., can be obtained by introducing more parameters into the basic model, as explained in reference [11]. These models can be introduced into the present formulation without any difficulty.

4.2 Equations of Motion for the System

Equations of motion for a discrete, N degree-of-freedom structural system subjected to earthquake ground motion can be written as follows:

$$\mathbf{M}\,\ddot{\mathbf{u}}(t) + \mathbf{C}\,\dot{\mathbf{u}}(t) + \mathbf{F}(t) \;=\; -\mathbf{M}\,\mathbf{r}\,\ddot{u}_g(t) \tag{4.2.1}$$

where

$\mathbf{u}(t) \;=\; [u_1(t),\, u_2(t), \ldots,\, u_N(t)]^T$ is the nodal point displacement vector, $\mathbf{u} \in \mathbb{R}^N$;

$\dot{\mathbf{u}}(t)$ = nodal point velocity vector;

$\ddot{\mathbf{u}}(t)$ = nodal point acceleration vector;

$\mathbf{M}$ = mass matrix of the system , $\mathbf{M} \in \mathbb{R}^N \times \mathbb{R}^N$;

$\mathbf{C}$ = structural damping matrix, $\mathbf{C} \in \mathbb{R}^N \times \mathbb{R}^N$;

$\mathbf{F}$ = nodal force vector, $\mathbf{F} \in \mathbb{R}^N$;

$\mathbf{r}$ = earthquake influence coefficient vector, $\mathbf{r} \in \mathbb{R}^N$. This vector represents displacements at nodal degrees of freedom resulting from a unit support displacement. For example, $r = (1,1,\ldots,1)^T$ for an N story shear frame (with one degree of freedom at each story) subjected to horizontal ground motion;

$\ddot{u}_g(t)$ = ground acceleration time history

4.3 Numerical Solution of the Differential Equations of Motion

The equations of motion (4.2.1) are solved numerically with the exact solution $\mathbf{u}(t)$, $\dot{\mathbf{u}}(t)$ and $\ddot{\mathbf{u}}(t)$ approximated by $\mathbf{u}_t$, $\dot{\mathbf{u}}_t$ and $\ddot{\mathbf{u}}_t$, respectively, at discrete time intervals. The step-by-step integration procedures start with the known initial conditions and march forward in time giving the solution at discrete points in time. The process for a nonlinear system has two distinct phases. The first phase is the linearization phase, in which the equations are linearized about the current state by retaining only first order terms of a Taylor series expansion. Estimates of the solution at the next step are then obtained by using these linearized equations. The second phase is the state determination phase, in which the internal forces in equilibrium with the new state of motion are calculated. If the discrepancy between these internal forces and the external applied loads is within some tolerance level, the solution is accepted and the process repeated for the next step. Otherwise, a Newton-Raphson type iteration is used until the unbalanced forces are within acceptable limits.

In this study, estimates of the solution are obtained using Newmark's method, and internal forces in the nonlinear elements are computed using a fourth-order Runge-Kutta scheme. Details of the process are given below.

The equations of motion (4.2.1) at time $\tau = t + \Delta t$ can be written as

$$\mathbf{M}\,\ddot{\mathbf{u}}_\tau + \mathbf{C}\,\dot{\mathbf{u}}_\tau + \mathbf{F}_\tau = \mathbf{P}_\tau \tag{4.3.1}$$

where

$$\mathbf{P}_\tau = -\mathbf{M}\,\mathbf{r}\,\ddot{u}_g(t)$$

Define the increments in acceleration, velocity, displacement and force occurring in the time increment Δt by

$$\begin{aligned} \Delta\ddot{\mathbf{u}}_t &= \ddot{\mathbf{u}}_\tau - \ddot{\mathbf{u}}_t \\ \Delta\dot{\mathbf{u}}_t &= \dot{\mathbf{u}}_\tau - \dot{\mathbf{u}}_t \\ \Delta\mathbf{u}_t &= \mathbf{u}_\tau - \mathbf{u}_t \\ \Delta\mathbf{F}_t &= \mathbf{F}_\tau - \mathbf{F}_t \\ &= \frac{\partial \mathbf{F}_t}{\partial \mathbf{u}_t}\,\Delta\mathbf{u}_t \\ &= \mathbf{K}_t\,\Delta\mathbf{u}_t \end{aligned} \tag{4.3.2}$$

Substituting these expressions in Equation (4.3.1), the incremental form of the equations of motion is obtained as follows:

$$\mathbf{M}\,\Delta\ddot{\mathbf{u}}_t + \mathbf{C}\,\Delta\dot{\mathbf{u}}_t + \mathbf{K}_t\,\Delta\mathbf{u}_t = \mathbf{P}_t^* \tag{4.3.3}$$

where

$$\mathbf{P}_t^* = \mathbf{P}_\tau - [\mathbf{M}\,\ddot{\mathbf{u}}_t + \mathbf{C}\,\dot{\mathbf{u}}_t + \mathbf{F}_t].$$

Newmark's Method

An implicit, single-step, two parameter family of integration operators described by Newmark [12] is used for the numerical integration of the equations of motion. The method assumes that the increments in velocity and acceleration are related to the increment in displacement and the state of motion at time t, as follows:

$$\Delta\dot{\mathbf{u}}_t = \frac{\gamma}{\beta\Delta t}\,\Delta\mathbf{u}_t - \frac{\gamma}{\beta}\,\dot{\mathbf{u}}_t - \Delta t\left[\frac{\gamma}{2\beta} - 1\right]\ddot{\mathbf{u}}_t \tag{4.3.4}$$

$$\Delta\ddot{\mathbf{u}}_t = \frac{1}{\beta(\Delta t)^2}\,\Delta\mathbf{u}_t - \frac{1}{\beta\Delta t}\,\dot{\mathbf{u}}_t - \frac{1}{2\beta}\,\ddot{\mathbf{u}}_t \tag{4.3.5}$$

where

Δt = time step of integration;

γ, β are integration parameters.

A "constant average acceleration" operator, which is unconditionally stable for linear problems, is obtained with $\beta = 1/4$ and $\gamma = 1/2$.

A "linear acceleration" operator is obtained with $\beta = 1/6$ and $\gamma = 1/2$.

Substituting (4.3.4) and (4.3.5) into the incremental equations of motion (4.3.3) and simplifying gives

$$\mathbf{K}_t^*\,\Delta\mathbf{u}_t = \mathbf{R}_t^* \tag{4.3.6}$$

where

$$\mathbf{K}_t^* = \frac{1}{\beta\Delta t}\,\mathbf{M} + \frac{\gamma}{\beta\Delta t}\,\mathbf{C} + \mathbf{K}_t$$

$$\mathbf{R}_t^* = \mathbf{P}_t^* + \mathbf{M}\left[\frac{1}{\beta\Delta t}\,\dot{\mathbf{u}}_t + \frac{1}{2\beta}\,\ddot{\mathbf{u}}_t\right] + \mathbf{C}\left[\frac{\gamma}{\beta}\,\dot{\mathbf{u}}_t + \Delta t\left[\frac{\gamma}{2\beta} - 1\right]\ddot{\mathbf{u}}_t\right].$$

Solution of $\mathbf{K}_t^* \, \Delta\mathbf{u}_t = \mathbf{R}_t^*$

The most expensive part of the integration process is the solution of the above set of linear equations. Fortunately, because of the localized nonlinearity of the problem, it is not necessary to form and decompose the whole matrix $\mathbf{K}_t^*$ at each step. The substructuring technique is used to separate effectively the nonlinear part from the linear part of the problem as follows:

Partition the displacement vector such that displacements corresponding to the nonlinear degrees of freedom are separated from the remaining displacements:

$$\Delta\mathbf{u}_t = \begin{bmatrix} \Delta\mathbf{u}^E \\ \Delta\mathbf{u}^N \end{bmatrix}$$

where

$\Delta\mathbf{u}^N$ = incremental displacements corresponding to the nonlinear degrees of freedom;

$\Delta\mathbf{u}^E$ = incremental displacements corresponding to the rest of the system.

Partition $\mathbf{K}_t^*$ and $\mathbf{R}_t^*$ accordingly, as follows:

$$\begin{bmatrix} \mathbf{K}_{EE} & \mathbf{K}_{EN} \\ \mathbf{K}_{NE} & \mathbf{K}_{NN} \end{bmatrix} \begin{Bmatrix} \Delta\mathbf{u}^E \\ \Delta\mathbf{u}^N \end{Bmatrix} = \begin{Bmatrix} \mathbf{R}^E \\ \mathbf{R}^N \end{Bmatrix}. \tag{4.3.7}$$

The first submatrix equation gives:

$$\mathbf{K}_{EE} \, \Delta\mathbf{u}^E + \mathbf{K}_{EN} \, \Delta\mathbf{u}^N = \mathbf{R}^E$$

or

$$\Delta\mathbf{u}^E = \mathbf{K}_{EE}^{-1} \left[\mathbf{R}^E - \mathbf{K}_{EN} \, \Delta\mathbf{u}^N \right] \tag{4.3.8}$$

The second submatrix equation in Equation (4.3.7) gives:

$$\mathbf{K}_{NE} \, \Delta\mathbf{u}^E + \mathbf{K}_{NN} \, \Delta\mathbf{u}^N = \mathbf{R}^N. \tag{4.3.9}$$

Substitute Equation (4.3.8) into Equation (4.3.9):

$$\mathbf{K}_{NE} \, \mathbf{K}_{EE}^{-1} \left[\mathbf{R}^E - \mathbf{K}_{EN} \, \Delta\mathbf{u}^N \right] + \mathbf{K}_{NN} \, \Delta\mathbf{u}^N = \mathbf{R}^N.$$

Define

$$\mathbf{Q} = -\mathbf{K}_{EE}^{-1}\,\mathbf{K}_{EN},$$

then

$$\mathbf{Q}^T = -\mathbf{K}_{NE}\,\mathbf{K}_{EE}^{-1}.$$

Thus,

$$\left[\mathbf{K}_{NE}\,\mathbf{Q} + \mathbf{K}_{NN}\right]\Delta\mathbf{u}^N = \mathbf{R}^N + \mathbf{Q}^T\,\mathbf{R}^E,$$

or

$$\Delta\mathbf{u}^N = \left[\mathbf{K}_{NE}\,\mathbf{Q} + \mathbf{K}_{NN}\right]^{-1}\left[\mathbf{R}^N + \mathbf{Q}^T\,\mathbf{R}^E\right]. \tag{4.3.10}$$

Once the $\Delta\mathbf{u}^N$ are known, $\Delta\mathbf{u}^E$ are calculated from Equation (4.3.8).

The computational steps can be summarized in the following algorithm.

Algorithm

In the beginning of the integration loop

(i) form $\mathbf{K}_{EE}$, $\mathbf{K}_{EN}$, $\mathbf{K}_{NE} = \mathbf{K}_{EN}^T$,

(ii) triangularize $\mathbf{K}_{EE}$,

(iii) obtain $\mathbf{Q}$ by forward reduction and back substitution from $\mathbf{K}_{EE}\,\mathbf{Q} = -\mathbf{K}_{EN}$,

(iv) form $\mathbf{Q}^T$ and the product $\mathbf{K}_{NE}\,\mathbf{Q}$.

At each time step of integration,

(i) form $\mathbf{K}_{NN}$ at the current step,

(ii) form load vectors $\mathbf{R}^E$ and $\mathbf{R}^N$,

(iii) solve $\left[\mathbf{K}_{NE}\,\mathbf{Q} + \mathbf{K}_{NN}\right]\Delta\mathbf{u}^N = \mathbf{R}^N + \mathbf{Q}^T\,\mathbf{R}^E$ for $\Delta\mathbf{u}^N$,

(iv) obtain $\Delta\mathbf{u}^E$ by forward reduction and back substitution from

$$\mathbf{K}_{EE}\,\Delta\mathbf{u}^E = \mathbf{R}^E - \mathbf{K}_{EN}\,\Delta\mathbf{u}^N.$$

Computation of Internal Resisting Forces

After the increments in the displacements and velocities are obtained, the next step is to compute the internal resisting forces in equilibrium with this new state of motion. The internal forces in the linear elements are obtained simply by multiplying the current displacements by the appropriate stiffnesses of these elements. Computation of forces in the nonlinear elements, however, is not so simple, because of lack of an algebraic expression for their force-deformation behavior, which is described by a set of first-order differential equations. These differential equations must be integrated numerically to obtain the internal forces in the nonlinear elements. An explicit fourth-order Runge-Kutta scheme, with the option of using a smaller time step than the one used in Newmark's method, is used in this study. An explicit scheme is favored over an implicit scheme because of the added complexity of an implicit scheme, which would involve an additional iteration cycle. The details of the process are given below.

To integrate force-deformation equations of nonlinear elements from time t to time $\tau = t + \Delta t$, some assumptions regarding the variation of acceleration, velocity and displacement during the time interval (t,τ) are needed. Since the Newmark's linear acceleration method has been demonstrated to be quite effective for solving nonlinear structural dynamic problems [13], it seems reasonable to assume linear variation in the acceleration during the time interval. This implies quadratic variation of velocity and cubic variation of displacement. These variations are shown in Figure 3.

The force corresponding to the i^{th} nonlinear degree of freedom is given by Equations (4.1.1) and (4.1.2).

$$\dot{F}_i(x) = K_o\left\{\dot{\delta}_i(x) - |\dot{\delta}_i(x)|\left[\frac{F_i(x)}{F_o} - S_i(x)\right]^n\right\} \tag{4.3.11}$$

$$S_i(x) = \alpha\left[\frac{\delta_i(x)}{\delta_o} - \frac{F_i(x)}{F_o}\right] \quad x \in [0,\Delta t], \tag{4.3.12}$$

where $\delta_i(x)$ is the deformation corresponding to the i^{th} degree of freedom. The deformations are related to nodal displacements by a transformation matrix which depends upon the type of structural system. For example, for a shear frame $\delta_i = U_i - U_{i-1}$, while more complicated expressions are required for other types of frames. Combining Equations (4.3.11) and (4.3.12) then

$$\dot{F}_i(x) = K_o\left[\dot{\delta}_i(x) - |\dot{\delta}_i(x)| \left\{(\alpha+1)\frac{F_i(x)}{F_o} - \alpha\frac{\delta_i(x)}{\delta_o}\right\}^n\right] \tag{4.3.13}$$

$$x \in [0,\Delta t].$$

Equation (4.3.13) is integrated by employing a fourth-order Runge-Kutta method with time step Δx, where $\Delta x \leqq \Delta t$, and initial condition $F_i(0) = F_i(t)$.

The following calculations advance the solution from $x_K \to x_{K+1} = x_K + \Delta x$.

$$K_1 = \Delta x\ K_0\left[\dot{\delta}_i(x_K) - |\dot{\delta}_i(x_K)| \left\{(\alpha+1)\frac{F_i(x_K)}{F_o} - \alpha\frac{\delta_i(x_K)}{\delta_o}\right\}^n\right]$$

$$K_2 = \Delta x\ K_0\left[\dot{\delta}_i(x_K+\tfrac{1}{2}\Delta x) - |\dot{\delta}_i(x_K+\tfrac{1}{2}\Delta x)| \left\{(\alpha+1)\frac{F_i(x_K)+\tfrac{1}{2}K_1}{F_o} - \alpha\frac{\delta_i(x_K+\tfrac{1}{2}\Delta x)}{\delta_o}\right\}^n\right]$$

$$K_3 = \Delta x\ K_0\left[\dot{\delta}_i(x_K+\tfrac{1}{2}\Delta x) - |\dot{\delta}_i(x_K+\tfrac{1}{2}\Delta x)| \left\{(\alpha+1)\frac{F_i(x_K)+\tfrac{1}{2}K_2}{F_o} - \alpha\frac{\delta_i(x_K+\tfrac{1}{2}\Delta x)}{\delta_o}\right\}^n\right]$$

$$K_4 = \Delta x\ K_0\left[\dot{\delta}_i(x_K+\Delta x) - |\dot{\delta}_i(x_K+\Delta x)| \left\{(\alpha+1)\frac{F_i(x_K)+K_3}{F_o} - \alpha\frac{\delta_i(x_K+\Delta x)}{\delta_o}\right\}^n\right]$$

where

$$\dot{\delta}_i(y) = \dot{\delta}_i(t) + \ddot{\delta}_i(t)\,y + \frac{\Delta\ddot{\delta}_i}{\Delta x}\frac{y^2}{2}$$

$$\delta_i(y) = \delta_i(t) + \dot{\delta}_i(t)\,y + \ddot{\delta}_i(t)\frac{y^2}{2} + \frac{\Delta\ddot{\delta}_i}{\Delta x}\frac{y^3}{6}.$$

then

$$F_i(x_{K+1}) = F_i(x_K) + \frac{1}{6}(K_1 + 2K_2 + 2K_3 + K_4).$$

Algorithm for Integration of the Equations of Motion

The process of numerical integration of the equations of motion (4.2.1) can now be summarized in the following algorithm.

A. INITIAL CALCULATIONS

DATA: Integration parameters, β, γ.

Time steps, Δt and Δx.

Convergence tolerance parameter, TOL.

Structural property matrices, $\mathbf{K}^E$, $\mathbf{M}$ and $\mathbf{C}$.

Parameters of hysteretic model for nonlinear elements, F_o, δ_o, α, and n.

STEP 1: Compute the constants

$$\alpha_1 = \frac{1}{\beta(\Delta t)^2} \qquad \alpha_2 = \frac{1}{\beta \Delta t} \qquad \alpha_3 = \frac{1}{2\beta}$$
$$\alpha_4 = \frac{\gamma}{\beta \Delta t} \qquad \alpha_5 = \frac{\gamma}{\beta} \qquad \alpha_6 = \Delta t\left[\frac{\gamma}{2\beta} - 1\right]$$

STEP 2: Initialize the state of motion, i.e. specify U_0, $\dot{\mathrm{U}}_0$, and $\ddot{\mathrm{U}}_0$.

STEP 3: Partition the stiffness matrix as explained in Equation (4.3.7), triangularize $\mathbf{K}_{EE}$ and form $\mathbf{Q}$.

B. FOR EACH TIME STEP

STEP 4: Form $\mathbf{K}_t^*$ and $\mathbf{R}_t^*$

$$\mathbf{K}_t^* = \alpha_1 \mathbf{M} + \alpha_4 \mathbf{C} + \mathbf{K}_t$$

$$\mathbf{R}_t^* = \mathbf{P}_t^* + \mathbf{M}\,[\alpha_2 \dot{\mathbf{U}}_t + \alpha_3 \ddot{\mathbf{U}}_t] + \mathbf{C}\,[\alpha_5 \dot{\mathbf{U}}_t + \alpha_6 \ddot{\mathbf{U}}_t]$$

where $\mathbf{P}_t^* = \mathbf{P}_\tau - [\mathbf{M}\ddot{\mathbf{U}}_t + \mathbf{C}\dot{\mathbf{U}}_t + \mathbf{F}_t]$

$$\mathbf{P}_\tau = -\mathbf{M}\,\mathbf{r}\,\ddot{U}_g(\tau).$$

STEP 5: Solve

$$\mathbf{K}_t^*\,\Delta \mathbf{U}_t = \mathbf{R}_t^*$$

for $\Delta \mathbf{U}_t$, using the algorithm given previously.

STEP 6: Update the state of motion at $\tau = t + \Delta t$

$$\ddot{\mathbf{U}}_\tau = \ddot{\mathbf{U}}_t + \alpha_1 \Delta \mathbf{U}_t - \alpha_2 \dot{\mathbf{U}}_t - \alpha_3 \ddot{\mathbf{U}}_t$$

$$\dot{\mathbf{U}}_\tau = \dot{\mathbf{U}}_t + \alpha_4 \Delta \mathbf{U}_t - \alpha_5 \dot{\mathbf{U}}_t - \alpha_6 \ddot{\mathbf{U}}_t$$
$$\mathbf{U}_\tau = \mathbf{U}_t + \Delta \mathbf{U}_t.$$

STEP 7: Compute the internal resisting forces, $\mathbf{F}_\tau$, in equilibrium with the current state, as explained previously.

STEP 8: Compute the unbalanced force at time τ

$$\hat{\mathbf{f}} = \mathbf{P}_\tau - [\mathbf{M}\ddot{\mathbf{U}}_\tau + \mathbf{C}\ddot{\mathbf{U}}_\tau + \mathbf{F}_\tau].$$

STEP 9: Compute $||\hat{\mathbf{f}}||_2$, the Euclidean norm of $\hat{\mathbf{f}}$. If $||\hat{\mathbf{f}}||_2 \leqq TOL$, no iteration is needed in this step. Go to Step 4 for the next step calculations, else proceed to Step 10.

C. ITERATION WITHIN A TIME STEP

STEP 10: Compute $\mathbf{K}_\tau^* = \alpha_1 \mathbf{M} + \alpha_4 \mathbf{C} + \mathbf{K}_\tau$.

STEP 11: Solve $\mathbf{K}_\tau^* \delta \mathbf{U}_\tau = \hat{\mathbf{f}}$ for $\delta \mathbf{U}_\tau$.

STEP 12: Update the state of motion

new $\ddot{\mathbf{U}}_\tau = \ddot{\mathbf{U}}_\tau + \alpha_1 \delta \mathbf{U}_\tau$

new $\dot{\mathbf{U}}_\tau = \dot{\mathbf{U}}_\tau + \alpha_4 \delta \mathbf{U}_\tau$

new $\mathbf{U}_\tau = \mathbf{U}_\tau + \delta \mathbf{U}_\tau$.

STEP 13: Compute the unbalance as in Step 8. See if convergence criterion of Step 9 is satisfied. If yes, go to Step 4 for next time step. Else go to Step 10.

4.4 Sensitivity Analysis

The method of feasible directions for optimization requires gradients of the constraint functions, which in turn require gradients of the response quantities with respect to the system parameters. The computation of these gradients, so-called sensitivity analysis, is intrinsically important because the information produced can be used directly for design trade-off studies.

One way of computing such sensitivity matrices is to integrate numerically the sensitivity equations obtained by differentiating the system equations of motion with respect to the system parameters [14,15]. In the present case, because of the complicated nature of the hysteretic model for the nonlinear elements, the analytical expressions for sensitivity equations are very complex. Numerical integration of these equations with the same time step as that used for the system equations poses additional difficulties. Because of these difficulties, a straight-forward approach using finite difference approximations is used. Partial derivatives are approximated by expressions of the type

$$\frac{\partial f(b)}{\partial b} \approx \frac{f(b+\Delta b) - f(b)}{\Delta b}$$

where

$f(\cdot)$ is any response function and

b is an element of the parameter vector.

Some errors are introduced by the above approximation, but by proper selection of the step size they can be controlled. Moreover, since these gradients are used only in the direction finding subproblem of the feasible directions method (Section 5), the optimal solution is relatively insensitive to these errors.

5. A METHOD OF FEASIBLE DIRECTIONS FOR PROBLEMS WITH FUNCTIONAL INEQUALITY CONSTRAINTS

This section presents an algorithm of the feasible direction type for the solution of nonlinear programming problems with functional inequality constraints (or time-dependent constraints). The basic algorithm is due to Gonzaga, Polak, and Trahan [16]. A short description of the algorithm is followed by details of actual implementation of the basic algorithm for the earthquake-resistant frame design problem. No convergence proof is given; readers interested in mathematical details and the convergence proof are referred to [16].

5.1 Definitions and Preliminaries

The nonlinear programming problem with functional inequality constraints is defined as

$$\min_{\mathbf{z}} \ f^{0}(\mathbf{z})$$

subject to

$$\begin{aligned} \max_{t\in T} \ \varphi^{j}(\mathbf{z},t) &\leqq 0 \ , \ j\in J_m \\ g^{j}(\mathbf{z}) &\leqq 0 \ , j\in J_l \end{aligned} \tag{5.1.1}$$

where

$\mathrm{T} = [t_0, t_f]$, specified time interval;

$J_l = \{1,2,\ldots,\mathrm{L}\}$;

$J_m = \{1,2,\ldots,\mathrm{M}\}$;

L = total number of conventional inequality constraints;

M = total number of functional inequality constraints;

$\mathbf{z}\in\mathbb{R}^{P}$ = the vector of optimization variables ;

P = total number of optimization variables;

$f^0 : \mathbb{R}^P \to \mathbb{R}$ and $g^j : \mathbb{R}^P \to \mathbb{R}, j \in J_l$ are continuously differentiable functions in **z**.

$\varphi^j : \mathbb{R}^P \times \mathbb{R} \to \mathbb{R}$, $j \in J_m$ are continuously differentiable functions in **z** and continuous in t.

The feasible domain, F, is defined by:

$$F = \left\{ \mathbf{z} \in \mathbb{R}^P \mid \max_{t \in T} \varphi^j(\mathbf{z}, t) \leq 0 , j \in J_m \ ; \ g^j(\mathbf{z}) \leq 0 , j \in J_l \right\}.$$

The interval T is discretized into q+1 points and is denoted by T_q .

Define:

$$\bar{\psi}_q(\mathbf{z}) = \max\left\{ \varphi^j(\mathbf{z}, t) , j \in J_m , t \in T_q \ ; \ g^j(\mathbf{z}) , j \in J_l \right\}$$

$$\psi_q(\mathbf{z}) = \max\{0 , \bar{\psi}_q(\mathbf{z})\} \tag{5.1.2}$$

Note that, if $\mathbf{z} \in F$, then $\psi_q(\mathbf{z}) = 0$.

The set of points at which a functional constraint is active is denoted by $\overline{T}^j_{q,\varepsilon}(\mathbf{z})$ and is defined as:

$$\overline{T}^j_{q,\varepsilon}(\mathbf{z}) = \left\{ t \in T_q \mid \varphi^j(\mathbf{z}, t) - \psi_q(\mathbf{z}) \geqq -\varepsilon \right\} , j \in J_m .$$

Next, define the intervals $I^j_{q,\varepsilon,k}(\mathbf{z}) \subset \overline{T}^j_{q,\varepsilon}(\mathbf{z})$ $k = 1,2,\ldots,k^j_{q,\varepsilon}(\mathbf{z})$, $j \in J_m$ recursively, as follows.

To define the first interval, $I^j_{q,\varepsilon,1}(\mathbf{z})$, let t_1 be the smallest number in $\overline{T}^j_{q,\varepsilon}(\mathbf{z})$ and let n_1 be the largest integer such that $(t_1 + n_1 \Delta t) \in \overline{T}^j_{q,\varepsilon}(\mathbf{z})$, but $\left[t_1 + (n_1+1)\Delta t \right] \not\subset \overline{T}^j_{q,\varepsilon}(\mathbf{z})$, where $\Delta t = (t_f - t_0)/q$.

Then

$$I^j_{q,\varepsilon,1}(\mathbf{z}) = \left\{ t_1, \ t_1+\Delta t, \ t_1+2\Delta t, \ \cdots \ , \ t_1+n_1\Delta t \right\}.$$

Next suppose that $I^j_{q,\varepsilon,k}(\mathbf{z})$ have been defined for k = 1,2,..., k_1 , then $I^j_{q,\varepsilon,(k_1+1)}(\mathbf{z})$ is defined as follows:

Let $t_{k_1+1} \in \overline{T}^j_{q,\varepsilon}(\mathbf{z})$ be the smallest number such that $t_{k_1+1} \not\in \bigcup_{k=1}^{k_1} I^j_{q,\varepsilon,k}(\mathbf{z})$ and let n_{k_1+1} be the smallest integer such that

$$\left[t_{k_1+1} + n_{k_1+1}\Delta t\right] \in \overline{T}^j_{q,\varepsilon}(\mathbf{z})$$

but

$$\left[t_{k_1+1} + (n_{k_1+1}+1)\,\Delta t\right] \not\in \overline{T}^j_{q,\varepsilon}(\mathbf{z}) .$$

Then

$$I^j_{q,\varepsilon,(k_1+1)}(\mathbf{z}) = \left\{t_{k_1+1} \,,\, t_{k_1+1}+\Delta t \,,\, t_{k_1+1}+2\Delta t \,,\, \cdots \,, t_{k_1+1}+n_{k_1+1}\Delta t\right\}.$$

For convenience, define

$$K^j_{q,\varepsilon}(\mathbf{z}) = \left\{1,2, \ldots , k^j_{q,\varepsilon}(\mathbf{z})\right\}.$$

Note that

$$\overline{T}^j_{q,\varepsilon}(\mathbf{z}) = \bigcup_{k \in K^j_{q,\varepsilon}(\mathbf{z})} I^j_{q,\varepsilon,k}(\mathbf{z}) .$$

The point at which a functional constraint is maximum in each of the above defined intervals is defined as:

$$t^j_{q,\varepsilon,k}(\mathbf{z}) = \left\{t^* \in I^j_{q,\varepsilon,k}(\mathbf{z}) \mid \varphi^j(\mathbf{z},t^*) \geqq \varphi^j(\mathbf{z},t) \,,\, t \in I^j_{q,\varepsilon,k}(\mathbf{z})\right\} \;\; k \in K^j_{q,\varepsilon}(\mathbf{z}).$$

The set of points at which a functional constraint is a local maximum is defined as:

$$T^j_{q,\varepsilon}(\mathbf{z}) = \bigcup_{k \in K^j_{q,\varepsilon}(\mathbf{z})} t^j_{q,\varepsilon,k}(\mathbf{z}) . \tag{5.1.3}$$

Now, the " ε - active constraint index " set for the functional constraints is defined as follows:

$$J^{\varphi}_{\varepsilon,q}(\mathbf{z}) = \left\{(j \,,\, t) \mid j \in J_m \,,\, t \in T^j_{q,\varepsilon}(\mathbf{z})\right\}. \tag{5.1.4}$$

The ε - active constraint index set for conventional inequality constraints is defined by:

$$J^g_{\varepsilon,q}(\mathbf{z}) = \left\{ j \mid g^j(\mathbf{z}) - \psi_q(\mathbf{z}) \geq -\varepsilon \, , \, j \in J_l \right\} . \tag{5.1.2}$$

The optimality function $\vartheta_{\varepsilon,q}(\mathbf{z}) : \mathbb{R}^P \to \mathbb{R}$ for the nonlinear programming problem (5.1.1) is defined as follows:

$$\vartheta_{\varepsilon,q}(\mathbf{z}) = \min_{\mathbf{h} \in \mathbb{R}^P} \left[\frac{1}{2} \| \mathbf{h} \|_2^2 + \max \left\{ <\nabla f^o(\mathbf{z}), \mathbf{h}> - \gamma \psi_q(\mathbf{z}) \, ; \right. \right.$$
$$<\nabla g^j(\mathbf{z}), \mathbf{h}> \, , \, j \in J^g_{\varepsilon,q}(\mathbf{z}) \, ;$$
$$\left. \left. <\nabla_z \varphi^j(\mathbf{z},t), \mathbf{h}> \, , \, (j,t) \in J^\varphi_{\varepsilon,q}(\mathbf{z}) \right\} \right] . \tag{5.1.6}$$

The dual form of (5.1.6), which is actually used in the following algorithm, is as follows:

$$\vartheta_{\varepsilon,q}(\mathbf{z}) = \max_{\mu \geq 0} \left[-\frac{1}{2} \Big\| \sum_{j \in J^g_{\varepsilon,q}(\mathbf{z})} \mu^j_g \nabla g^j(\mathbf{z}) + \sum_{(j,t) \in J^\varphi_{\varepsilon,q}(\mathbf{z})} \mu^{j,t}_\varphi \nabla_z \varphi^j(\mathbf{z},t) + \right.$$
$$\left. \mu^o \nabla f^o(\mathbf{z}) \Big\|_2^2 - \gamma \mu^o \psi_q(\mathbf{z}) \;\Big|\; \sum_{j \in J^g_{\varepsilon,q}(\mathbf{z})} \mu^j_g + \sum_{(j,t) \in J^\varphi_{\varepsilon,q}(\mathbf{z})} \mu^{j,t}_\varphi + \mu^o = 1 \right] \tag{5.1.7}$$

and

$$-\mathbf{h}_{\varepsilon,q}(\mathbf{z}) = \sum_{j \in J^g_{\varepsilon,q}(\mathbf{z})} \mu^j_g \nabla g^j(\mathbf{z}) + \sum_{(j,t) \in J^\varphi_{\varepsilon,q}(\mathbf{z})} \mu^{j,t}_\varphi \nabla_z \varphi^j(\mathbf{z},t) + \mu^o \nabla f^o(\mathbf{z}) . \tag{5.1.8}$$

where

$\nabla f(\mathbf{x})$ denotes the gradient of function $f : \mathbb{R}^P \to \mathbb{R}$ at $\mathbf{x}$. The gradient vector is treated as a column vector.

$<.,.>$ denotes the scalar product in $\mathbb{R}^P$ and is defined by $<\mathbf{x} \, , \, \mathbf{y}> = \sum_{i=1}^{P} x_i y_i$.

$\| . \|_2$ denotes the Euclidean norm in $\mathbb{R}^P$ and is defined by $\| \mathbf{x} \|_2 = \sqrt{<\mathbf{x} \, , \, \mathbf{x}>}$.

Theorem [16]

If $\mathbf{z}$ is optimal for nonlinear programming problem (5.1.1), then the function $\vartheta_{0,q}(\mathbf{z})$ given by Equation (5.1.7) is equal to zero.

5.2 A Feasible Directions Algorithm

A feasible directions algorithm for the solution of the nonlinear programming problem (5.1.1) can now be presented.

Algorithm

DATA: $\alpha \in (0,1)$, $\beta \in (0,1)$, $\gamma \geqq 1$

$\delta \in (0,1]$, $\varepsilon_0 > 0$

$\mu_1 > 0$, $\mu_2 > 0$, $M > 0$

q_0 , $q_{\max} \geqq q_0$, $\mathbf{z}_0 \in \mathbb{R}^P$.

STEP 0: Set i = 0 , q = q_0.

STEP 1: Set $\varepsilon = \varepsilon_0$.

STEP 2: Compute $\left[\vartheta_{\varepsilon,q}(\mathbf{z}^i)\ ,\ \mathbf{h}_{\varepsilon,q}(\mathbf{z}^i)\right]$ by solving (5.1.7) and (5.1.8).

STEP 3: If $\vartheta_{\varepsilon,q}(\mathbf{z}^i) \leqq -2\varepsilon\delta$, go to step 6; Else set $\varepsilon = \varepsilon/2$ and go to step 4.

STEP 4: If $\varepsilon < \varepsilon_0 \dfrac{\mu_1}{q}$ and $\psi_q(\mathbf{z}^i) < \dfrac{\mu_2}{q}$, set q = 2q and go to step 5; Else go to step 2.

STEP 5: If $q > q_{\max}$, STOP; Else, go to step 1.

STEP 6: Compute the largest step size $\lambda(\mathbf{z}^i) = \beta^{k(\mathbf{z}^i)} \in (0, M^*]$, where $M^* = \max\left\{1, \dfrac{M}{\|\mathbf{h}_{\varepsilon,q}(\mathbf{z}^i)\|_\infty}\right\}$ and $k(\mathbf{z}^i)$ is an integer, such that

(i) if $\mathbf{z}^i \in F^C$ (the complement of F in $\mathbb{R}^P$)

$$\psi_q\left[\mathbf{z}^i + \lambda(\mathbf{z}^i)\mathbf{h}_{\varepsilon,q}(\mathbf{z}^i)\right] - \psi_q(\mathbf{z}^i) \leqq -\alpha\lambda(\mathbf{z}^i)\delta\varepsilon,$$

(ii) if $\mathbf{z}^i \in F$

$$f^0\left[\mathbf{z}^i + \lambda(\mathbf{z}^i)\mathbf{h}_{\varepsilon,q}(\mathbf{z}^i)\right] - f^0(\mathbf{z}^i) \leq -\alpha\lambda(\mathbf{z}^i)\delta\varepsilon$$
$$g^j\left[\mathbf{z}^i + \lambda(\mathbf{z}^i)\mathbf{h}_{\varepsilon,q}(\mathbf{z}^i)\right] \leqq 0 \quad j \in J_l$$
$$\varphi^j\left[\mathbf{z}^i + \lambda(\mathbf{z}^i)\mathbf{h}_{\varepsilon,q}(\mathbf{z}^i), t\right] \leqq 0\ ,\ j \in J_m\ ,\ t \in T_q .$$

STEP 7: Set $\mathbf{z}^{i+1} = \mathbf{z}^i + \lambda(\mathbf{z}^i)\mathbf{h}_{\varepsilon,q}(\mathbf{z}^i)$. Set i = i+1 and go to Step 2.

Remark

The algorithm as presented above does not require an initial feasible point. If $\mathbf{z}_0 \not\in F$, then $\psi_q(\mathbf{z}_0)$ is non-zero and the algorithm constructs a sequence of points which forces the point into the feasible domain. This aspect of the algorithm is very advantageous in the case of complicated problems where the choice of an initial feasible point is not obvious. For example, in earthquake-resistant design if the relative drift of a particular story in a framed structure is to be limited to a certain value, it is not easy to find an initial design that will satisfy that requirement. Of course, the algorithm is more efficient if one can start from an initial feasible point.

5.3 Explanation of the Algorithm

The algorithm has two distinct phases. First, a direction is computed by solving (5.1.7) and (5.1.8). A step is then taken in this direction in such a way that, if the current $\mathbf{z}$ is in the feasible domain, there is a maximum reduction in the objective function while still maintaining feasibility. When the current point is outside the feasible domain, the step length is chosen so as to move as close to the feasible domain as possible.

Direction Finding Subproblem

As noted, a feasible direction is found by solving the problem:

$$\vartheta_{\varepsilon,q}(\mathbf{z}) = \max_{\mu \geqq 0}\left[-\frac{1}{2}\left|\left| \sum_{j \in J^g_{\varepsilon,q}(\mathbf{z})} \mu_g^j \nabla g^j(\mathbf{z}) + \sum_{(j,t) \in J^\varphi_{\varepsilon,q}(\mathbf{z})} \mu_\varphi^{j,t} \nabla_z \varphi^j(\mathbf{z},t) + \right.\right.\right.$$

$$\mu^o \nabla f^o(\mathbf{z}) \,||_2^2 - \gamma \mu^o \psi_q(\mathbf{z}) \;\Big|\; \sum_{j \in J^g_{\varepsilon,q}(\mathbf{z})} \mu^j_g + \sum_{(j,t) \in J^\varphi_{\varepsilon,q}(\mathbf{z})} \mu^{j,t}_\varphi + \mu^o = 1 \Bigg] \quad (5.3.1)$$

and then computing the direction from

$$-\mathbf{h}_{\varepsilon,q}(\mathbf{z}) = \sum_{j \in J^g_{\varepsilon,q}(\mathbf{z})} \mu^j_g \nabla g^j(\mathbf{z}) + \sum_{(j,t) \in J^\varphi_{\varepsilon,q}(\mathbf{z})} \mu^{j,t}_\varphi \nabla_z \varphi^j(\mathbf{z},t) + \mu^o \nabla f^o(\mathbf{z}) \,. \quad (5.3.2)$$

Equation (5.3.1) can be transcribed into a standard quadratic programming problem as follows. Let k_g be the total number of points in $J^g_{\varepsilon,q}(\mathbf{z})$ and (j_φ, l_φ) be the total number of points in $J^\varphi_{\varepsilon,q}(\mathbf{z})$. Define the vector $\mu \in \mathbb{R}^{1+k_g+j_\varphi l_\varphi}$ as follows:

$$\mu^T = \left[\mu^o, \mu_g^{k_1}, \mu_g^{k_2}, \ldots, \mu_g^{k_g}, \mu_\varphi^{j_1, l_1}, \ldots, \mu_\varphi^{j_\varphi, l_\varphi}\right]. \quad (5.3.3)$$

where

$k_i \in J^g_{\varepsilon,q}(\mathbf{z})$ for $i = 1, \ldots, k_g$

$(j_i, l_j) \in J^\varphi_{\varepsilon,q}(\mathbf{z})$ for $i = 1, \ldots, j_\varphi$ $j = 1, \ldots, l_\varphi$

Define the matrix $\mathbf{A} \in \mathbb{R}^{1+k_g+j_\varphi l_\varphi} \times \mathbb{R}^P$ as:

$$\mathbf{A} = \begin{bmatrix} \left[\nabla f^o(\mathbf{z})\right]^T \\ \left[\nabla g^{k_1}(\mathbf{z})\right]^T \\ \vdots \\ \left[\nabla g^{k_g}(\mathbf{z})\right]^T \\ \left[\nabla_z \varphi^{j_1}(\mathbf{z}, t^{j_1}_{q,\varepsilon,l_1})\right]^T \\ \vdots \\ \left[\nabla_z \varphi^{j_\varphi}(\mathbf{z}, t^{j_\varphi}_{q,\varepsilon,l_\varphi})\right]^T \end{bmatrix}. \quad (5.3.4)$$

Then Equation (5.3.1) can be written as:

$$\max_{\mu \ge 0} \left[-\frac{1}{2} (\mu^T \mathbf{A}) \, (\mu^T \mathbf{A})^T - \gamma \mu^o \psi_q(\mathbf{z}) \;\Big|\; \sum_{j=0}^{1+k_g+j_\varphi l_\varphi} \mu^j = 1 \right]$$

or

$$\min_{\mu \ge 0} \left[\frac{1}{2} \mu^T \, \mathbf{A} \, \mathbf{A}^T \, \mu \; + \; \gamma \, \mu^o \, \psi_q(\mathbf{z}) \;\Big|\; \sum_{j=0}^{1+k_g+j_\varphi l_\varphi} \mu^j = 1 \right]. \quad (5.3.5)$$

Define a vector $\mathbf{D} \in \mathbb{R}^{1+k_g+j_\varphi l_\varphi}$ such that

$$\mathbf{D}^T = \left[\gamma\psi_g(\mathbf{z}) \; , \; 0 \; , \; 0 \; , \cdots\right] \tag{5.3.6}$$

and a matrix $\mathbf{Q} \in \mathbb{R}^{1+k_g+j_\varphi l_\varphi} \times \mathbb{R}^{1+k_g+j_\varphi l_\varphi}$ by

$$\mathbf{Q} = \mathbf{A}\,\mathbf{A}^T \,. \tag{5.3.7}$$

Then Equation (5.3.5) can be written as:

$$\min_{\mu \geq 0} \left[\frac{1}{2} \, \mu^T \, \mathbf{Q} \, \mu \; + \; \mathbf{D}^T \, \mu \; \middle| \; \sum_{j=1}^{1+k_g+j_\varphi l_\varphi} \mu^j = 1 \right] \tag{5.3.8}$$

which is a standard quadratic programming problem. Once μ 's are obtained by solving (5.3.8), the direction is computed from

$$-\mathbf{h}_{\varepsilon,q}(\mathbf{z})^T = \mu^T \, \mathbf{A} \,. \tag{5.3.9}$$

Step Length Computation

After a feasible direction is obtained, the next step is to compute the step length in that direction. If the current design is inside the feasible design, the step length should be chosen in such a way that there is a maximum reduction in the objective function, while still maintaining feasibility. When the current design is outside the feasible domain, the objective is to take a step such that the new design is as close to the feasible domain as possible. The step size calculations begin by minimizing the objective function along the feasible direction and then checking whether any of the constraints is violated. If any of the constraints is violated, the step length is reduced and the process repeated until the new design satisfies all of the constraints. A number of methods are available for this unidirectional search, the most popular among them being Fibonacci search, Newton's method, quadratic or cubic fit, etc. [6,17]. For general non-convex problems, these methods tend to be very expensive. Since computation of the exact minimum along the feasible direction is not absolutely necessary, an approximate line search technique, known as the Armijo step size rule, is often used [6,18]. The method performs only an approximate line search and is quite efficient for general non-convex problems. The method is as follows.

Given the constants α, δ, ε, β, M, current design vector $\mathbf{z}^i$, $\mathbf{h}_{\varepsilon,q}(\mathbf{z}^i)$ and $\psi_q(\mathbf{z}^i)$, compute the largest step size $\lambda(\mathbf{z}^i) = \beta^{k(\mathbf{z}^i)} \in (0, M^*]$ where $M^* = \max\left\{1 \, , \, \frac{M}{||\mathbf{h}_{\varepsilon,q}(\mathbf{z}^i)||_\infty}\right\}$,

such that

(i) if $\psi_q(\mathbf{z}^i) > 0$ (i.e. $\mathbf{z}^i \notin F$), then

$$\psi_q\left[\mathbf{z}^i + \lambda(\mathbf{z}^i)\mathbf{h}_{\varepsilon,q}(\mathbf{z}^i)\right] - \psi_q(\mathbf{z}^i) \leqq -\alpha\lambda(\mathbf{z}^i)\delta\varepsilon;$$

(ii) if $\psi_q(\mathbf{z}^i) = 0$, i.e. $\mathbf{z}^i \in F$, then

$$f^o\left[\mathbf{z}^i + \lambda(\mathbf{z}^i)\mathbf{h}_{\varepsilon,q}(\mathbf{z}^i)\right] - f^o(\mathbf{z}^i) \leqq -\alpha\lambda(\mathbf{z}^i)\delta\varepsilon \, ,$$

$$g^j\left[\mathbf{z}^i + \lambda(\mathbf{z}^i)\mathbf{h}_{\varepsilon,q}(\mathbf{z}^i)\right] \leqq 0 \quad j \in J_l \, ,$$

$$\varphi^j\left[\mathbf{z}^i + \lambda(\mathbf{z}^i)\mathbf{h}_{\varepsilon,q}(\mathbf{z}^i) \, , \, t\right] \leqq 0 \quad j \in J_m \, , \, t \in T_q \, .$$

The algorithm to implement the above process is as follows.

STEP 1: Set $\lambda = \beta$. Compute $M^* = \max\left\{1, \frac{M}{||\mathbf{h}_{\varepsilon,q}(\mathbf{z}^i)||_\infty}\right\}$. Set FLAG = 0. Set n = 0.

STEP 2: Compute $\mathbf{z}_n^{i+1} = \mathbf{z}^i + \lambda\mathbf{h}_{\varepsilon,q}(\mathbf{z}^i)$.

STEP 3: If $\psi_q(\mathbf{z}^i) > 0$, go to step 5. Else , go to step 4.

STEP 4: Compute $f^o(\mathbf{z}_n^{i+1})$. If $f^o(\mathbf{z}_n^{i+1}) + \alpha\lambda\delta\varepsilon \leqq -f^o(\mathbf{z}^i)$, go to step 6. Otherwise, go to step 8.

STEP 5: If $\psi_q(\mathbf{z}_n^{i+1}) + \alpha\lambda\delta\varepsilon \leqq \psi_q(\mathbf{z}^i)$, go to step 7. Otherwise, go to step 8.

STEP 6: Compute $g^j(\mathbf{z}_n^{i+1}), j \in J_l$ and $\varphi^j(\mathbf{z}_n^{i+1}, t), j \in J_m\ t \in T_q$. If $g^j(\mathbf{z}_n^{i+1}) \leqq 0, j \in J_l$ and $\varphi^j(\mathbf{z}_n^{i+1}, t) \leqq 0\ j \in J_m, t \in T_q$, go to step 7. Otherwise, go to step 8.

STEP 7: If $\lambda / \beta > M^*$ or FLAG = -1, go to step 9. Otherwise, set $\lambda = \lambda / \beta$, FLAG = 1, n = n + 1 and go to step 2.

STEP 8: Set $\lambda = \lambda \beta$. If FLAG = 1, got to step 9. Otherwise, set FLAG = -1, n = n + 1 and go to step 2.

STEP 9: Set $\lambda = \lambda^*$ and the new design vector is $\mathbf{z}^{i+1} = \mathbf{z}^i + \lambda^* \mathbf{h}_{\varepsilon,q}(\mathbf{z}^i)$.

5.4 Computational Considerations

The quadratic programming problem as formulated in Equation (5.3.8) may be computationally ill-posed because of different magnitudes of the gradients of different functions. Proper scaling is therefore essential to make the problem computationally efficient. In the present version the following scaling was used. Define

$$\begin{aligned} s_g^j &= \| \nabla g^j(\mathbf{z}) \|_\infty, \ j \in J_{\varepsilon,q}^g(\mathbf{z}) ; \\ s_\varphi^{j,t} &= \| \nabla_z \varphi^j(\mathbf{z},t) \|_\infty, \ (j,t) \in J_{\varepsilon,q}^\varphi(\mathbf{z}) ; \\ s_o &= \| \nabla f^o(\mathbf{z}) \|_\infty . \end{aligned} \tag{5.4.1}$$

where

$\| \,.\, \|_\infty$ is the maximum norm in $\mathbb{R}^P$ defined by

$$\| \mathbf{x} \|_\infty = \max_{i \in \mathbb{R}^P} |x_i| .$$

The matrix **A** defined in (5.3.4) is scaled as follows.

$$\mathbf{A} = \begin{bmatrix} \left[\nabla f^o(\mathbf{z})\right]^T / s^o \\ \left[\nabla g^{k_1}(\mathbf{z})\right]^T / s_g^{k_1} \\ \vdots \\ \left[\nabla_z \varphi^{j_1}(\mathbf{z}, t_{q,\varepsilon,l_1}^{j_1})\right]^T / s_\varphi^{j_1,l_1} \\ \vdots \end{bmatrix} \tag{5.4.2}$$

Define a vector $\mathbf{R} \in \mathbb{R}^{1+k_g+j_\varphi l_\varphi}$ as:

$$\mathbf{R} = \left[1/s_o, \xi^{k_1}, \xi^{k_2}, \ldots, \xi^{k_g}, \rho^{j_1,l_1}, \rho^{j_2,l_2}, \ldots, \rho^{j_\varphi,l_\varphi}\right]^T \tag{5.4.3}$$

where ξ^j , $j=1, \ldots, k_g$ and $\rho^{j,l}$, $j=1, \ldots, j_\varphi$ $l=1, \ldots, l_\varphi$ are called " push-off " factors and can be adjusted to force the direction vector toward or away from a constraint. If any of these factors is large as compared to the rest, then the constraint corresponding to that factor will dominate the direction finding problem. If the constraint functions are well scaled, all the push-off factors could be set equal to one in which case all the active constraints will get equal importance. For a general case the following scheme of choosing the push-off factors seems to work well.

$$\xi^j = 1 + \eta \left[1 + \frac{g^j(\mathbf{z}) - \psi_q(\mathbf{z})}{\varepsilon}\right]^2 \quad j=1, \ldots, k_g \tag{5.4.4}$$

$$\rho^{j,l} = 1 + \eta \left[1 + \frac{\varphi^j(\mathbf{z},t) - \psi_q(\mathbf{z})}{\varepsilon}\right]^2 \quad t \in T^j_{q,\varepsilon}(\mathbf{z}) \;\; j \in J_m \tag{5.4.5}$$

where η is an input parameter.

An arbitrary upper limit of fifty was set for these push-off factors in the present study to prevent any instability in the direction finding process.

With these definitions, the scaled version of the quadratic programming problem (5.3.8) can be written as:

$$\min_{\mu \geq 0} \left\{ \frac{1}{2} \mu^T \mathbf{Q} \mu + \mathbf{D}^T \mu \mid \mathbf{R}^T \mu = 1 \right\} \tag{5.4.6}$$

where $\mathbf{Q} = \mathbf{A}\mathbf{A}^T$ with $\mathbf{A}$ defined by (5.4.2) and

$$\mathbf{D}^T = \left[\gamma \psi_q(\mathbf{z})/s_o, 0, 0, \cdots\right].$$

The direction vector is still computed from Equation (5.4.9).

5.5 Evaluation of Constraint Funtions and their Gradients

As is clear from the previous sections, the feasible directions algorithm requires computation of constraint functions and gradients of "active" constraint functions at each iteration. The computation of conventional inequality constraints (functions 'g' in the previous section) and their gradients presents no great difficulty. The funtional constraints (functions ' φ ' in the previous section) , however, are very expensive to compute because they require the computation of the time history of response of the structure, which for a nonlinear system is not a trivial matter. The problem becomes even more complicated because the algorithm requires computation of the gradients of the functional constraints, which in turn require sensitivity analysis, i.e., computation of gradients of the response quantities with respect to design parameters, using the chain rule, to obtain differential equations for senstivity analysis [14,15]. Numerical integration of the sensitivity equations then gives the required gradients of the response quantities. For a nonlinear system of the type considered here the analytical form of the sensitivity equations becomes quite complicated, so that the direct finite difference scheme of computing these derivatives seems to be more appropriate. The finite difference scheme requires an additional p time history analyses, where p is the total number of design parameters. Thus, computation of functional constraints and their gradients requires p + 1 time history analyses of an "N" degree of freedom nonlinear system, clearly a major computational task. Therefore, any reduction in the number of times that these calculations are executed will significantly reduce the total computational cost.

In the actual implementation of the algorithm for the type problem under consideration a number of things can be done to reduce the computational cost. The most obvious is to make the integration of response equations as efficient as possible. This is done by exploiting the localized nonlinear nature of the problem, using sub-structuring techniques. An efficient Newmark's method with optional Newton-Raphson iteration is used to carry out numerical integration of the equations of motion. Provision is made in the program to do the structural and/or sensitivity analysis only if the design parameters are changed "appreciably". Thus, if at a particular iteration, design parameters are changed very little, so that the maximum difference between the new and old design parameters is less than a certain prescribed value, the program does not compute the new time history analysis; instead, it uses the previous values.

A closer look at the algorithm shows that, when none of the functional constraints is active, gradients of the response quantities are not needed. In the program, therefore, constraint functions are first computed and then checked to determine if any of the constraints is active. If none of the constraints is active, the sensitivity analysis part is skipped, resulting in a significant saving in computation. Another source of considerable savings is the observation that gradients of response quantities are required only at those times included in the ε - active constraint set defined in the previous section. In earthquake problems, structural response typically builds up slowly and then dies down, whence the ε - active times are for the most part much smaller than the total duration of the response time history. Therefore, when performing sensitivity analysis, it is not necessary to compute the response time history beyond the maximum time included in the ε - active set. This feature has been incorporated into the program.

6. APPLICATIONS

The general techniques described in the previous sections are applied to a three-story steel test frame supported on an earthquake isolation system consisting of rubber bearings and a mild steel energy-absorbing device. The same frame was used as an example in reference [19] but with only one level of performance constraint. This section describes the formulation of a mathematical model for the test structure and presents numerical results for two design problems.

6.1 Steel Test Frame with an Earthquake Isolation System

A half-scale model of a three-story steel-framed structure with an isolation system consisting of rubber bearings and energy-absorbing devices was tested on the earthquake simulator at the University of California. This section gives a brief description of the test frame and the isolation system used. Further details of design and fabrication are given in references [20-24].

Steel Test Frame

The test structure consisted of two identical, three-story, single-bay steel frames interconnected by floor diaphragm systems which were essentially rigid in their planes, as shown in Figure 4. The model weighed 39.5 kips, was 20 ft. high and 12 ft. by 6 ft. in plan. The columns and beams were W5 x 12 and W6 x 12 rolled sections, respectively, and were welded together by typical moment-resistant connections. A heavy W10 x 49 girder was used at the base to ensure that the rubber bearings would have little tendency to undergo bending deformations. Concrete blocks weighing 8 kips were added to each floor to simulate the dead weight of the building. The model was supported on rubber bearings and energy-absorbing devices were attached to the base floor through a horizontal link.

Natural Rubber Bearings

A typical natural rubber bearing used in the test is shown in Figure 5. Each layer of a multi-layer bearing was hand-fabricated from sheets of rubber vulcanization bonded to aluminum foil. The aluminum foil was in turn bonded to the mild steel interleaves using adhesive tape over two-thirds of the surface area and epoxy resin, for greater shear strength, over the remaining one-third area.

The vertical stiffness characteristics of the rubber bearings are shown in Figure 6. After an initial soft cycle, the bearings showed little hysteresis. The vertical stiffness under the working load is of the order of 150 kips/in.

Horizontal stiffness characteristics are shown in Figure 7. The initial tangent stiffness at zero deflection is 320 lb./in., reducing to about 250 lb/in. at 2.5 in. deflection. The hysteresis loops represent approximately 10% critical damping.

Torsional Energy-Absorbing Devices

A typical energy-absorbing device is shown in Figure 8. The key element in the device is the mild steel torsion bar of rectangular cross section to which four clamps are welded. The outer clamping arms are used to attach the device to structural and foundation elements, with the inner arms linked to the active structural element. When this element is displaced, it pushes the inner arms introducing torsion in the mild steel bar.

In this steel frame test, devices were attached to the base floor in such a way that they applied a horizontal force to the model structure. The devices were tested under sinusoidal and random loadings to establish their capability of withstanding many cycles of large plastic deformation without appreciable deterioration in their energy absorption capacity. Under small excitations, the devices are elastic and the system behaves as a rigid foundation system, while under strong excitations the devices yield and produce large hysteresis loops, thus absorbing a considerable amount of energy.

6.2 Equations of Motion for the Test Frame

The test frame geometry is shown in Figure 9. Masses are assumed to be lumped at the floor levels and rotary inertia is neglected. If the axial deformations in beams and columns are neglected, the frame has 12 degrees of freedom as shown in Figure 10.

The equations of motion for the frame can be written as:

$$\overline{\mathbf{M}}\,\ddot{\overline{\mathbf{u}}}(t) + \overline{\mathbf{C}}\,\dot{\overline{\mathbf{u}}}(t) + \overline{\mathbf{K}}^E\,\overline{\mathbf{u}}(t) + \overline{\mathbf{F}}(t) = -\overline{\mathbf{M}}\,\overline{\mathbf{r}}\,\ddot{u}_g(t) \qquad (6.2.1)$$

where

$\overline{u}$, $\dot{\overline{u}}$, $\ddot{\overline{u}}$ = displacement, velocity and acceleration vectors of the 12 degrees of freedom;

$\overline{\mathbf{M}}$ = 12 x 12 diagonal mass matrix, whose diagonal elements are [0.02438 0.02438 0.02514 0.02832 0 ... 0];

$\overline{\mathbf{C}}$ = 12 x 12 damping matrix;

$\overline{\mathbf{K}}^E$ = 12 x 12 stiffness matrix of the frame including the rubber bearings but not the energy-absorbing device. This matrix is given in Table 1;

$\overline{\mathbf{F}}$ = force in the energy-absorbing device. The only nonzero entry in this vector corresponds to the degree of freedom at which the energy-absorbing device is connected. In this case, only F_4 will be nonzero;

$\overline{\mathbf{r}}^T$ = [1 1 1 1 0 0 ... 0];

$\ddot{u}_g(t)$ = ground acceleration time history.

In order to eliminate rotational degrees of freedom from the system, the matrices $\overline{\mathbf{M}}$, $\overline{\mathbf{C}}$, and $\overline{\mathbf{K}}^E$ are partitioned corresponding to the rotational and translational degrees of freedom. The system of equations than has the form

$$\begin{bmatrix}\mathbf{M} & 0\\ 0 & 0\end{bmatrix}\begin{Bmatrix}\ddot{\mathbf{u}}\\ \ddot{\mathbf{u}}_\vartheta\end{Bmatrix} + \begin{bmatrix}\mathbf{C} & 0\\ 0 & 0\end{bmatrix}\begin{Bmatrix}\dot{\mathbf{u}}\\ \dot{\mathbf{u}}_\vartheta\end{Bmatrix} + \begin{bmatrix}\mathbf{K}^E_{tt} & \left[\mathbf{K}^E_{\vartheta t}\right]^T\\ \mathbf{K}^E_{\vartheta t} & \mathbf{K}^E_{\vartheta\vartheta}\end{bmatrix}\begin{Bmatrix}\mathbf{u}\\ \mathbf{u}_\vartheta\end{Bmatrix} + \begin{Bmatrix}\mathbf{F}\\ 0\end{Bmatrix} = -\begin{bmatrix}\mathbf{M} & 0\\ 0 & 0\end{bmatrix}\begin{Bmatrix}\mathbf{e}\\ 0\end{Bmatrix}\ddot{u}_g(t) \tag{6.2.2}$$

where

$$\begin{aligned}\mathbf{u} &= [u_1, u_2, u_3, u_4]^T\\ \mathbf{u}_\vartheta &= [u_5, \cdots, u_{12}]^T\\ \mathbf{e} &= [1,1,1,1]^T.\end{aligned}$$

The second sub-matrix equation gives:

$$\mathbf{u}_\vartheta = -[\mathbf{K}^E_{\vartheta\vartheta}]^{-1}\,\mathbf{K}^E_{\vartheta t}\,\mathbf{u}. \tag{6.2.3}$$

The first sub-matrix equation gives:

$$\mathbf{M}\,\ddot{\mathbf{u}} + \mathbf{C}\dot{\mathbf{u}} + \mathbf{K}^E_{tt}\,\mathbf{u} + [\mathbf{K}^E_{\vartheta t}]^T\mathbf{u}_\vartheta + \mathbf{F} = -\mathbf{M}\mathbf{e}\ddot{u}_g(t); \tag{6.2.4}$$

Substituting for $\mathbf{u}_\vartheta$ from Equation (6.2.3) into Equation (6.2.4) yields

$$\mathbf{M}\ddot{\mathbf{u}}(t) + \mathbf{C}\dot{\mathbf{u}}(t) + \mathbf{K}^E\,\mathbf{u}(t) + \mathbf{F} = -\mathbf{M}\mathbf{e}\ddot{u}_g(t) \tag{6.2.5}$$

where

$$\mathbf{K}^E = \mathbf{K}^E_{tt} - [\mathbf{K}^E_{\vartheta t}]^T[\mathbf{K}^E_{\vartheta\vartheta}]^{-1}\,\mathbf{K}_{\vartheta t}. \tag{6.2.6}$$

The 4 x 4 condensed stiffness matrix for the frame can be evaluated by carrying out the matrix operations in Equation (6.2.6), which gives (in kip-inch units):

$$\mathbf{K}^E = \begin{bmatrix} 46.38 & -66.64 & 23.04 & -2.78\\ & 144.40 & -96.50 & 18.74\\ & & 122.43 & -48.97\\ SYMMETRIC & & & 34.21\end{bmatrix}. \tag{6.2.7}$$

The mass matrix of the structure corresponding to the lateral degrees of freedom is, from Equation (6.2.1) (in kip-inch units):

$$\mathbf{M} = \begin{bmatrix}0.02438 & & & \\ & 0.02438 & & \\ & & 0.02514 & \\ & & & 0.02832\end{bmatrix}.$$

Rayleigh damping is assumed in constructing the damping matrix:

$$\mathbf{C} = \alpha\mathbf{M} + \beta\mathbf{K}^E.$$

The coefficients α and β are computed from:

$$\begin{bmatrix} \frac{1}{\omega_1} & \omega_1 \\ \frac{1}{\omega_2} & \omega_2 \end{bmatrix} \begin{Bmatrix} \alpha \\ \beta \end{Bmatrix} = \begin{Bmatrix} \xi_1 \\ \xi_2 \end{Bmatrix},$$

where ω_1 and ω_2 are first and second mode frequencies, and ξ_1 and ξ_2 are the respective critical damping ratios in these modes. The damping matrix for the present structures, assuming $\xi_1 = 3\%$ and $\xi_2 = 1\%$, is given below.

$$\mathbf{C} = \begin{bmatrix} 0.0279 & -0.0332 & 0.0115 & -0.0014 \\ & 0.0768 & -0.0481 & 0.0093 \\ & & 0.0660 & -0.0244 \\ SYMMETRIC & & & 0.0226 \end{bmatrix}.$$

The force in the energy absorber is computed from Equations (4.1.1) and (4.2.2):

$$\dot{F}_4(t) = K_0\left[\dot{u}_4(t) - |\dot{u}_4(t)| \left[\frac{F_4(t)}{F_0} - S\right]^n\right] \tag{6.2.8}$$

$$S(t) = \alpha\left[\frac{u_4(t)}{\delta_o} - \frac{F_4(t)}{F_0}\right].$$

where

$K_0 = F_0/\delta_0$;

F_0, δ_0, α and n *are device parameters.*

For linear analysis, the stiffness matrix for the complete structure is obtained by adding K_0 to K_{44}^E. Thus, the following **K** matrix is used in Equation (3.1.1).

$$\mathbf{K} = \begin{bmatrix} 46.38 & -66.64 & 23.04 & -2.78 \\ & 144.40 & -96.50 & 18.74 \\ SYMMETRIC & & 122.43 & -48.97 \\ & & & 34.21+K_0 \end{bmatrix}.$$

For nonlinear analysis, the tangent stiffness matrix $\mathbf{K}_t$ at any time is obtained by adding $\dfrac{\partial F_4(t)}{\partial u_4}$ to K_{44}^E as follows:

Equation (6.2.8) gives

$$\dot{F}_4(t) = K_0\dot{u}_4(t)\left[1 - sign\left[\frac{F_4(t)}{F_0} - S(t)\right]^n\right]$$

$$S(t) = \alpha\left[\frac{u_4(t)}{\delta_0} - \frac{F_4(t)}{F_0}\right]$$

where

$$\begin{aligned} sign &= 1 \text{ if } \dot{u}_4(t) > 0 \\ &= -1 \text{ if } \dot{u}_4(t) < 0. \end{aligned}$$

Thus,

$$\frac{\dot{F}_4(t)}{\dot{u}_4(t)} = K_0\left[1 - sign\left[\frac{F_4(t)}{F_0} - S(t)\right]^n\right]$$

or

$$\frac{\partial F_4(t)}{\partial u_4} = K_0\left[1 - sign\left[\frac{F_4(t)}{F_0} - S(t)\right]^n\right].$$

Thus, $\mathbf{K}_t$ for Equation (4.3.3) is:

$$\mathbf{K}_t(t) = \begin{bmatrix} 46.38 & -66.64 & 23.04 & -2.78 \\ SYMMETRIC & 144.40 & -96.50 & 18.74 \\ & & 122.43 & -48.97 \\ & & & 34.21+\dfrac{\partial F_4(t)}{\partial u_4} \end{bmatrix}.$$

6.3 Design Parameters

It is assumed here that the characteristics of the rubber bearings are fixed. Therefore, only the parameters of the energy-absorbing device will be adjusted to obtain the optimal design. The two basic variables in the design of energy absorbers are the elastic stiffness and the post-yield stiffness. These variables are controlled by the parameters F_0 , δ_0, and α in the hysteretic model of the energy absorbers. The elastic stiffness is approximately equal to F_0/δ_0 and the post-yield stiffness is approximately equal to $\frac{F_0}{\delta_0}\left(\frac{\alpha}{1+\alpha}\right)$. Thus, the design variables are F_0, δ_0, and α. Another parameter which may influence the design is the exponent "n" in the hysteretic model, but it is not considered as a variable in the present study.

6.4 Optimal Design Problems

The purpose of an earthquake isolation system is to minimize some measure of the response of the structure. There is a number of response quantities which could be minimized, e.g., the maximum acceleration in the structure, maximum base shear, maximum story shear, maximum interstory drift, etc. In order to get meaningful results, response constraints are also needed. Some of the constraints are dictated by the problem itself, e.g., the design parameters F_0, δ_0, and α are not allowed to attain negative values. Such constraints constitute conventional inequality constraints. Constraints on the response quantities are also needed; e.g., when accelerations in the frame are minimized, the displacement at the base must not be arbitrarily large. These restrictions give rise to functional inequality constraints. Thus, a number of design problems could be formulated depending upon the objective function and the type of constraints placed on the response. In what follows, two design problems of interest are considered.

6.4.1 Design Problem 1

In this problem, the base shear in the frame subjected to a large earthquake (El Centro span 750 test shaking table motion) is minimized while maintaining the bottom floor displacement within a prescribed limit under that earthquake. Since large deformations are not desirable under small earthquakes which occur frequently, an additional constraint to limit the bottom floor displacement due to a small earthquake is incorporated.

Mathematically, the problem can be expressed as:

$$\min_{\mathbf{z}} \max_{t \in T} \; [V_0^l(t)]^2$$

subject to

$$\begin{aligned} \max_{t \in T} [u_4^l(t)]^2 &\leq \delta \\ F_{\max}^S &\leq F_0 \\ F_0, \delta_0, \alpha &> 0 \end{aligned}$$

where

V_o^l = base shear from a large earthquake. The base shear is computed by first computing the story shears from

$$\mathbf{f}_s^l(t) = \mathbf{K}^E \mathbf{u}^l(t),$$

and then adding the story shears

$$V_o^l(t) = \mathbf{e}^T \mathbf{f}_s^l(t).$$

where

$$\mathbf{e}^T = [1,1,1,1],$$

$\mathbf{K}^E$ is given in Equation (6.2.7), $\mathbf{u}^l(t)$ is the displacement vector from a large earthquake;

$\mathbf{z}$ = $[z_1, z_2, z_3]^T = [F_0, \delta_0, \alpha]^T$ is the design parameter vector;

T = $[t_o, t_f]$, given time interval;

δ = prescribed limit on u_4 (specified as 4 inches in the example);

$F_{\max}^s$ = maximum force in the energy-absorbing device subjected to a small earthquake.

As explained in Section 2.2, the design problem can be transcribed into a mathematical programming problem, as follows.

The parameter vector $\mathbf{z}$ is augmented by a dummy cost parameter z_4 and the above problem is then equivalent to the problem:

$$\min_{\mathbf{z}} \; z_4$$

subject to

$$\begin{aligned} \max_t \; [V_o^l(\mathbf{z},t)]^2 &\leq z_4 \\ \max_t \; [u_4^l(\mathbf{z},t)]^2 &\leq \delta \\ (F_{\max}^s(\mathbf{z}))^2 &\leq (F_0)^2 \\ F_0, \delta_0, \alpha &> 0 \end{aligned}$$

In terms of the canonical form of nonlinear programming problem, Section 2.2, the above problem is expressed as:

$$\begin{aligned}
\varphi^1(\mathbf{z},t) &= \frac{1}{z_4}\,[V_0^l(\mathbf{z},t)]^2 - 1.0 \\
\varphi^2(\mathbf{z},t) &= \frac{1}{\delta}\,[u_4^l(\mathbf{z},t)]^2 - 1.0 \\
g^1(\mathbf{z}) &= \left[\frac{F_{\max}^S(\mathbf{z})}{z_1}\right]^2 - 1.0 \\
g^2(\mathbf{z}) &= -z_1 + 1.0E-5 \\
g^3(\mathbf{z}) &= -z_2 + 1.0E-10 \\
g^4(\mathbf{z}) &= -z_3 + 1.0E-10 \\
f^o(\mathbf{z}) &= z_4 \\
z &= [z_1, z_2, z_3, z_4] \\
&= [F_0, \delta_0, \alpha, z_4]
\end{aligned}$$

The gradients of objective and constraint functions are:

$$\nabla_z \varphi^1(\mathbf{z},t) = \frac{2}{z_4}\, V_o^l(\mathbf{z},t) \begin{bmatrix} \partial V_o^l(\mathbf{z},t)/\partial z_1 \\ \partial V_o^l(\mathbf{z},t)/\partial z_2 \\ \partial V_o^l(\mathbf{z},t)/\partial z_3 \\ -\dfrac{1}{2z_4}\, V_o^l(\mathbf{z},t) \end{bmatrix}$$

Since

$$V_o^l(\mathbf{z},t) = \mathbf{e}^T f_S^l(\mathbf{z},t) = \mathbf{e}^T\, \mathbf{K}^E\, \mathbf{u}^l(\mathbf{z},t).$$

Therefore,

$$\frac{\partial V_0^l(\mathbf{z},t)}{\partial z_j} = \mathbf{e}^T\, \mathbf{K}^E \begin{bmatrix} \partial u_1^l(\mathbf{z},t)/\partial z_j \\ \partial u_2^l(\mathbf{z},t)/\partial z_j \\ \partial u_3^l(\mathbf{z},t)/\partial z_j \\ \partial u_4^l(\mathbf{z},t)/\partial z_j \end{bmatrix} \quad j=1,2,3.$$

$$\nabla_z \varphi^2(\mathbf{z},t) = \frac{2}{\delta}\, u_4^l(\mathbf{z},t) \begin{bmatrix} \partial u_4^l(\mathbf{z},t)/\partial z_1 \\ \partial u_4^l(\mathbf{z},t)/\partial z_2 \\ \partial u_4^l(\mathbf{z},t)/\partial z_3 \\ 0 \end{bmatrix}$$

$$\nabla g^1(\mathbf{z}) = \frac{2F_{\max}^s(\mathbf{z})}{(z_1)^2} \begin{bmatrix} \partial F_{\max}^s(\mathbf{z})/\partial z_1 - F_{\max}^s(\mathbf{z})/z_1 \\ \partial F_{\max}^s(\mathbf{z})/\partial z_2 \\ \partial F_{\max}^s(\mathbf{z})/\partial z_3 \\ 0 \end{bmatrix}$$

$$\begin{aligned}
\nabla g^2(\mathbf{z}) &= [-1,0,0,0]^T \\
\nabla g^3(\mathbf{z}) &= [0,-1,0,0]^T
\end{aligned}$$

$$\nabla g^4(\mathbf{z}) = [0,0,-1,0]^T$$
$$\nabla f^o(\mathbf{z}) = [0,0,0,1]^T$$

Numerical Results

A computer program based on the algorithms presented in Sections 3, 4, and 5 was used to solve the above design problem. El Centro span 750 ground motion, as used in the experimental investigation in reference [20], was used to represent a large earthquake. This ground motion is the same as the El Centro 1940 NS component with modified time scale and amplitude and is shown in Figure 10. For the small earthquake, a response spectrum approach is used, as indicated in Section 3. The response spectrum chosen corresponds to an earthquake with 50% probability of being exceeded, along with the assumption that the critical damping is 5%. The maximum absolute acceleration for the small earthquake was set at 0.15 g. δ , the upper limit on the bottom floor displacement, was set equal to four inches.

Initial values of the design parameters were obtained from experimental data on the energy-absorbing devices [20,22]. The following numerical values were used:

$$F_0 = 5.0 \qquad \delta_0 = 0.11 \qquad \alpha = 0.064 \qquad n = 1.$$

Initial value for the dummy cost parameter was $z_4 = 8.75$, which was an upper bound for the square of the maximum base shear for a large earthquake.

The optimal values obtained for these parameters were:

$$F_0 = 5.011661 \quad \delta_0 = 0.054741 \quad \alpha = 0.0102178$$
$$z_4 = 4.538479.$$

Figure 11 shows the decrease in the cost parameter, which is the same as the decrease in the square of maximum base shear, versus the number of design iterations. Story shears, bottom floor displacement and hysteresis loops for both optimal and initial parameters are plotted in Figures 12 - 17. The plots of the story shears show that the peaks are reduced in the large acceleration range. Since the optimal design is stiffer than the initial design, the stiffness being increased from 45.5 to 91.55, the displacements at the floor levels are reduced too.

6.4.2 Design Problem 2

It has been observed that the inter-story drift is one of the important parameters which controls damage to the structural and non-structural components. Since story shears are proportional to the inter-story drift, the objective function for this problem is chosen as the sum of squares of story shears due to a large earthquake. Constraints are placed on the bottom floor displacement due to both a large and a small earthquake and on the force in the energy-absorber when subjected to a small earthquake. Mathematically, the problem can be expressed as:

$$\min_{\mathbf{z}} \max_{t \in T} \left[\sum_{j=1}^{3} \left\{ K_j \left[u_j^l(\mathbf{z},t) - u_{j+1}^l(\mathbf{z},t) \right] \right\}^2 \right]$$

subject to

$$\begin{aligned} \max_{t \in T} [u_4^l(t)]^2 &\leq \delta^2 \\ \left[u_{4,\max}^s \right]^2 &\leq \delta_1^2 \\ \left[F_{\max}^s \right]^2 &\leq F_0^2 \\ F_0, \delta_0, \alpha &> 0 \end{aligned}$$

where

$u_j;\ j=1,4$ = story displacements (top down). Superscripts l and s refer to a large and a small earthquake respectively;

$K_j;\ j=1,4$ = story stiffnesses, (top down);

$F_{\max}^s$ = maximum force in the energy-absorbing device when subjected to a small earthquake;

$\mathbf{z} = [z_1, z_2, z_3]^T = [F_0, \delta_0, \alpha]^T$ is the design parameter vector;

$T = [t_o, t_f]$, given time interval;

δ = prescribed limit on u_4^l (taken as 4 inches in the example);

δ_1 = prescribed limit on u_4^s (taken as 0.25 inches).

The corresponding nonlinear programming problem can be written as:

$$\min_{\mathbf{z}} \; z_4$$

subject to

$$\max_{t \in T} \left[\sum_{j=1}^{3} \left\{ K_j \left[u_j^l(\mathbf{z},t) - u_{j+1}^l(\mathbf{z},t) \right] \right\}^2 \right] \leq z_4$$

$$\max_{t \in T} \; [u_4^l(\mathbf{z},t)]^2 \leq \delta^2$$

$$[u_{4,max}^s(\mathbf{z})]^2 \leq \delta_1^2$$

$$[F_{\max}^s(\mathbf{z})]^2 \leq F_0^2$$

$$F_0, \delta_0, \alpha > 0$$

In terms of the canonical form of nonlinear programming problem, Section 2.2, the above problem is expressed as:

$$\varphi^1(\mathbf{z},t) = \frac{1}{z_4} \left[\sum_{j=1}^{3} \left\{ K_j \left[u_j^l(\mathbf{z},t) - u_{j+1}^l(\mathbf{z},t) \right] \right\}^2 \right] - 1.0$$

$$\varphi^2(\mathbf{z},t) = \frac{1}{\delta^2} [u_4^l(\mathbf{z},t)]^2 - 1.0$$

$$g^1(\mathbf{z}) = \left[\frac{u_{4,max}^s(\mathbf{z})}{\delta^1} \right]^2 - 1.0$$

$$g^2(\mathbf{z}) = \left[\frac{F_{\max}^s(\mathbf{z})}{z_1} \right]^2 - 1.0$$

$$g^3(\mathbf{z}) = -z_1 + 1.0E-5$$

$$g^4(\mathbf{z}) = -z_2 + 1.0E-10$$

$$g^5(\mathbf{z}) = -z_3 + 1.0E-10$$

$$f^o(\mathbf{z}) = z_4$$

$$z = [z_1, z_2, z_3, z_4] = [F_0, \delta_0, \alpha, z_4]$$

The gradients of objective and constraint functions are:

$$\nabla_z \varphi^1(\mathbf{z},t) = \frac{2}{z_4} V_0 \begin{bmatrix} \partial u_j^l(\mathbf{z},t)/\partial z_1 - \partial u_{j+1}^l(\mathbf{z},t)/\partial z_1 \\ \partial u_j^l(\mathbf{z},t)/\partial z_2 - \partial u_{j+1}^l(\mathbf{z},t)/\partial z_2 \\ \partial u_j^l(\mathbf{z},t)/\partial z_3 - \partial u_{j+1}^l(\mathbf{z},t)/\partial z_3 \\ -\dfrac{1}{2z_4} V_0 \end{bmatrix}$$

where

$$V_0 = \sum_{j=1}^{3}\left\{K_j\left[u_j^l(\mathbf{z},t) - u_{j+1}^l(\mathbf{z},t)\right]\right\}$$

$$\nabla_z \varphi^2(\mathbf{z},t) = \frac{2}{\delta^2} u_4^l(\mathbf{z},t)\begin{bmatrix}\partial u_4^l(\mathbf{z},t)/\partial z_1\\ \partial u_4^l(\mathbf{z},t)/\partial z_2\\ \partial u_4^l(\mathbf{z},t)/\partial z_3\\ 0\end{bmatrix}$$

$$\nabla g^1(\mathbf{z}) = \frac{2u_{4,max}^s(\mathbf{z})}{\delta_1^2}\begin{bmatrix}\partial u_{4,max}^s(\mathbf{z})/\partial z_1\\ \partial u_{4,max}^s(\mathbf{z})/\partial z_2\\ \partial u_{4,max}^s(\mathbf{z})/\partial z_3\\ 0\end{bmatrix}$$

$$\nabla g^2(\mathbf{z}) = \frac{2F_{\max}^s(\mathbf{z})}{(z_1)^2}\begin{bmatrix}\partial F_{\max}^s(\mathbf{z})/\partial z_1 - F_{\max}^s(\mathbf{z})/z_1\\ \partial F_{\max}^s(\mathbf{z})/\partial z_2\\ \partial F_{\max}^s(\mathbf{z})/\partial z_3\\ 0\end{bmatrix}$$

$$\nabla g^3(\mathbf{z}) = [-1,0,0,0]^T$$

$$\nabla g^4(\mathbf{z}) = [0,-1,0,0]^T$$

$$\nabla g^5(\mathbf{z}) = [0,0,-1,0]^T$$

$$\nabla f^o(\mathbf{z}) = [0,0,0,1]^T$$

Numerical Results

Initial values of the design parameters for this problem were the same as those for the first problem. The dummy cost parameter was $z_4 = 30.0$, which was an upper bound on the sum of squares of story shears. The optimal values obtained for these parameters were:

$$F_0 = 4.337126 \quad \delta_0 = 0.25028 \quad \alpha = 0.0583057$$
$$z_4 = 16.89978.$$

Figure 18 shows the decrease in the cost parameter, which is the same as the decrease in the sum of square of story shears, versus the number of design iterations. Story shears, bottom floor displacement time history and hysteresis loops for both optimal and initial parameters are plotted in Figures 19 - 23. The optimal design is softer than the initial design; the stiffness being reduced from 45.5 to 17.33.

It is interesting to compare the results of this problem with the one solved in reference [19], which was essentially the same except that there were no constraints under small earthquake excitation. In that case the stiffness of the optimal energy absorber was 2.4, which is considerably lower than that obtained here. Thus, the present design shows that the previous design was not satisfactory since it will have excessive deformations under small excitations.

6.4.3 Discussion

As is evident from the solution of two design problems presented in sections 6.4.1 and 6.4.2, the optimal solution depends upon the objective function and the constraints imposed on the system. Two completely different solutions were obtained for the same physical problem by choosing different objective and constraint functions. In the first problem, the optimal design was stiffer than the initial one while in the second problem it was softer. Thus, there is no unique way of defining an optimal problem. Different objective and/or constraint functions should be tried and the results compared. The solution exhibiting best overall behavior should be chosen.

From the study of two design problems considered here, it seems that the solution given by the second problem is better since in this case the story shears are reduced considerably. Although the bottom floor displacements are larger in this case , they are still within the acceptable limits defined for the problem.

6.5 Sensitivity of the Optimal Design to Different Earthquake Ground Motions

As is clear from the preceding development, only one earthquake ground motion is used in the optimal design process. Since earthquakes are random in nature, it is unlikely that the same earthquake ground motion will be repeated at some future time. Therefore, it becomes necessary to see the effectiveness of the optimal design process for different earthquakes. To get meaningful results, these additional earthquakes should have characteristics similar to the one used in the design process. This requirement prohibits the use of actual past earthquake records, inasmuch as for a given site there is typically an insufficient number of past records. An alternative is the use of artificially generated earthquakes of the same class.

For the present study a family of five earthquakes having characteristics similar to the El Centro 1940 NS earthquake was generated using the computer program PSEQGN developed by P. Ruiz and J. Penzien [25] and later modified by M. Murakami [26]. The earthquake accelerograms were generated by passing nonstationary shot noise through two second-order linear filters and applying a base line correction. Each accelerogram was of thirty seconds duration with four seconds of parabolic built up, eleven seconds of constant intensity followed by fifteen seconds of exponential decay. The maximum acceleration in each record was about 0.30g.

The structure was analyzed twice, first with initial parameters and then with optimal parameters obtained from problem 2, subjected to these five earthquakes. Story shears and bottom floor displacements are compared for the initial and optimal parameters and are shown in Figures 24-33.

7. CONCLUDING REMARKS

The main objective of the current study was to formulate and solve a problem of design of earthquake-resistant structural systems with dual design criteria. The techniques were applied to the design of an earthquake isolation system for a three-story frame. The same frame was used as an example in reference [19] with constraints only on the nonlinear response. Comparison of the optimal solution obtained here with the one obtained in reference [19] clearly shows that the current strategy gives a much more practical design, since both the limit states could be explicitly satisfied. Although, numerical results obtained so far are encouraging, further research is needed with more practical design problems to establish the superiority of the designs obtained with the dual design criteria approach.

Since the earthquake ground motions are probabilistic in nature, the optimal design obtained using one ground motion may not be optimal for some other ground motion. Better methods for characterization of ground motion are urgently needed. It should be pointed out that the techniques presented here can be extended to obtain an optimal design with constraints on response under a number of earthquakes without any difficulty. The only drawback is the excessive amount of computer time used in this approach.

The limited numerical experience with the feasible directions algorithm used here indicates that the effectiveness of the algorithm depends, among other things, on a number of tolerance parameters. Some experience with these parameters is needed before arriving at the most suitable set of parameters for a particular problem. An interactive computer system, where the user can change these parameters during the optimization process, seems to be a more efficient way of handling this situation. Work on the interactive implementation of this algorithm is underway.

Another factor which apparently affects the computational efficiency of the algorithm is the number of design parameters. As the number of design parameters increases, the computational efficiency decreases. One way of decreasing the number of design parameters at a particular stage of design process is to use the so-called "multi-level optimization techniques" which break down the problem into a number of sub-problems. At the moment, it is not clear whether this approach will increase the overall computational efficiency, but more research is being done on this approach.

APPENDIX A - Derivatives of Eigenvalues and Eigenvectors

Computation of derivatives of eigenvalues and eigenvectors has been the subject of a number of recent publications. Current state-of-the-art is reviewed in reference [5]. The particular formulation used in the present study is summarized below for completeness.

The generalized eigenvalue problem is written as:

$$\mathbf{K(z)}\ \varphi_i(\mathbf{z}) = \lambda_i(\mathbf{z})\ \mathbf{M}\ \varphi_i(\mathbf{z}) \tag{A.1}$$

or

$$[\mathbf{K(z)} - \lambda_i(\mathbf{z})\mathbf{M}]\ \varphi_i(\mathbf{z}) = 0 \tag{A.2}$$

Derivatives of Eigenvalues

Premultiply (A.2) by $\varphi_i^T(\mathbf{z})$ and differentiate with respect to design parameter z_l;

$$\varphi_i^T(\mathbf{z})\left[\frac{\partial \mathbf{K(z)}}{\partial z_l} - \frac{\partial \lambda_i(\mathbf{z})}{\partial z_l}\mathbf{M}\right]\varphi_i(\mathbf{z}) = 0$$

or

$$\frac{\partial \lambda_i(\mathbf{z})}{\partial z_l}\ \varphi_i^T(\mathbf{z})\ \mathbf{M}\ \varphi_i(\mathbf{z}) = \varphi_i^T(\mathbf{z})\ \frac{\partial \mathbf{K(z)}}{\partial z_l}\ \varphi_i(\mathbf{z})$$

Therefore,

$$\frac{\partial \lambda_i(\mathbf{z})}{\partial z_l} = \frac{\varphi_i^T(\mathbf{z})\ \dfrac{\partial \mathbf{K(z)}}{\partial z_l}\ \varphi_i(\mathbf{z})}{M_i^*} \tag{A.3}$$

where

$$M_i^* = \varphi_i^T(\mathbf{z})\ \mathbf{M}\ \varphi_i(\mathbf{z})$$

(A.3) gives the required eigenvalue derivatives.

Derivatives of Eigenvectors

Differentiate (A.2) with respect to z_l;

$$\left[\mathbf{K(z)} - \lambda_i(\mathbf{z})\mathbf{M}\right]\frac{\partial \varphi_i(\mathbf{z})}{\partial z_l} + \left[\frac{\partial \mathbf{K(z)}}{\partial z_l} - \frac{\partial \lambda_i(\mathbf{z})}{\partial z_l}\mathbf{M}\right]\varphi_i(\mathbf{z}) = 0$$

Premultiply by $\varphi_j^T(\mathbf{z})\ j \neq i$ to get:

$$\left[\varphi_j^T(\mathbf{z})\ \mathbf{K}(\mathbf{z})\ -\ \lambda_i(\mathbf{z})\ \varphi_j^T(\mathbf{z})\ \mathbf{M}\right] \frac{\partial \varphi_i(\mathbf{z})}{\partial z_l}\ =\ -\ \varphi_j^T(\mathbf{z})\ \frac{\partial \mathbf{K}(\mathbf{z})}{\partial z_l}\ \varphi_i(\mathbf{z}) \qquad \text{(A.4)}$$

From (A.1):

$$\varphi_j^T(\mathbf{z})\ \mathbf{K}(\mathbf{z})\ =\ \lambda_j(\mathbf{z})\ \varphi_j^T(\mathbf{z})\ \mathbf{M}$$

Therefore, (A.4) gives:

$$\left[\lambda_j(\mathbf{z}) - \lambda_i(\mathbf{z})\right] \varphi_j^T(\mathbf{z})\ \mathbf{M}\ \frac{\partial \varphi_i(\mathbf{z})}{\partial z_l}\ =\ -\ \varphi_j^T(\mathbf{z})\ \frac{\partial \mathbf{K}(\mathbf{z})}{\partial z_l}\ \varphi_i(\mathbf{z})$$

or

$$\varphi_j^T(\mathbf{z})\ \mathbf{M}\ \frac{\partial \varphi_i(\mathbf{z})}{\partial z_l}\ =\ \frac{1}{\lambda_i(\mathbf{z}) - \lambda_j(\mathbf{z})}\ \varphi_j^T(\mathbf{z})\ \frac{\partial \mathbf{K}(\mathbf{z})}{\partial z_l}\ \varphi_i(\mathbf{z}) \qquad j \neq i \qquad \text{(A.5)}$$

Equation (A.5) represents (n-1) equations in n unknowns. To make the set complete an additional equation is needed. The orthogonality of mode shapes with respect to the mass matrix is used for this purpose.

$$\varphi_i^T(\mathbf{z})\ \mathbf{M}\ \varphi_i(\mathbf{z})\ =\ 1 \qquad \text{(A.6)}$$

Differentiation of (A.6) with respect to z_l gives

$$2\ \varphi_i^T(\mathbf{z})\ \mathbf{M}\ \frac{\partial \varphi_i(\mathbf{z})}{\partial z_l}\ =\ 0 \qquad \text{(A.7)}$$

Define a matrix $\mathbf{X} \in \mathbb{R}^N \times \mathbb{R}^N$ such that:

$$X_{ij}\ =\ \frac{1 - \delta_{ij}}{\lambda_i(\mathbf{z}) - \lambda_j(\mathbf{z})} \left[\varphi_j^T(\mathbf{z})\ \frac{\partial \mathbf{K}(\mathbf{z})}{\partial z_l}\ \varphi_i(\mathbf{z})\right] \qquad \text{(A.8)}$$

where

$$\delta_{ij}\ =\ \begin{cases} 0 & \text{if } i \neq j \\ 1 & \text{if } i = j \end{cases}$$

With the matrix $\mathbf{X}$ defined in (A.8), (A.5) and (A.7) can be combined as:

$$\Phi^T\ \mathbf{M}\ \frac{\partial \Phi(\mathbf{z})}{\partial z_l}\ =\ \mathbf{X}$$

or

$$\frac{\partial \Phi(\mathbf{z})}{\partial z_l}\ =\ \left[\Phi^T\ \mathbf{M}\right]^{-1} \mathbf{X} \qquad \text{(A.9)}$$

But from (A.6) $\left[\Phi^T \mathbf{M}\right]^{-1} = \Phi$. Therefore,

$$\frac{\partial \Phi(\mathbf{z})}{\partial z_l} = \Phi \, \mathbf{X} \qquad \text{(A.10)}$$

(A.10) gives the required derivatives of eigenvectors with respect to design parameter z_l .

APPENDIX B - Derivatives of Pseudo-Velocity Response Spectrum

In the sensitivity analysis of a linear system using the response spectrum approach, derivatives of the pseudo-velocity response spectrum with respect to the system eigenvalues are needed. This appendix derives the expressions for these derivatives.

The response spectrum shape is defined as follows:

$$S_{v,n}(\xi,\lambda_n) = \frac{D\,a}{\sqrt{\lambda_n}} \tag{B.1}$$

where

$$a = \max_t |\ddot{u}_g(t)|$$

and D is defined for different time periods $T=2\pi/\omega$ as:

(i) For $T_A < T \leqq T_B$

$$D = D_A + (T-T_A)\,\frac{D_B - D_A}{T_B - T_A} \tag{B.2}$$

(ii) For $T_B < T \leqq T_C$

$$D = D_B + (T-T_B)\,\frac{D_C - D_B}{T_C - T_B} \tag{B.3}$$

(iii) For $T > T_C$

$$D = b\,T^{-\vartheta} \tag{B.4}$$

T_A , D_A etc. are defined in Figures 1 and 2.

Differentiating (B.1) with respect to λ_n , we get:

$$\frac{\partial S_{v,n}}{\partial \lambda_n} = \frac{\partial D}{\partial \lambda_n}\,\frac{a}{\sqrt{\lambda_n}} - \frac{D\,a}{2\,\lambda_n^{3/2}} \tag{B.5}$$

$\frac{\partial D}{\partial \lambda_n}$ is computed by differentiating (B.2), (B.3) and (B.4) as follows:

(i) For $T_A < T \leqq T_B$

$$\frac{\partial D}{\partial \lambda_n} = -\frac{\pi}{\lambda_n^{3/2}}\,\frac{D_B - D_A}{T_B - T_A} \tag{B.6}$$

(ii) For $T_B < T \leqq T_C$

$$\frac{\partial D}{\partial \lambda_n} = - \frac{\pi}{\lambda_n^{3/2}} \frac{D_C - D_B}{T_C - T_B} \tag{B.7}$$

(iii) For $T > T_C$

$$\frac{\partial D}{\partial \lambda_n} = \frac{1}{2} \frac{b\ \vartheta}{(2\ \pi)^{\vartheta}} \lambda_n{}^{0.5\vartheta - 1} \tag{B.8}$$

REFERENCES

1. Bertero, V. V., "Identification of Research Needs for Improving Aseismic Design of Building Structures," *Report No. EERC 75-27*, Earthquake Engineering Research Center, University of California, Berkeley, September 1975.

2. Pierson, B. L., "A Survey of Optimal Structural Design Under Dynamic Constraints," *International Journal of Numerical Methods in Engineering*, Vol. 4, 491-499 (1972).

3. Rao, S. S., "Structural Optimization Under Shock and Vibration Environment," *The Shock and Vibration Digest*, Vol. 11, No. 2, February 1979.

4. Walker, N. D., "Automated Design of Earthquake-Resistant Multistory Steel Building Frames," *Report No. UCB/EERC 77-12*, Earthquake Engineering Research Center, University of California, Berkeley, May 1977.

5. Ray, D., Pister, K. S. and Chopra, A. K., "Optimum Design of Earthquake-Resistant Shear Buildings," *Report No. EERC 74-3*, Earthquake Engineering Research Center, University of California, Berkeley, January 1974.

6. Polak, E., **Computational Methods in Optimization**, Academic Press, New York, 1971.

7. Polak, E. and Mayne, D. Q., "An Algorithm for Optimization Problems with Functional Inequality Constraints," *IEEE Transaction on Automatic Control*, Vol. AC-21, No. 2, April 1976.

8. Clough, R. W. and Penzien, J., **Dynamics of Structures,** McGraw-Hill, 1975.

9. Blume, J. A., Sharpe, R. L. and Dalal, J. S., "Recommendations for Shape of Earthquake Response Spectra," John A. Blume & Associates, Engineers, San Francisco, California, February 1973.

10. Matzen, V. C. and McNiven, H. D., "Investigation of the Inelastic Characteristics of a Single-Story Steel Structure Using System Identification and Shaking Table Experiments," *Report No. EERC 76- 20,* Earthquake Engineering Research Center, University of California, Berkeley, August 1976.

11. Ozdemir, H., "Nonlinear Transient Dynamic Analysis of Yielding Structures," *Ph.D. Dissertation,* Division of Structural Engineering and Structural Mechanics, Department of Civil Engineering, University of California, Berkeley, 1976.

12. Newmark, N. M., "A Method of Computation for Structural Dynamics," *Journal of the Engineering Mechanics Division,* ASCE, Vol. 85, No. EM3, 67-94 (1959).

13. Mondkar, D. P. and Powell, G. H., "Static and Dynamic Analysis of Nonlinear Structures," *Report No. EERC 75- 10,* Earthquake Engineering Research Center, University of California, Berkeley, March 1975.

14. Ray, D., "Sensitivity Analysis for Hysteretic Dynamic Systems: Application to Earthquake Engineering," *Report No. EERC 74- 5*, Earthquake Engineering Research Center, University of California, Berkeley, April 1974.

15. Ray, D., Pister, K. S. and Polak, E., "Sensitivity Analysis for Hysteretic Dynamic Systems: Theory and Applications," *Report No. EERC 76- 12*, Earthquake Engineering Research Center, University of California, Berkeley, February 1976.

16. Gonzaga, G., Polak, E. and Trahan, R., "An Improved Algorithm for Optimization Problems with Functional Inequality Constraints," *Memorandum No. UCB/ERL M78/56*, Electronics Research Laboratory, University of California, Berkeley, September 1977.

17. Luenberger, D. G., **Introduction to Linear and Nonlinear Programming,** Addison-Wesley, 1973.

18. Armijo, L., "Minimization of Functions Having Continuous Partial Derivatives," *Pacific Jr. Math. 16*, 1-3 (1966).

19. Bhatti, M. A., Pister, K. S. and Polak, E., "Optimal Design of an Earthquake Isolation System," *Report No. UCB/EERC- 78/22*, Earthquake Engineering Research Center, University of California, Berkeley, October 1978.

20. Kelly, J. M., Eidinger, J. M. and Derham, C. J., "A Practical Soft-Story Earthquake Isolation System," *Report No. UCB/EERC- 77/27*, Earthquake Engineering Research Center, University of California, Berkeley, November 1977.

21. Kelly, J. M. and Tsztoo, D. F., "Earthquake Simulation Testing of a Stepping Frame with Energy-Absorbing Devices," *Report No. UCB/EERC- 77/17*, Earthquake Engineering Research Center, University of California, Berkeley, August 1977.

22. Kelly, J. M. and Tsztoo, D. F., "The Development of Energy-Absorbing Devices for Aseismic Base Isolation System," *Report No. UCB/EERC- 78/01*, Earthquake Engineering Research Center, University of California, Berkeley, January 1978.

23. Eidinger, J. M. and Kelly, J. M., "Experimental Results of an Earthquake Isolation System Using Natural Rubber Bearings," *Report No. UCB/EERC-78/03*, Earthquake Engineering Research Center, University of California, Berkeley, February 1978.

24. Clough, R. W. and Tang, D. T., "Earthquake Simulator Study of a Steel Frame Structure, Vol. 1: Experimental Results," *Report No. EERC 75- 6*, Earthquake Engineering Research Center, University of California, Berkeley, April 1975.

25. Ruiz, P. and Penzien, J., "PSEQGN - Artificial Generation of Earthquake Accelerograms," A Computer Program Distributed by NISEE/Computer Applications, U. C. Berkeley, March 1969.

26. Murakami, M. and Penzien, J., "Nonlinear Response Spectra for Probablistic Seismic Design and Damage Assesment of Reinforced Concrete Structures," *Report No. EERC 75- 38,* Earthquake Engineering Research Center, U. C. Berkeley, November 1975.

TABLE 1

58.81	-58.81	0	0	-940.90	-940.90	-940.90	-940.90	0	0	0	0
	117.61	-58.81	0	940.90	940.90	0	0	-940.90	-940.90	0	0
		81.82	-23.01	0	0	940.90	940.90	437.53	437.53	-503.37	-503.37
			23.01	0	0	0	0	503.37	503.37	503.37	503.37
				57658.3	8756.67	20072.5	0	0	0	0	0
					57658.3	0	20072.5	0	0	0	0
						97803.3	8756.67	20072.5	0	0	0
	SYMMETRIC						97803.3	0	20072.5	0	0
								87021.5	8756.67	14681.6	0
									87021.5	0	14681.6
										253748.0	112192.0
											253748.0

[Units are kip-inches]

Stiffness Matrix of the Test Frame

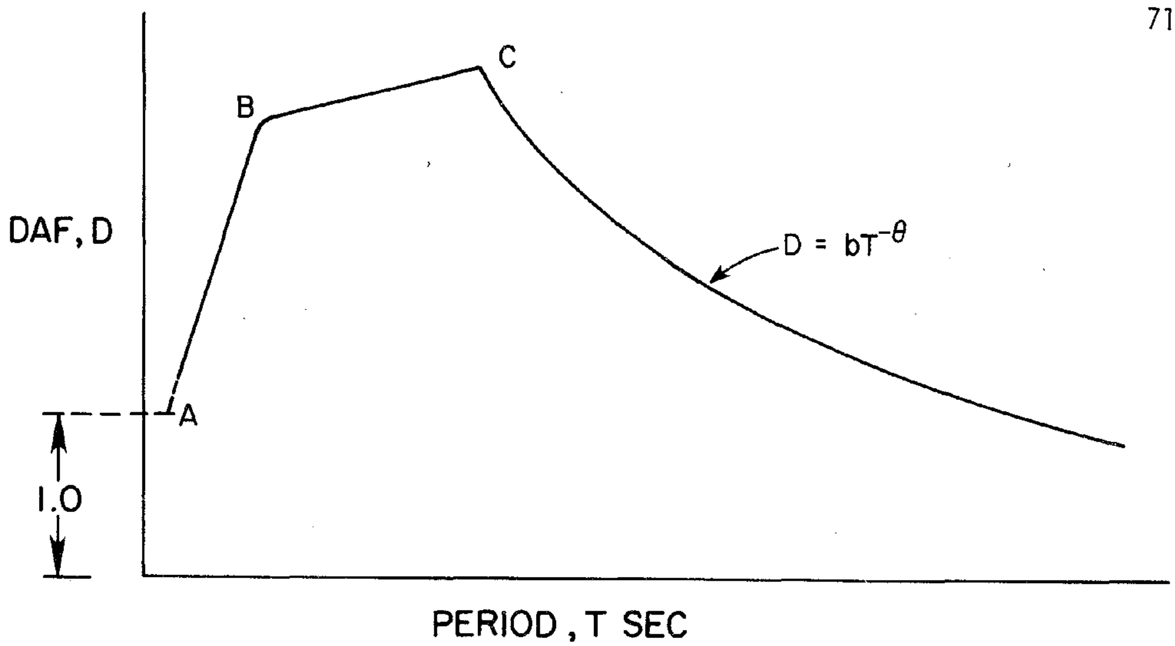

Probability of Being Exceeded	Damping Ratio	Point A		Point B		Point C		Curve	
		T	DAF	T	DAF	T	DAF	b	θ
Large (50%)	0.005	0.03	1.0	0.12	3.2	0.35	4.0	1.20	1.46
	0.01	0.032	1.0	0.12	3.8	0.35	3.5	1.08	1.16
	0.02	0.034	1.0	0.12	2.5	0.35	2.9	0.93	1.075
	0.05	0.036	1.0	0.12	2.0	0.35	2.3	0.76	1.053
	0.07	0.038	1.0	0.12	1.85	0.35	2.0	0.67	1.038
	0.10	0.040	1.0	0.12	1.7	0.35	1.75	0.59	1.032
Small (15.8%)	0.005	0.028	1.0	0.11	5.1	0.35	6.2	2.34	0.928
	0.01	0.029	1.0	0.11	4.1	0.35	5.0	2.00	0.872
	0.02	0.030	1.0	0.11	3.5	0.35	4.2	1.73	0.843
	0.05	0.031	1.0	0.11	2.6	0.35	3.1	1.35	0.794
	0.07	0.032	1.0	0.11	2.2	0.35	2.6	1.13	0.790
	0.10	0.033	1.0	0.11	2.0	0.35	2.3	1.02	0.776
Negligible (2.3%)	0.005	0.025	1.0	0.09	8.1	0.35	9.6	4.32	0.761
	0.01	0.026	1.0	0.09	6.2	0.35	7.6	3.68	0.692
	0.02	0.027	1.0	0.09	4.8	0.35	5.9	3.12	0.604
	0.05	0.028	1.0	0.09	3.2	0.35	4.1	2.40	0.511
	0.07	0.029	1.0	0.09	2.6	0.35	3.4	2.03	0.489
	0.10	0.030	1.0	0.09	2.3	0.35	2.9	1.77	0.470

Figure 1 Recommended Design Response Spectrum Shapes

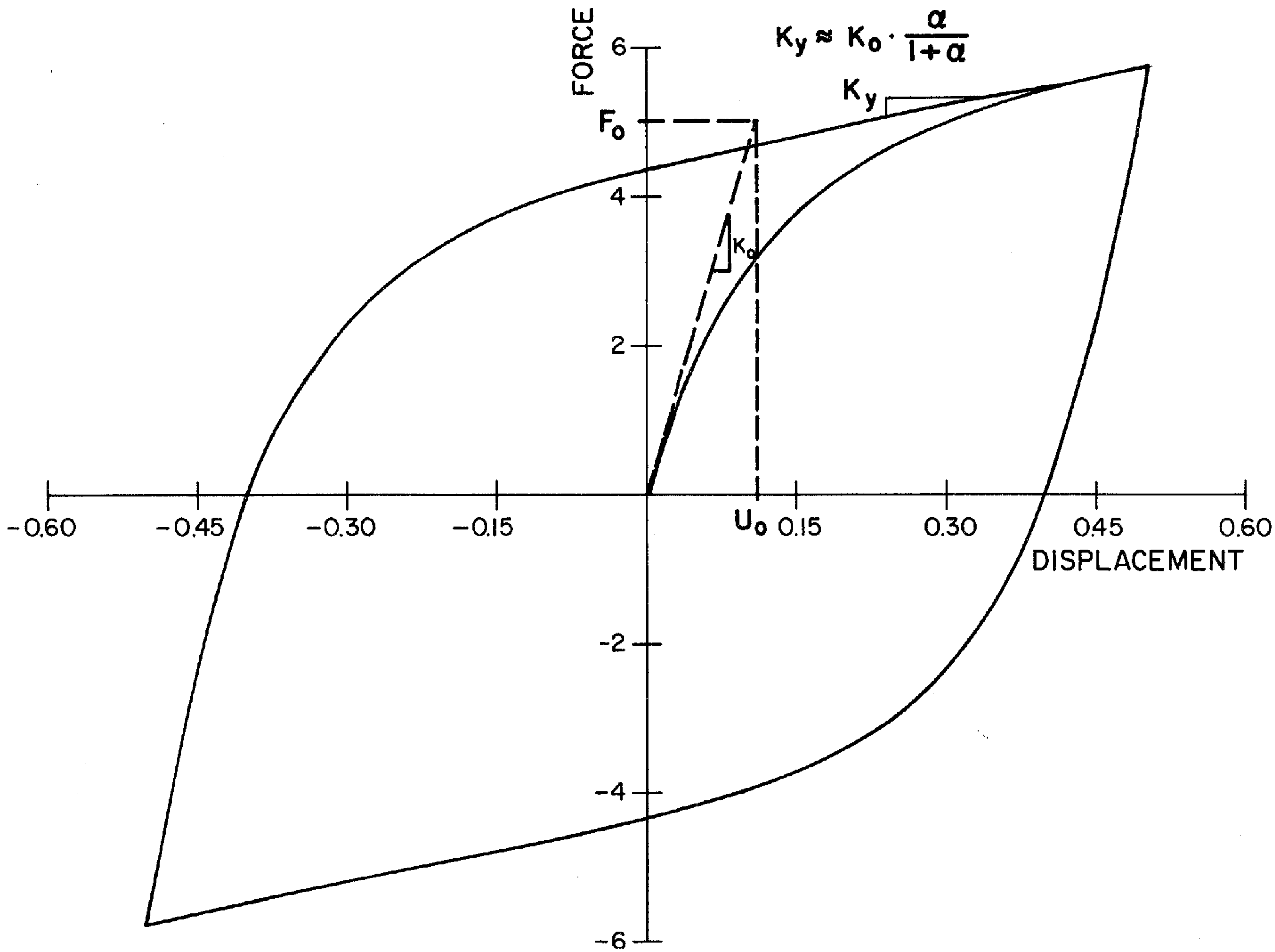

Figure 2 Hysteresis Loops Generated by Rate-Independent Hysteresis Model under Sinusoidal Excitation

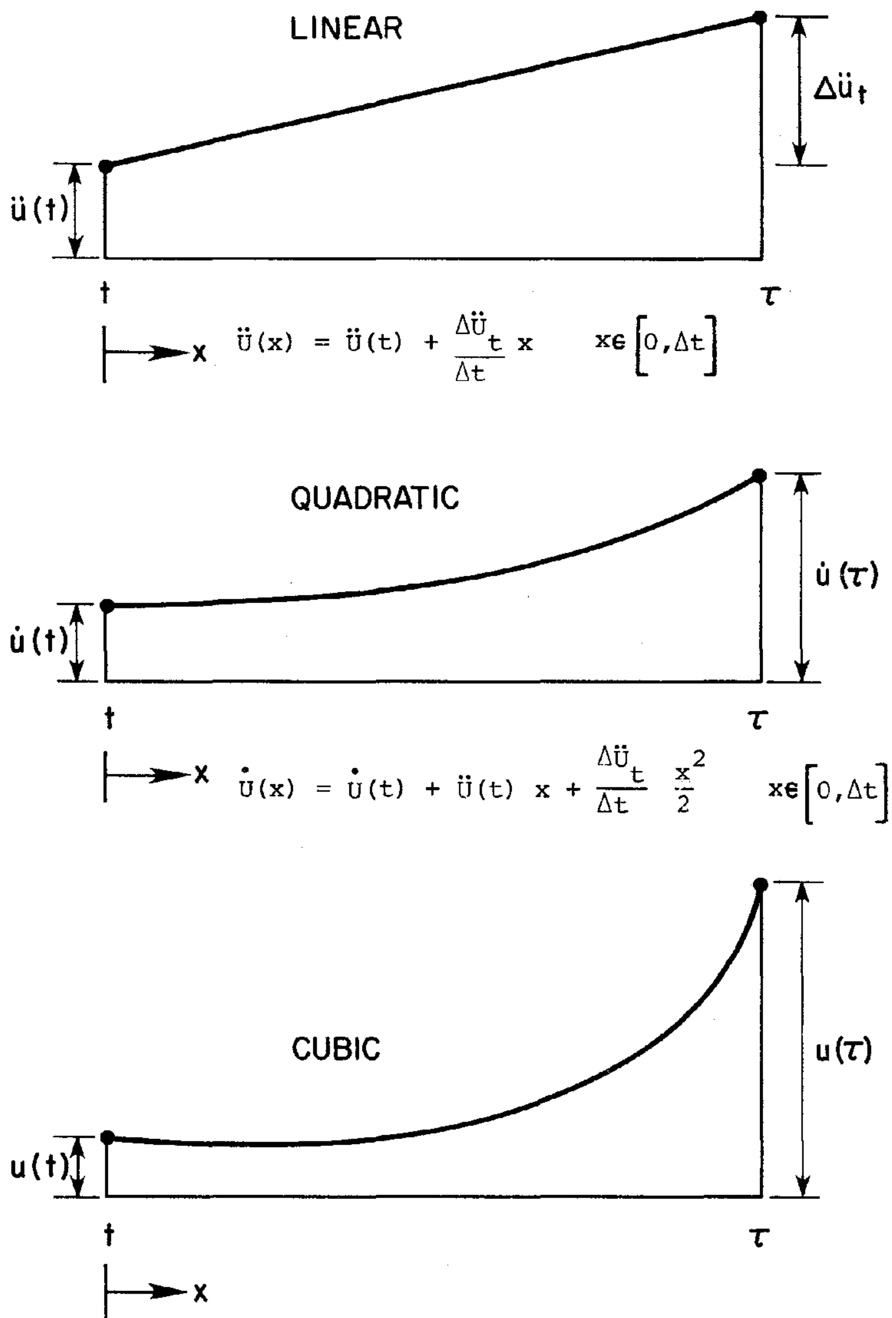

$$\ddot{U}(x) = \ddot{U}(t) + \frac{\Delta\ddot{U}_t}{\Delta t}\, x \qquad x \in \left[0, \Delta t\right]$$

$$\dot{U}(x) = \dot{U}(t) + \ddot{U}(t)\, x + \frac{\Delta\ddot{U}_t}{\Delta t}\,\frac{x^2}{2} \qquad x \in \left[0, \Delta t\right]$$

$$U(x) = U(t) + \dot{U}(t)x + \ddot{U}(t)\,\frac{x^2}{2} + \frac{\Delta\ddot{U}_t}{\Delta t}\,\frac{x^3}{6} \qquad x \in \left[0, \Delta t\right]$$

Figure 3 Variations in Acceleration, Velocity and Displacement During Time Interval $[t \,, \tau = t + \Delta t\,]$

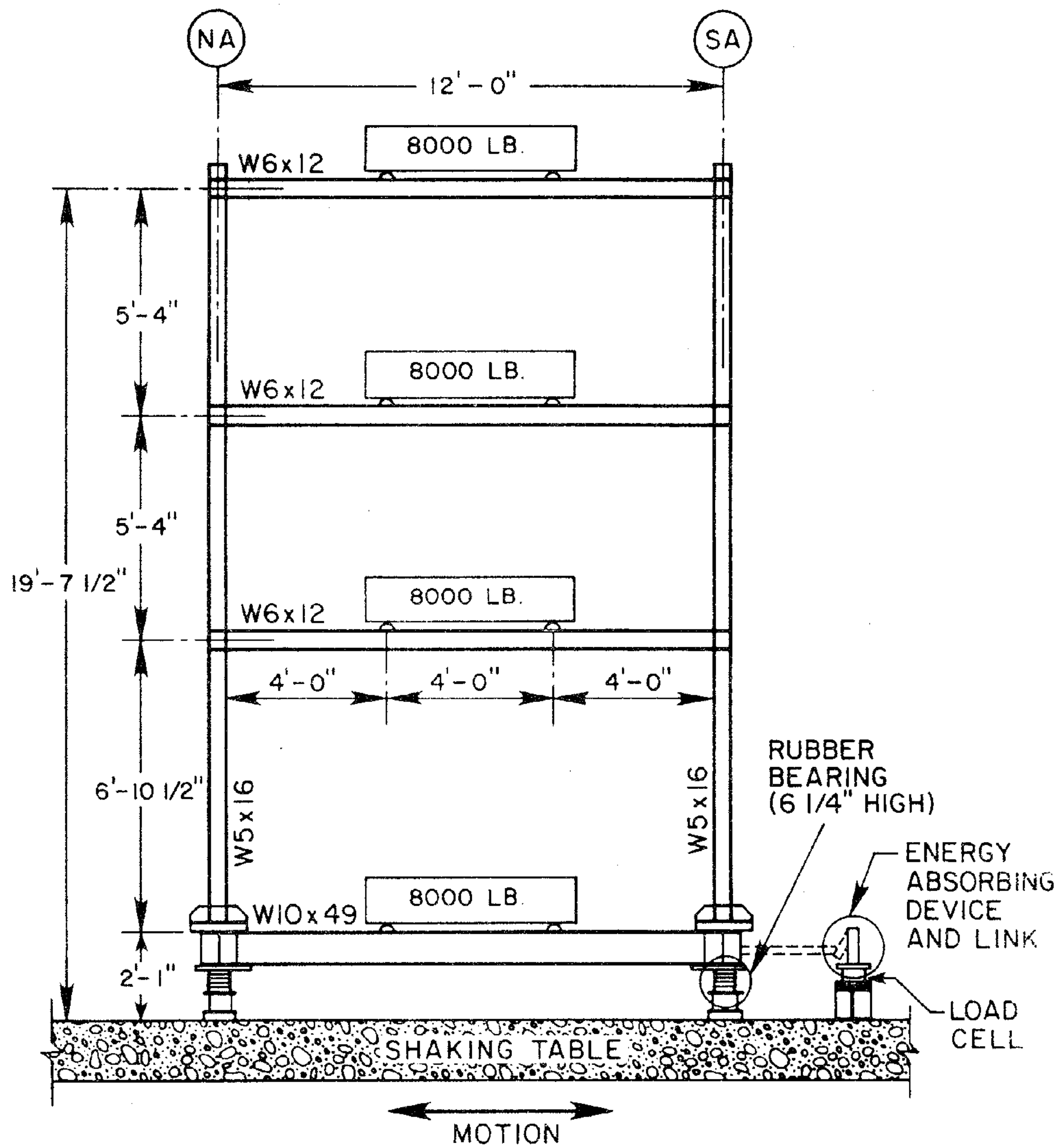

Figure 4 Test Structure

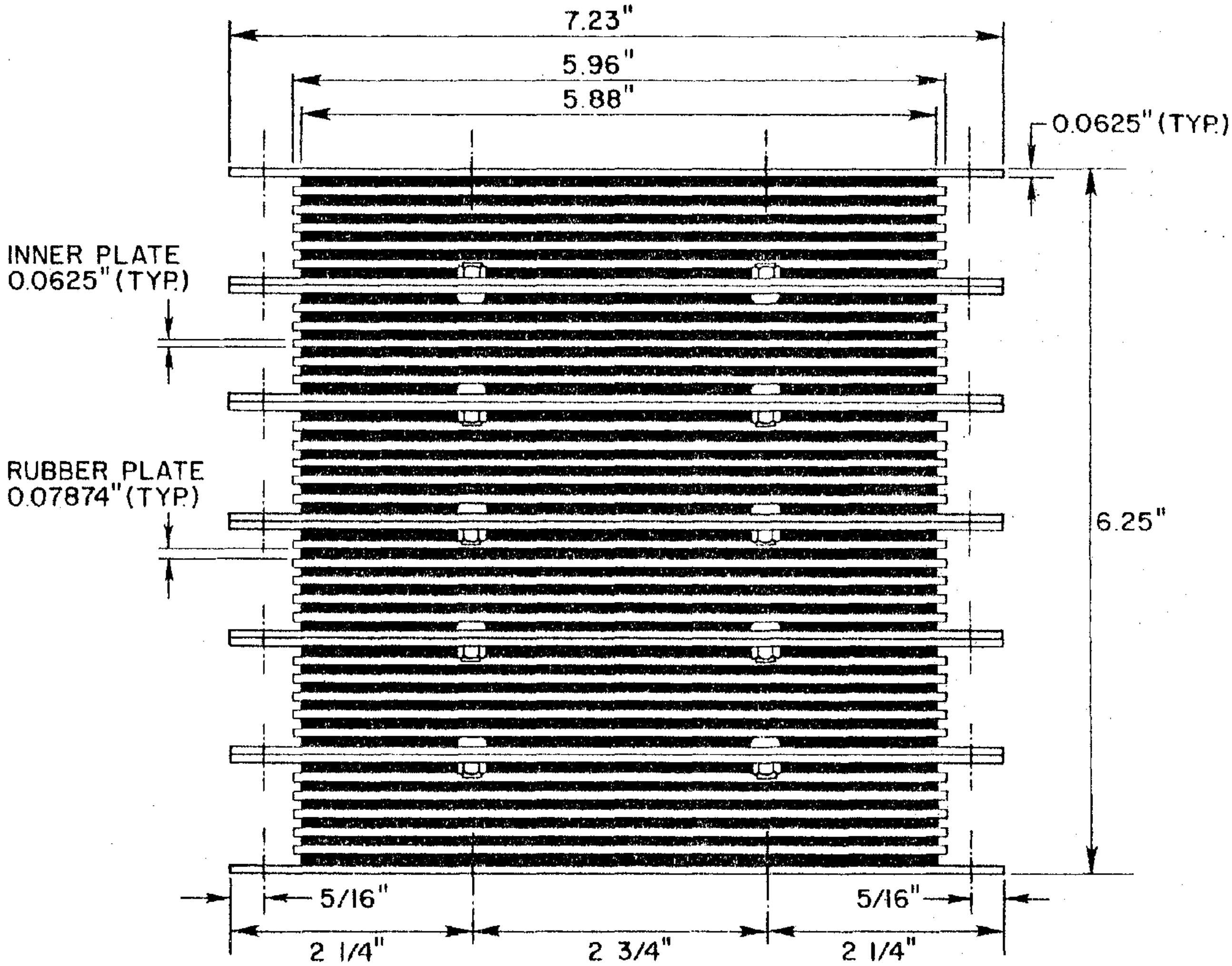

Figure 5 Typical Natural Rubber Bearing

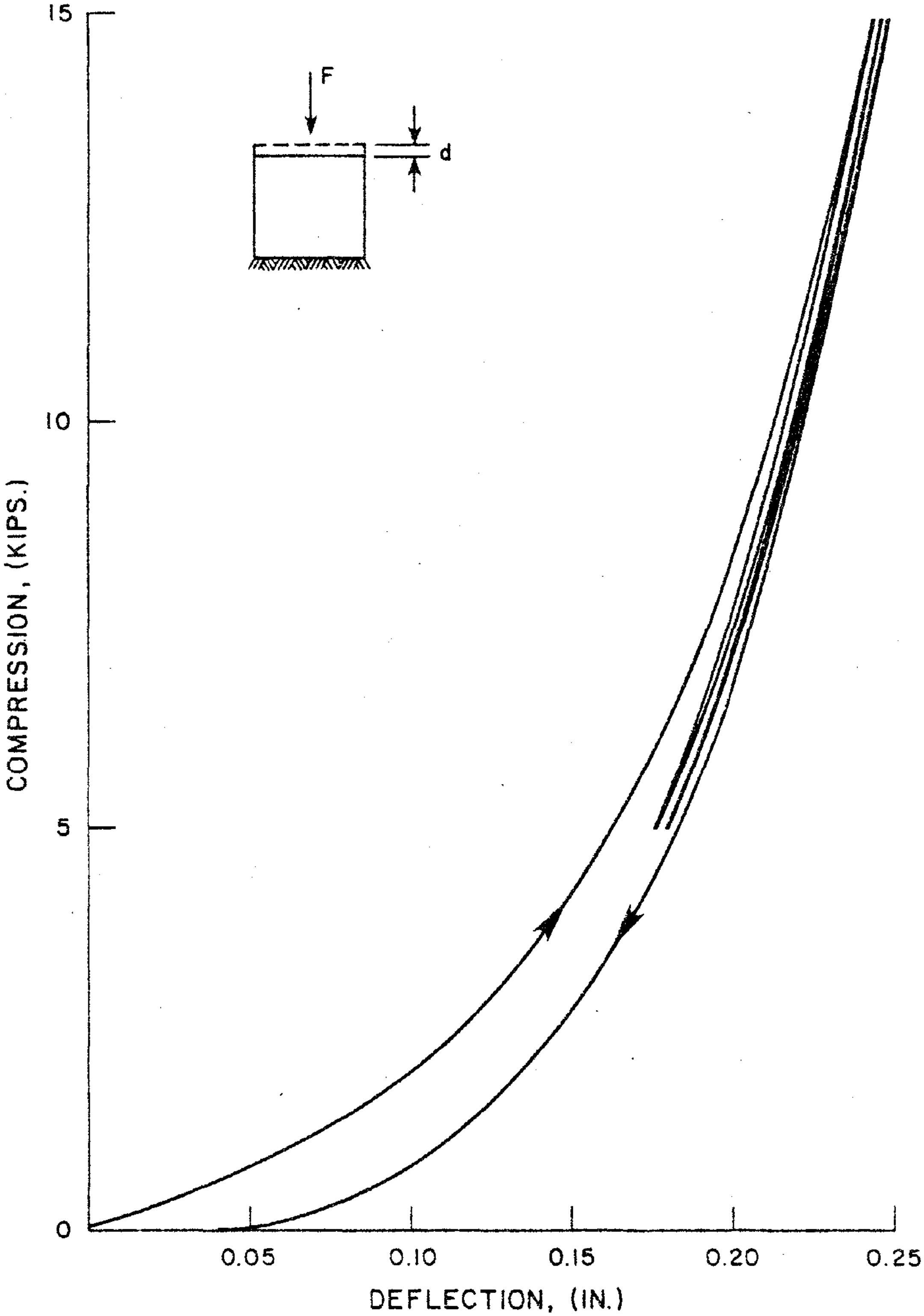

Figure 6 Vertical Stiffness of Bearings

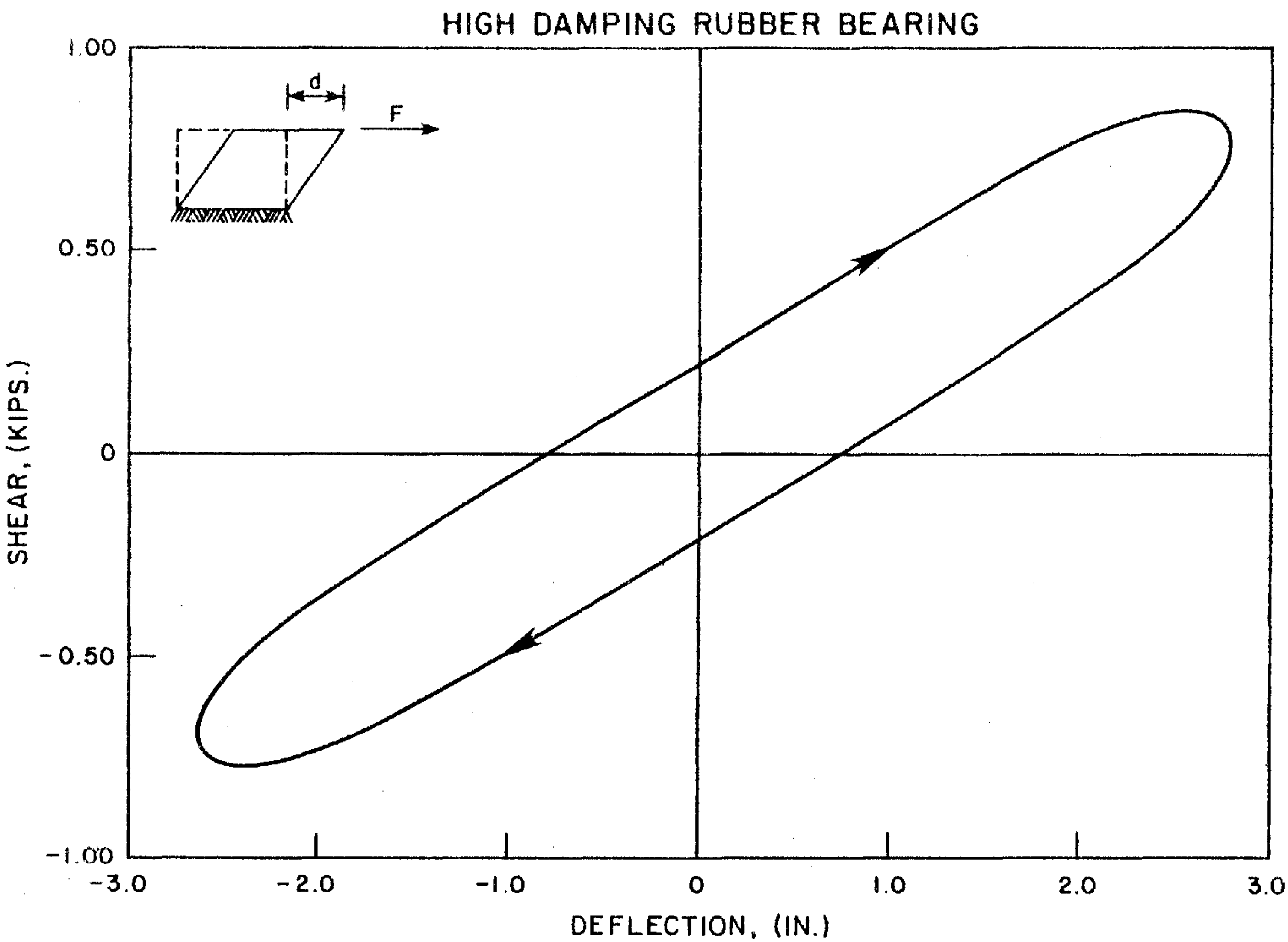

Figure 7 Horizontal Stiffness of Bearings

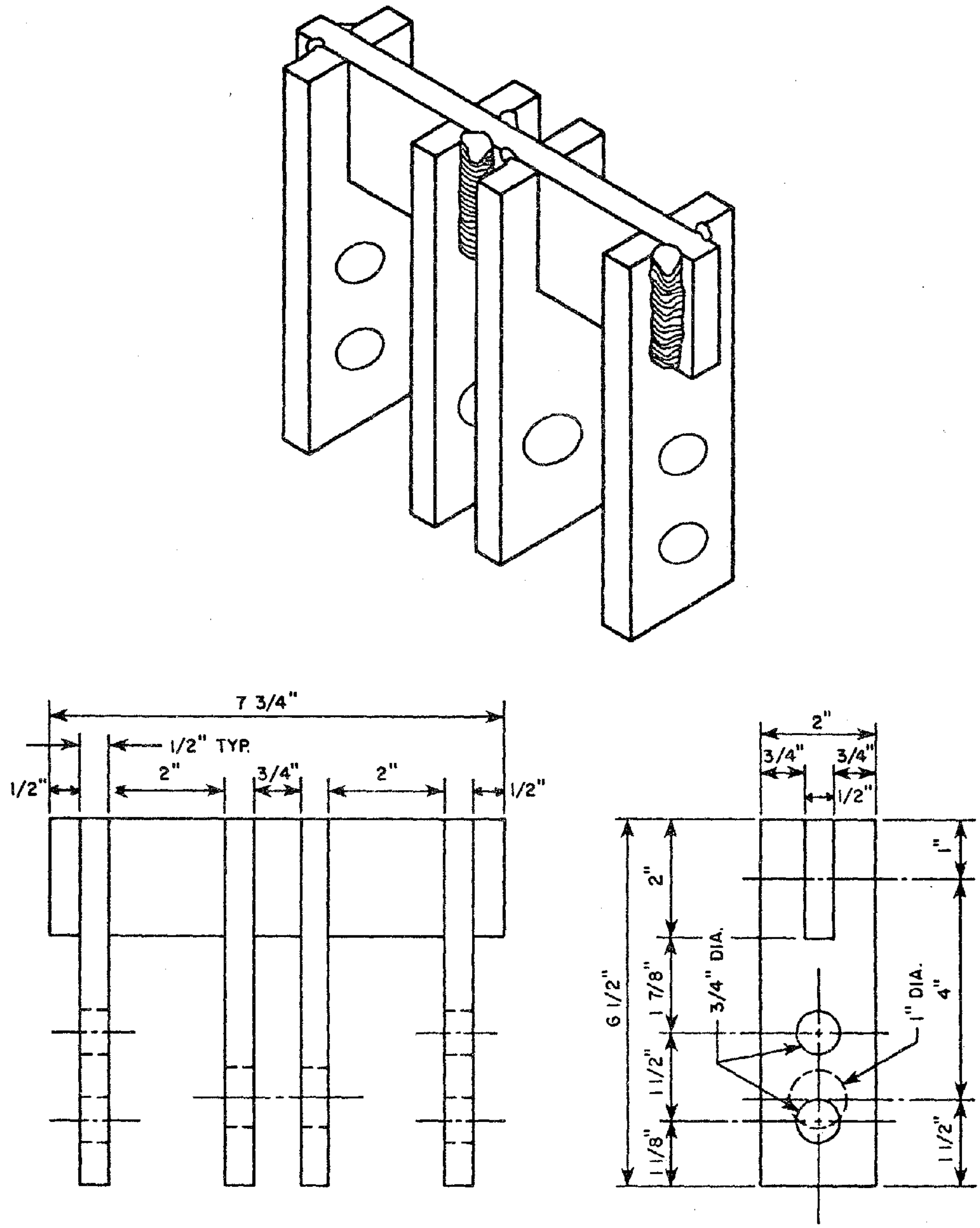

Figure 8 Typical Energy-Absorbing Device

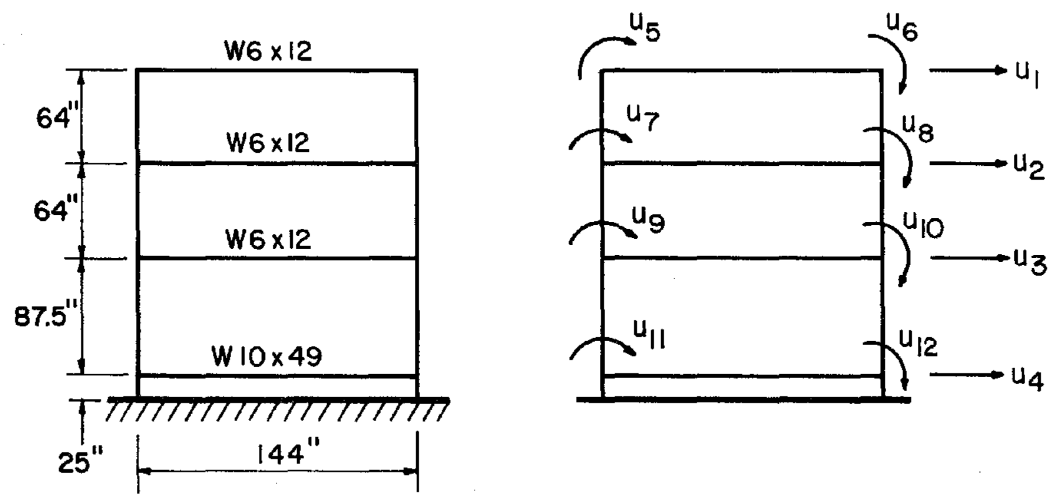

Columns are W5x16

Stiffness of rubber bearings = 1.2 k/in

Section properties:	Area (in^2)	Moment of Inertia (in^4)
W6x12	3.54	21.7
W5x16	4.70	21.3
W10x49	14.40	272.9

Figure 9 Structural Data

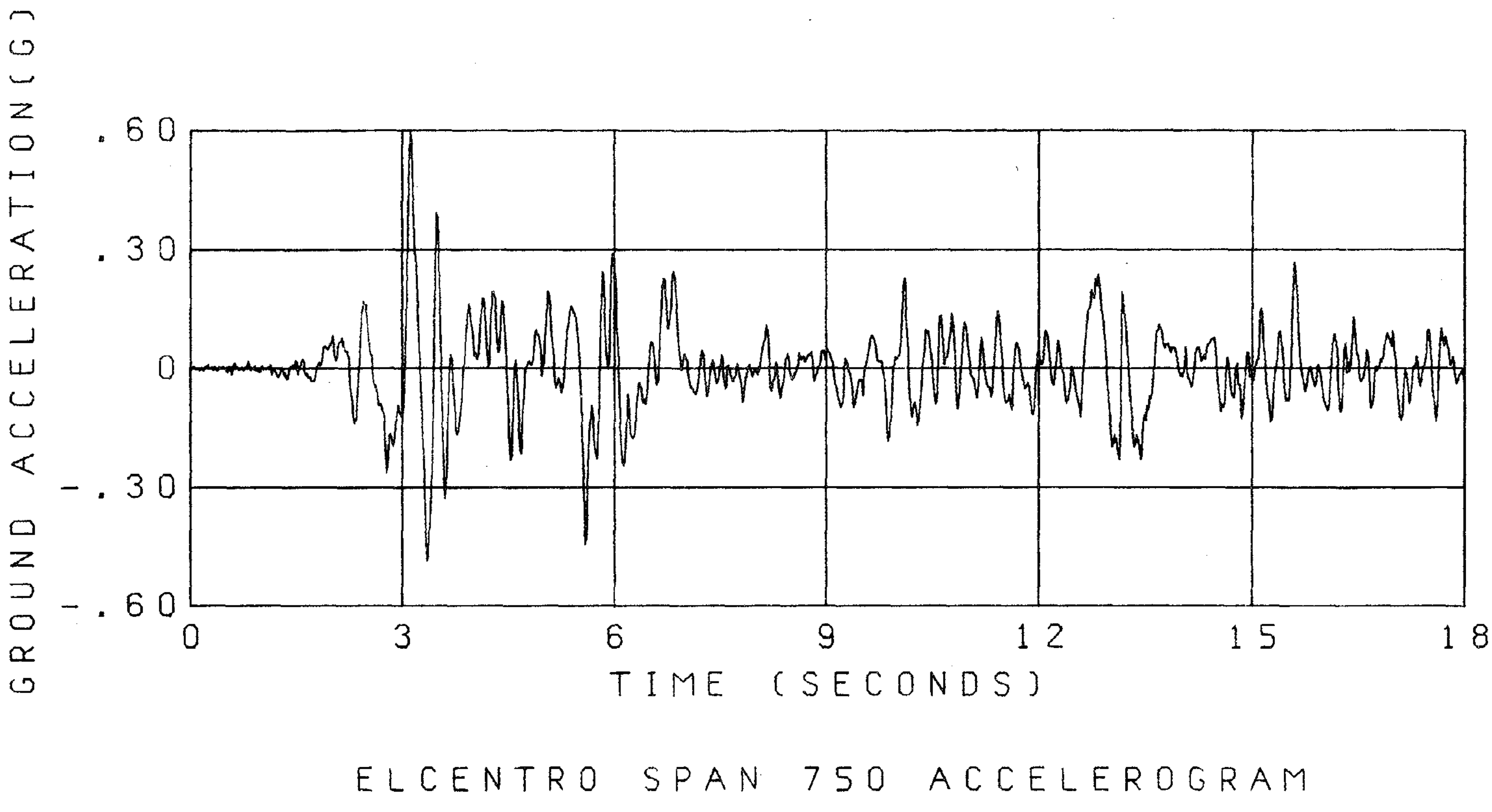

Figure 10 El Centro Span 750 Accelerogram

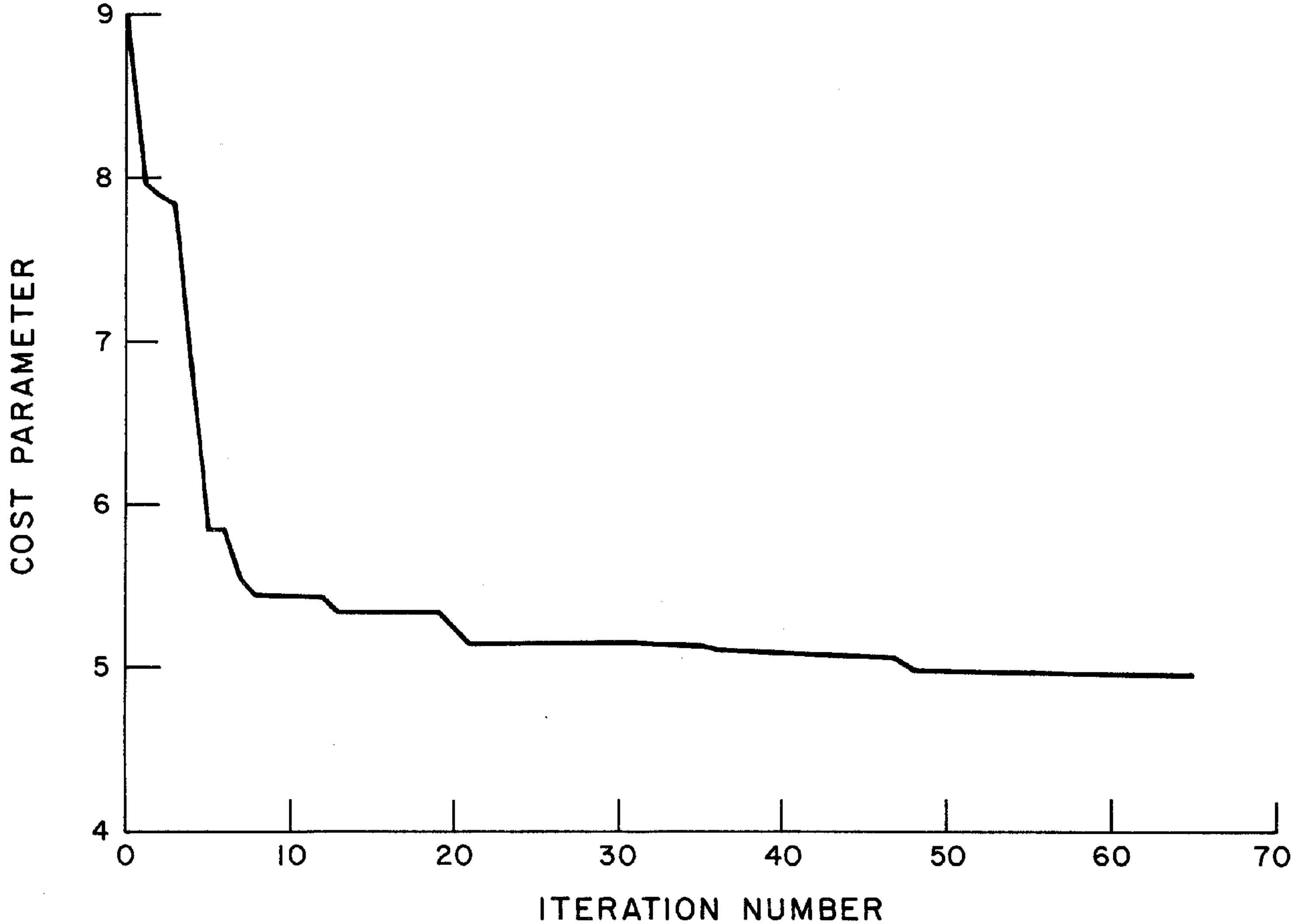

Figure 11 Cost Parameter Versus Iteration Number (Design Problem 1)

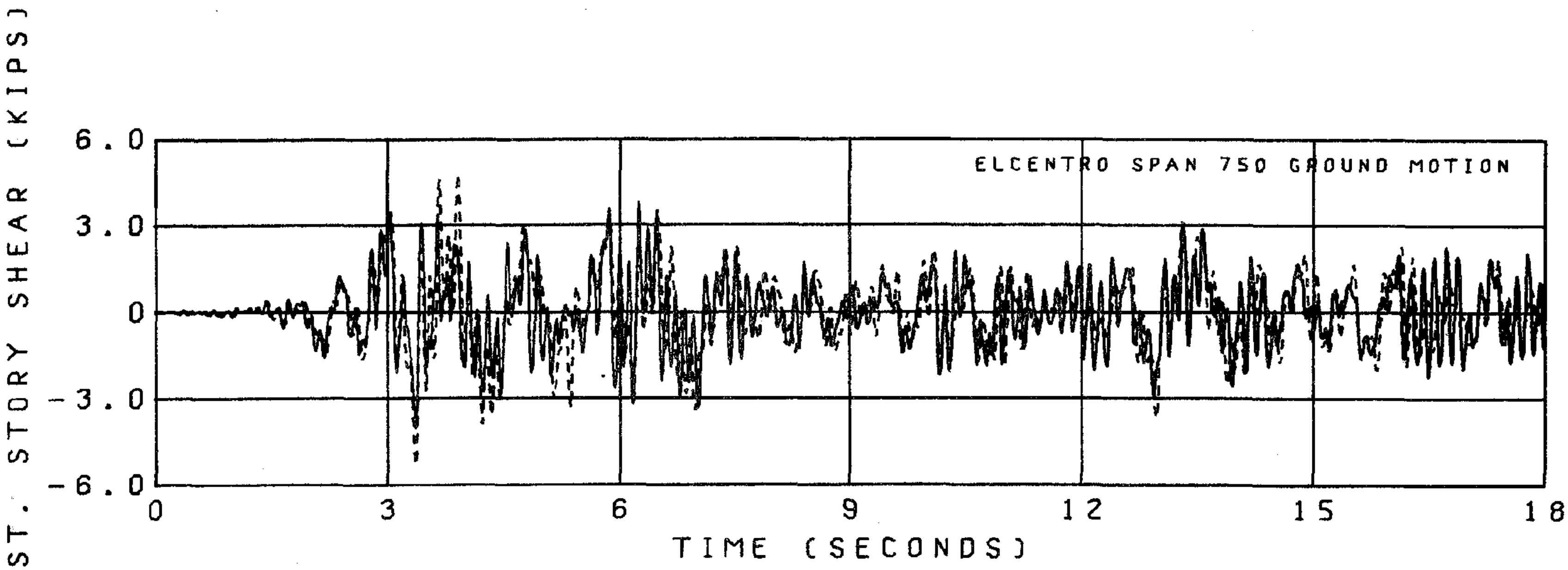

Figure 12 First Story Shear Time History (Design Problem 1)

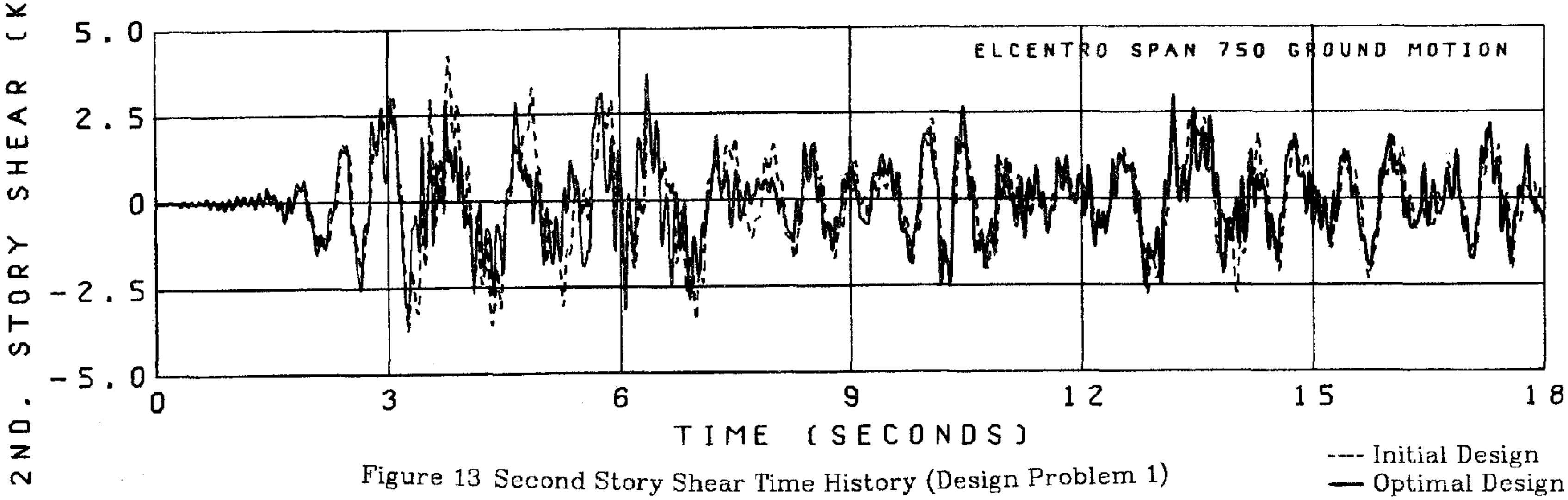

Figure 13 Second Story Shear Time History (Design Problem 1)

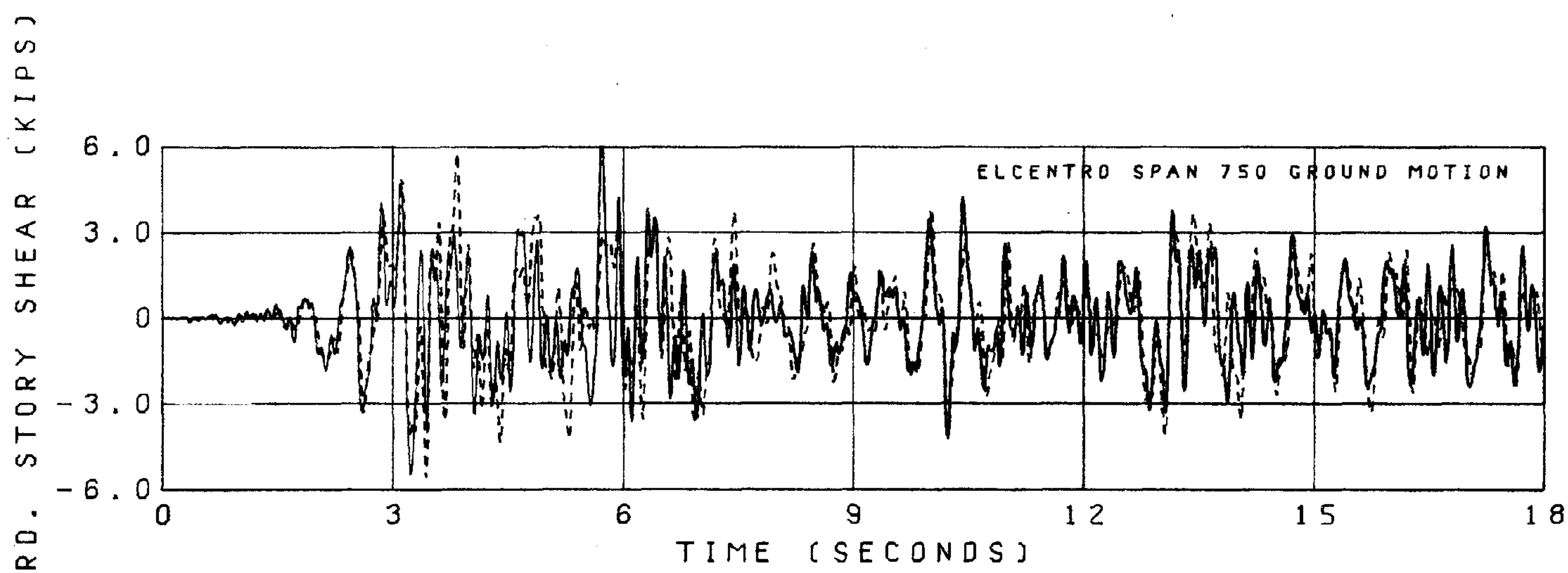

Figure 14 Third Story Shear Time History (Design Problem 1)

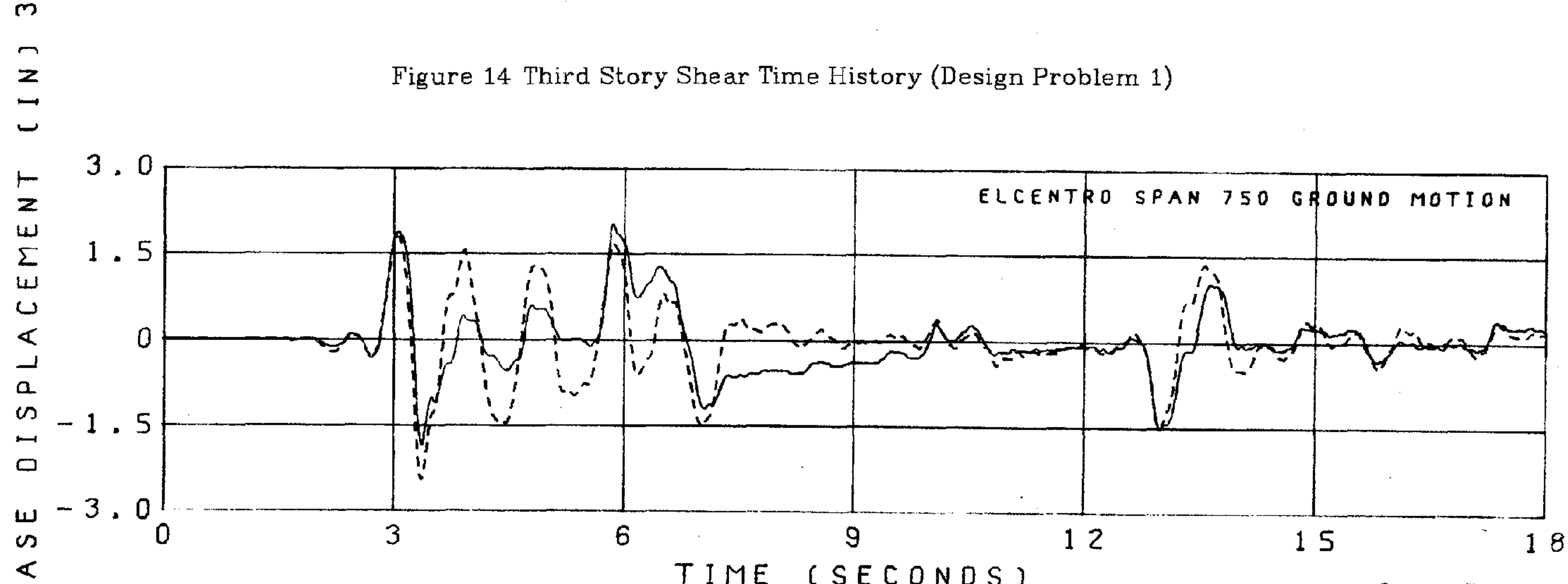

Figure 15 Base Displacement Time History (Design Problem 1)

---- Initial Design
—— Optimal Design

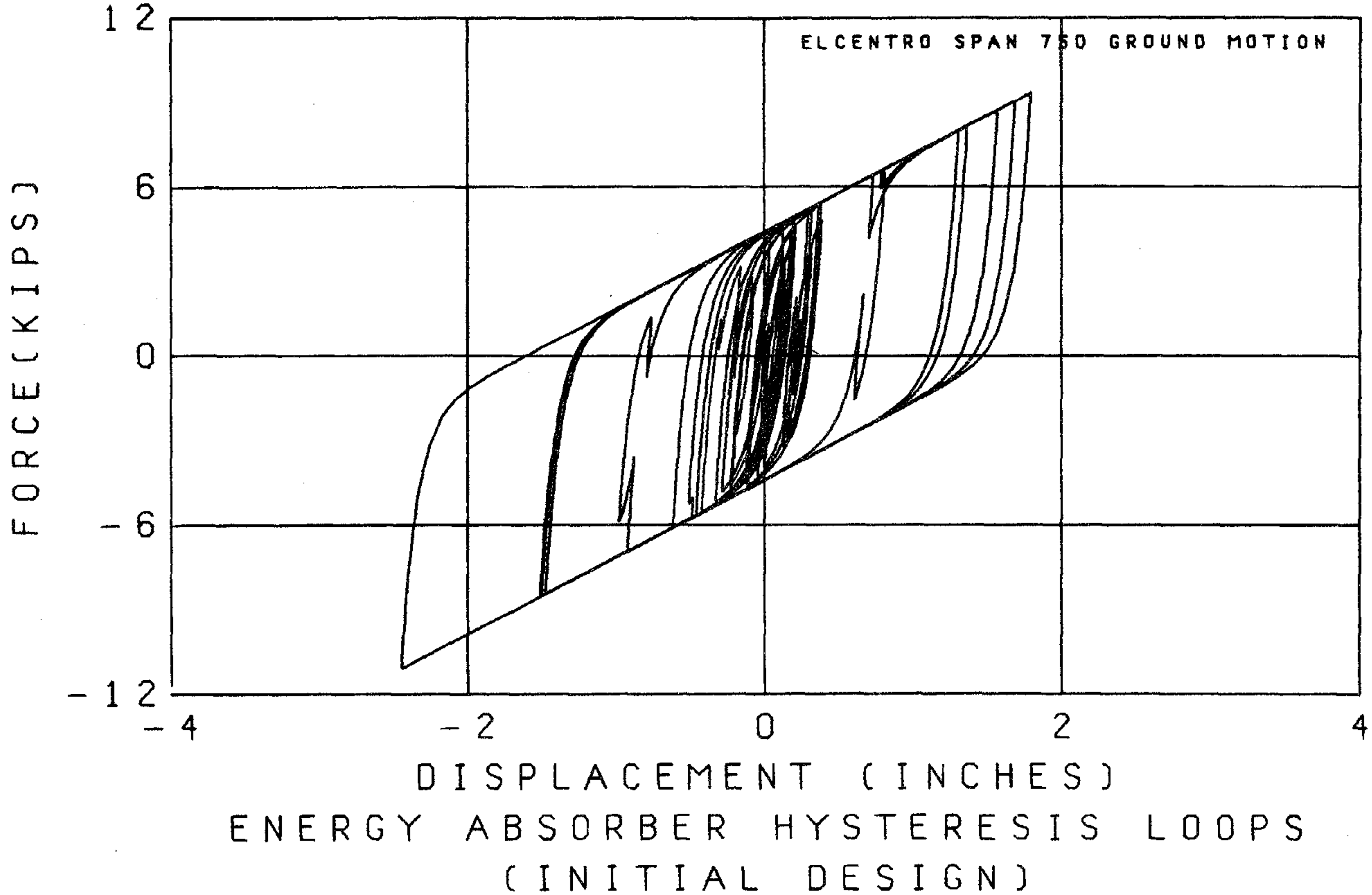

Figure 16 Energy-Absorber Hysteresis Loops (Initial Design)

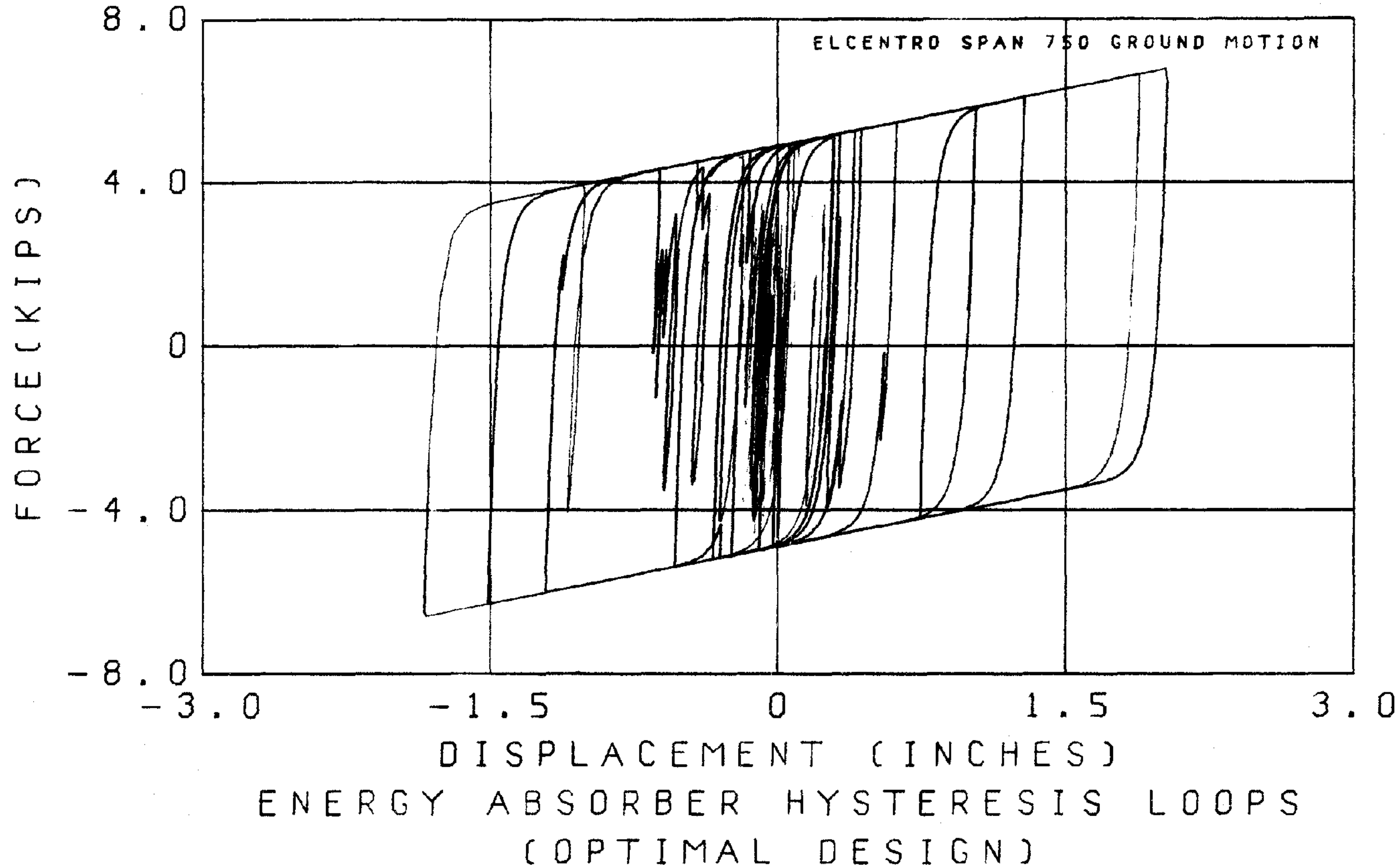

Figure 17 Energy-Absorber Hysteresis Loops (Design Problem 1)

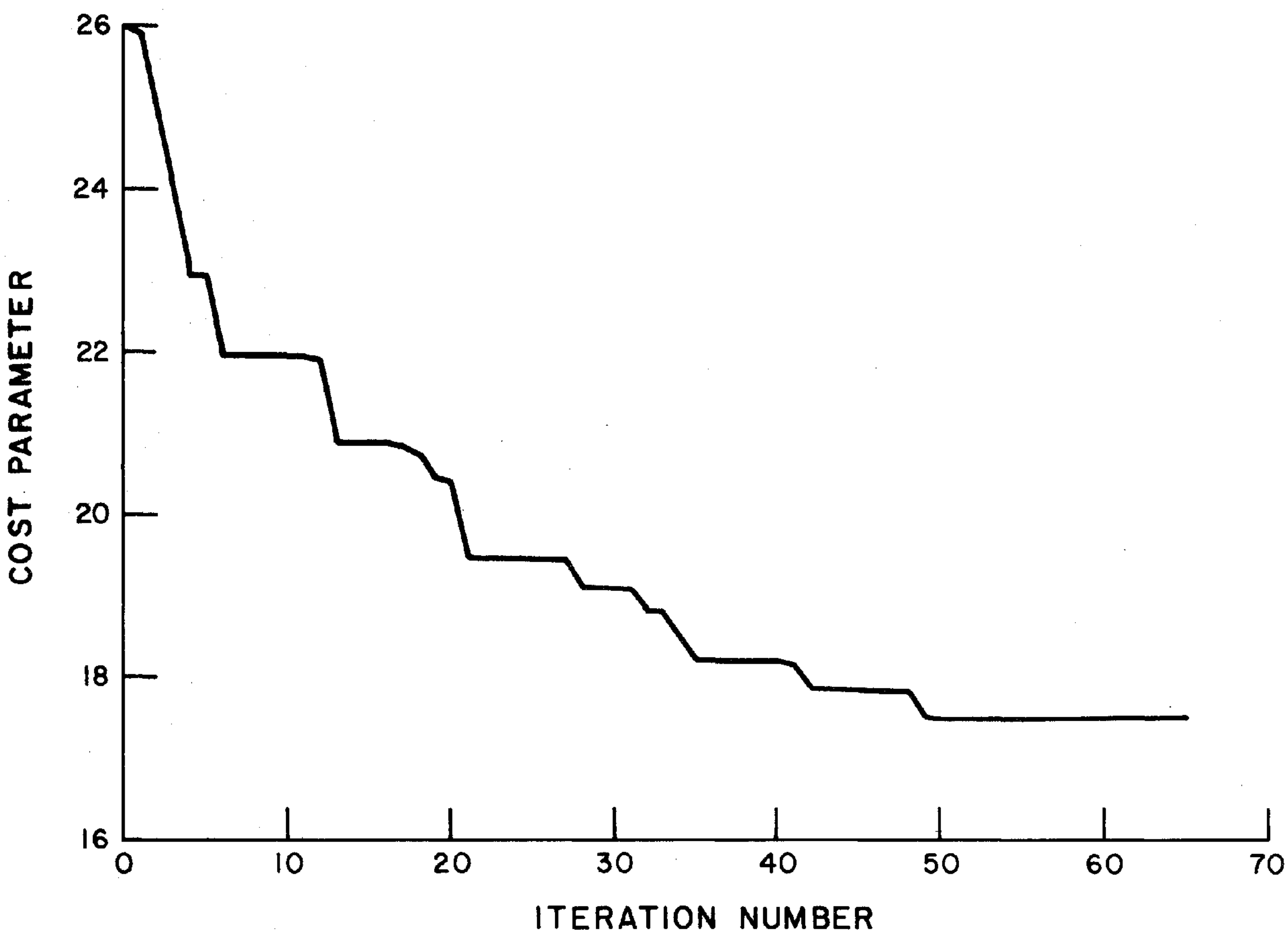

Figure 18 Cost Parameter Versus Iteration Number (Design Problem 2)

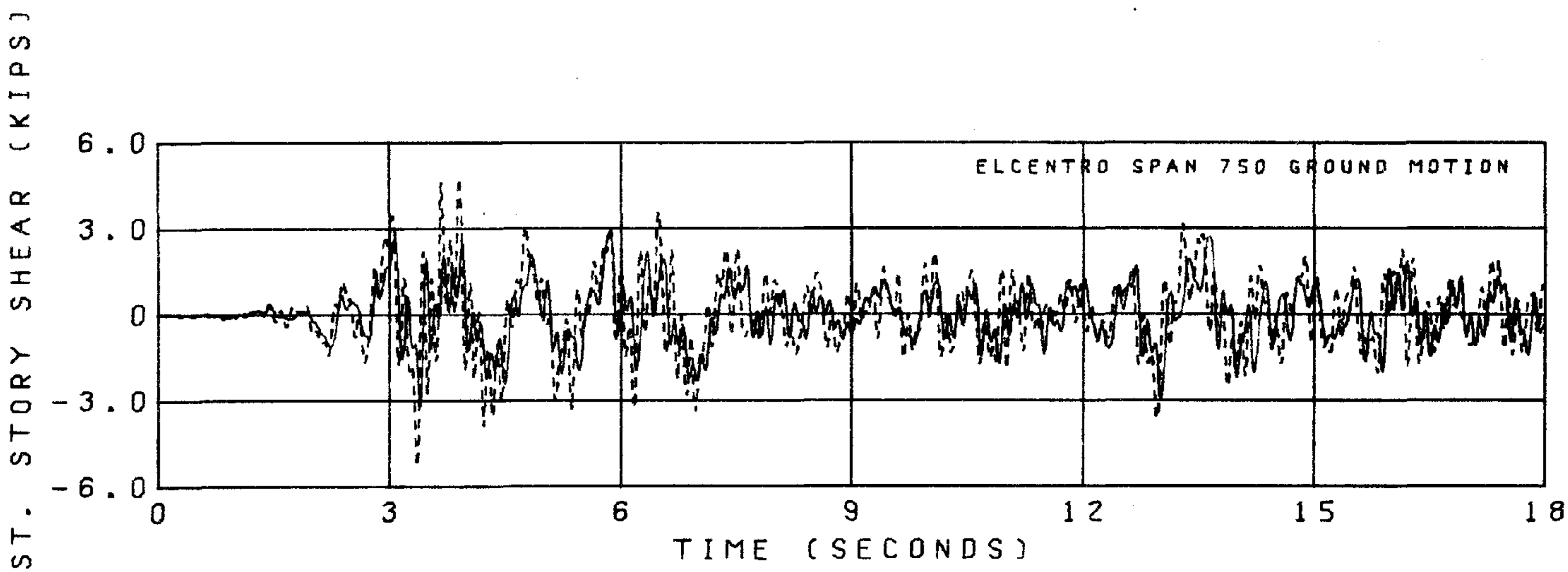

Figure 19 First Story Shear Time History (Design Problem 2)

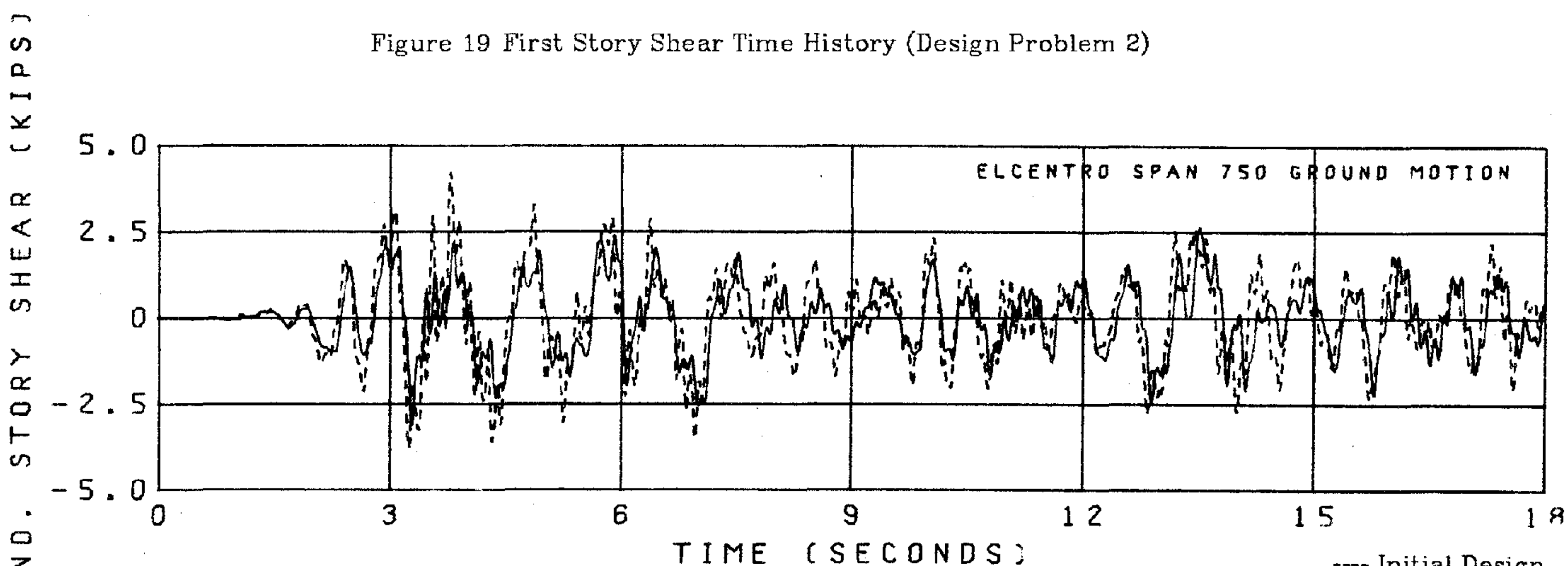

Figure 20 Second Story Shear Time History (Design Problem 2)

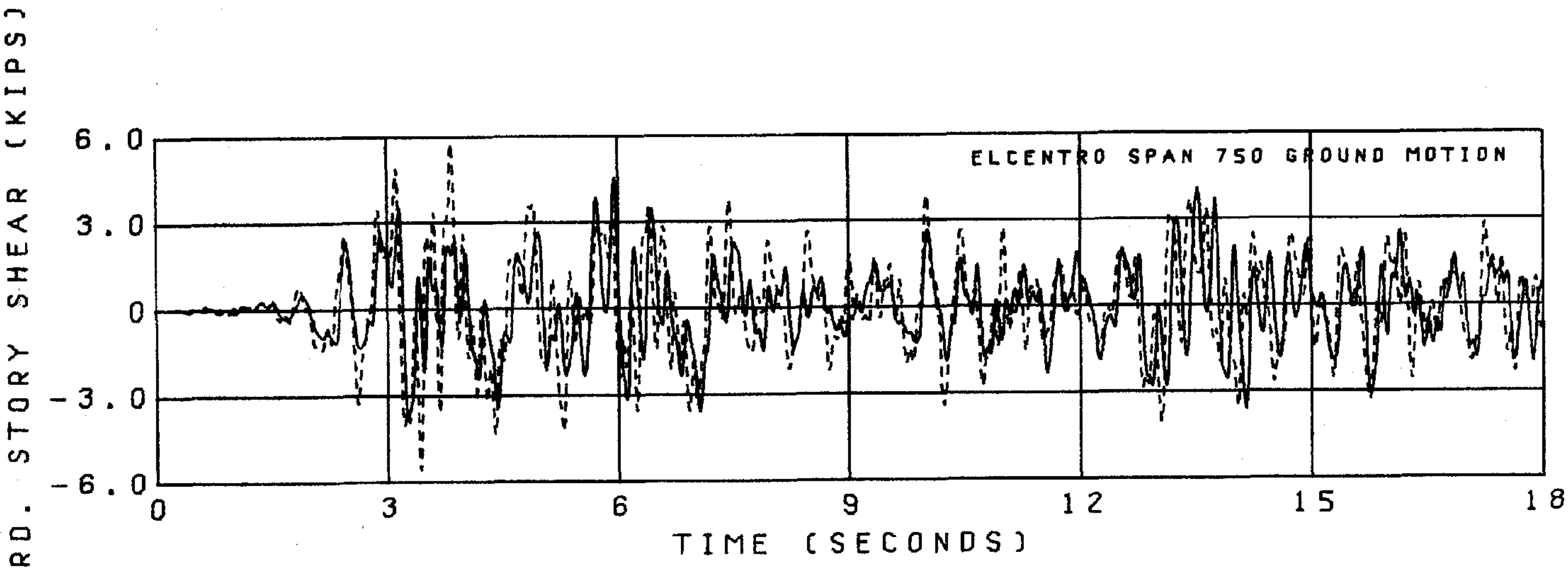

Figure 21 Third Story Shear Time History (Design Problem 2)

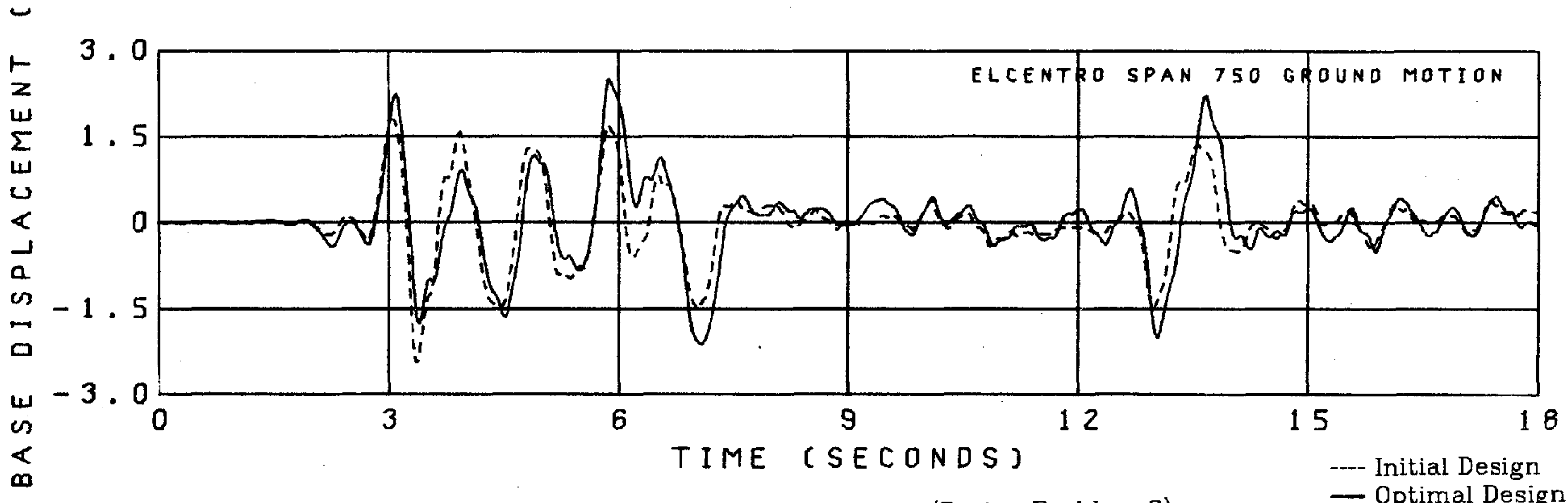

Figure 22 Base Displacement Time History (Design Problem 2)

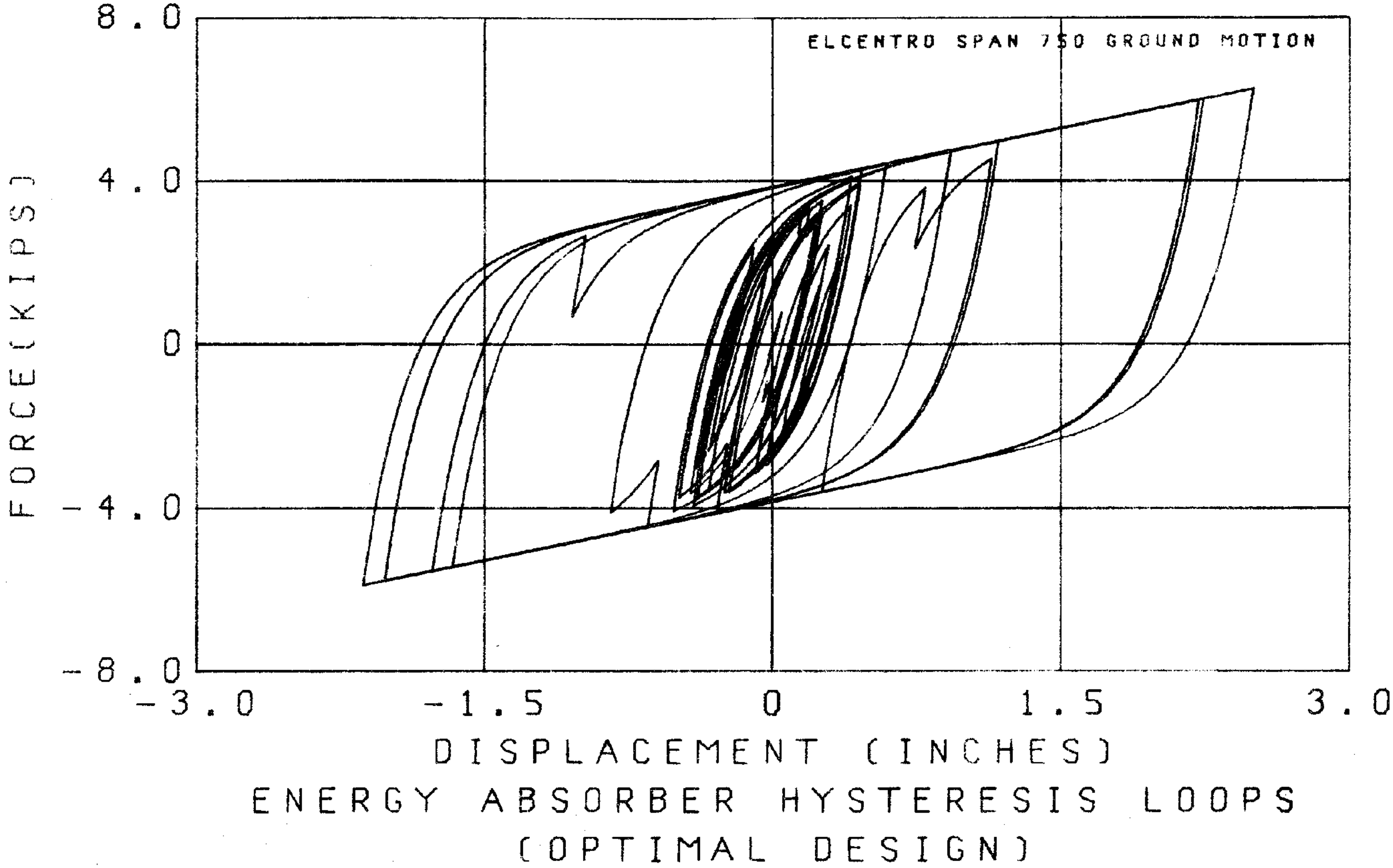

Figure 23 Energy-Absorber Hysteresis Loops (Design Problem 2)

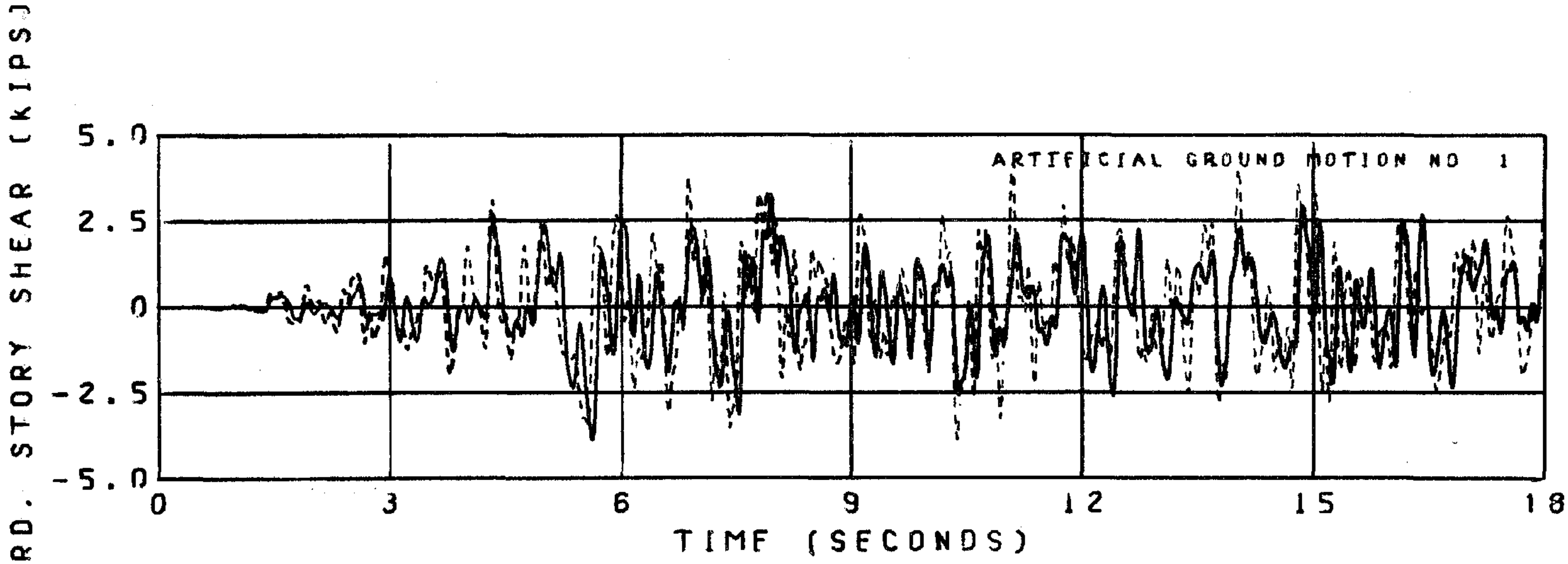

Figure 24 Third Story Shear Time History (Design Problem 2)

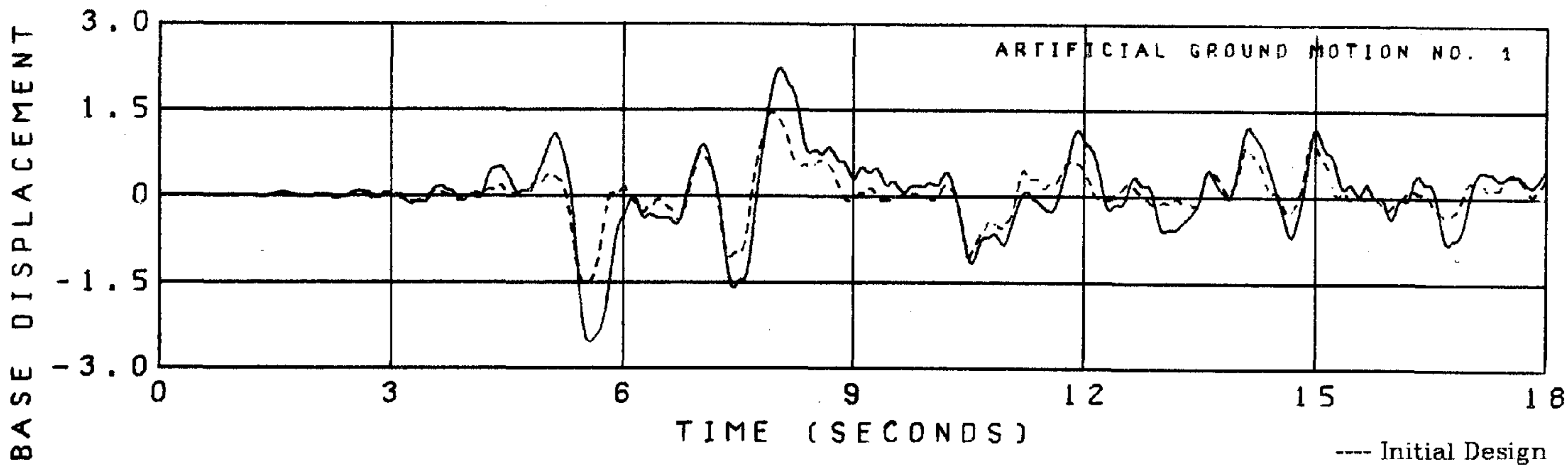

Figure 25 Base Displacement Time History (Design Problem 2)

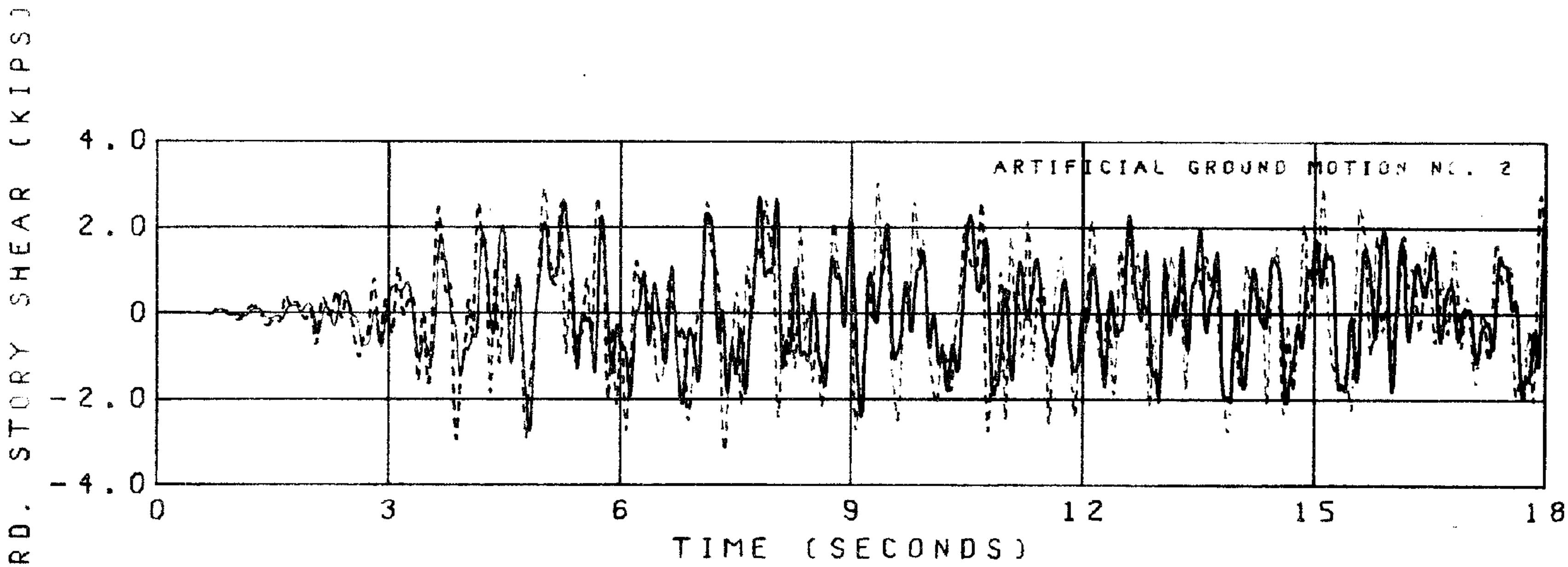

Figure 26 Third Story Shear Time History (Design Problem 2)

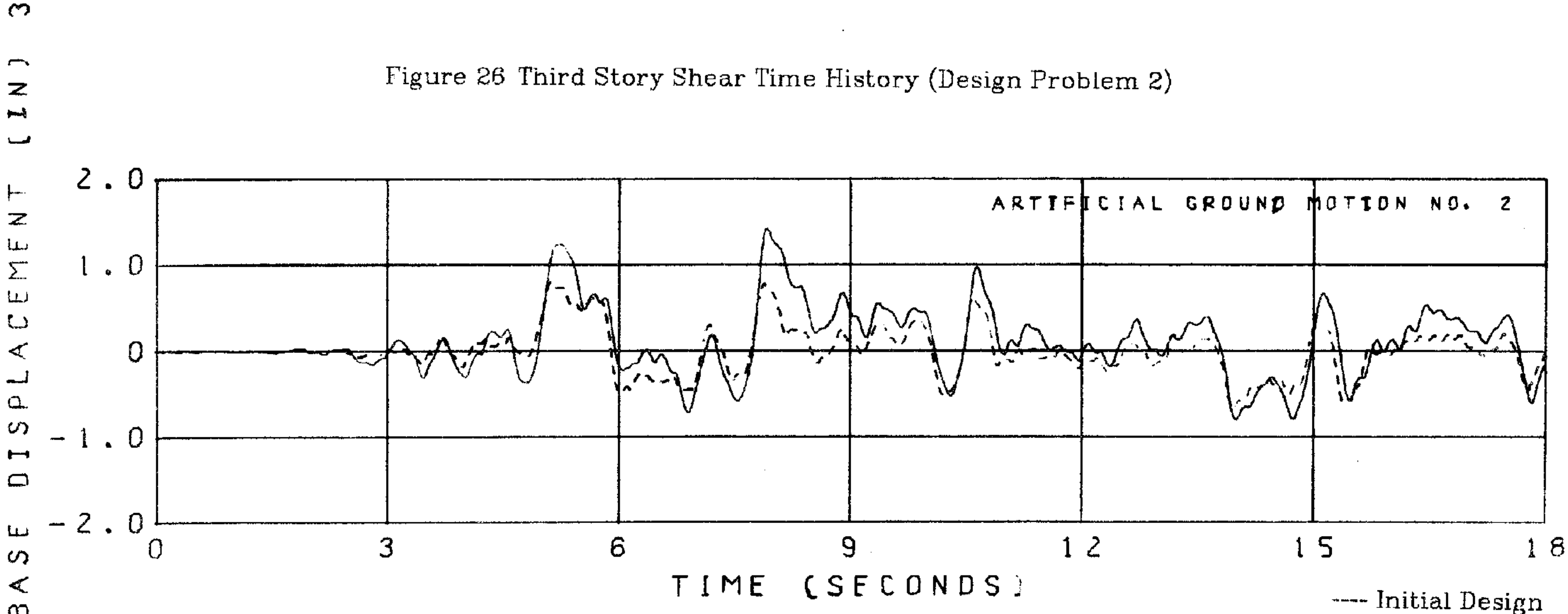

Figure 27 Base Displacement Time History (Design Problem 2)

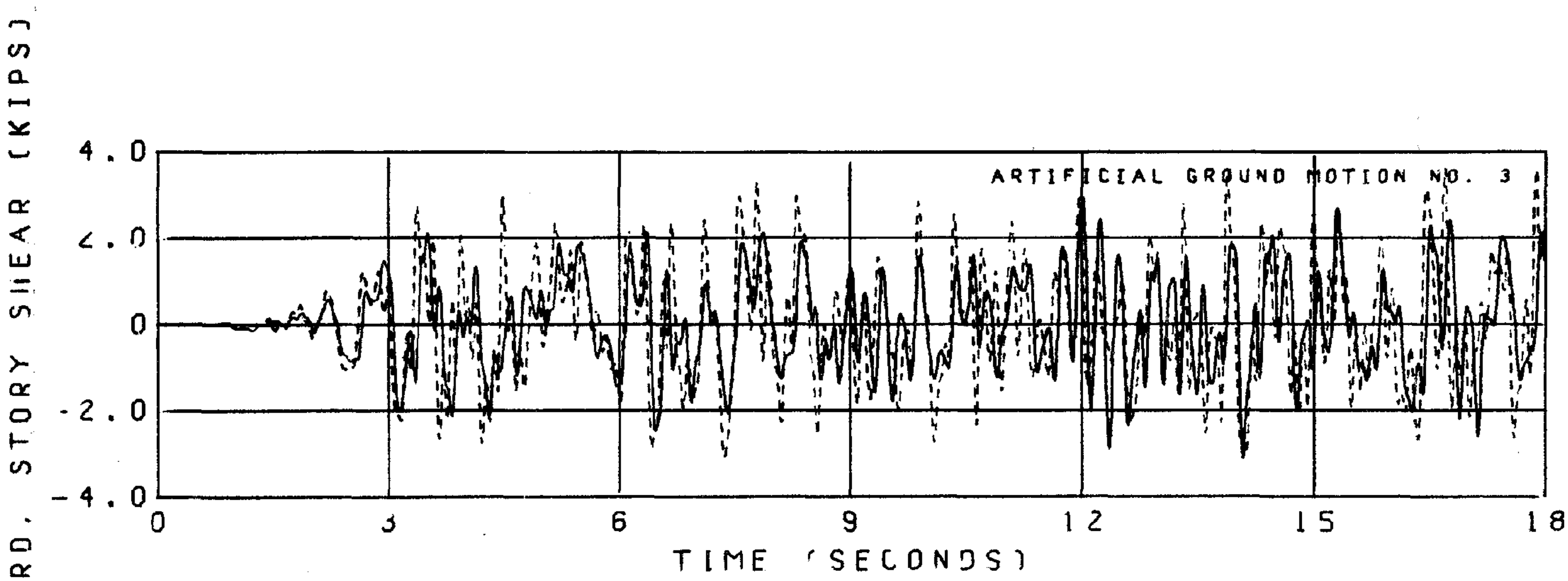

Figure 28 Third Story Shear Time History (Design Problem 2)

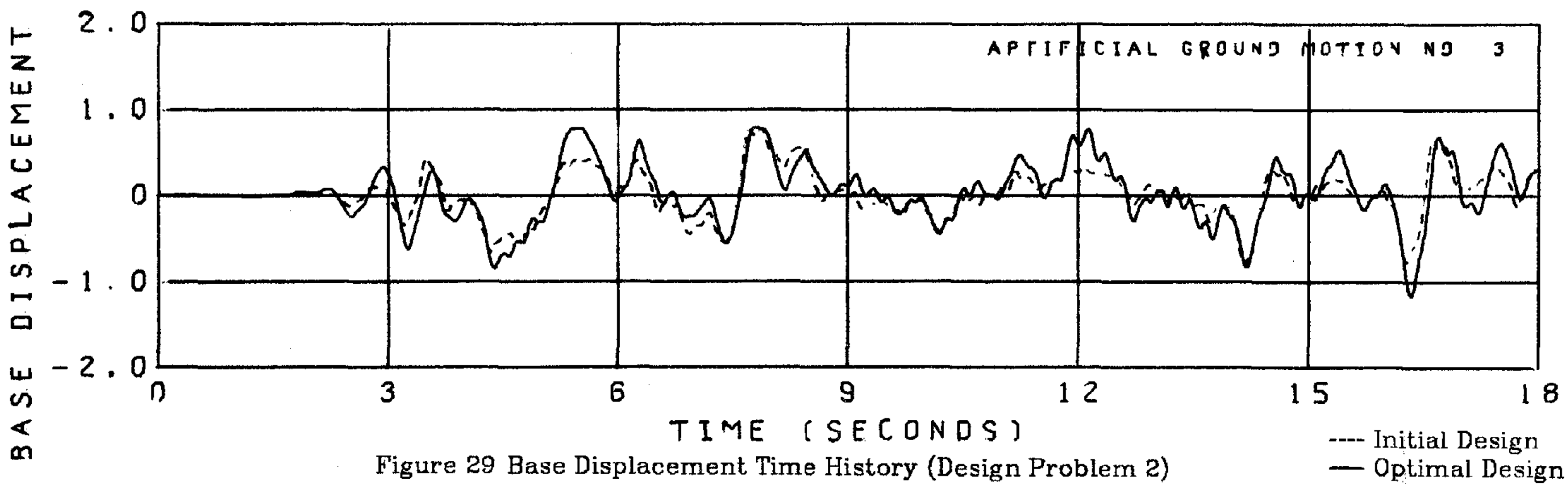

Figure 29 Base Displacement Time History (Design Problem 2)

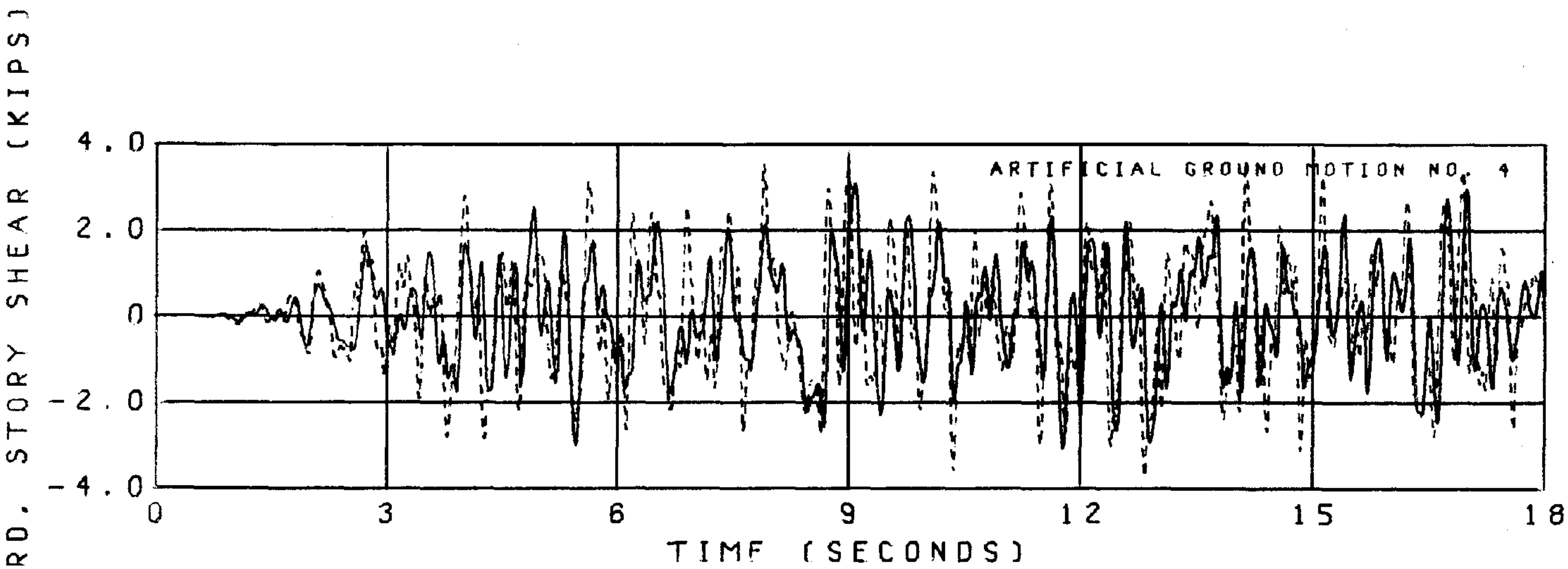

Figure 30 Third Story Shear Time History (Design Problem 2)

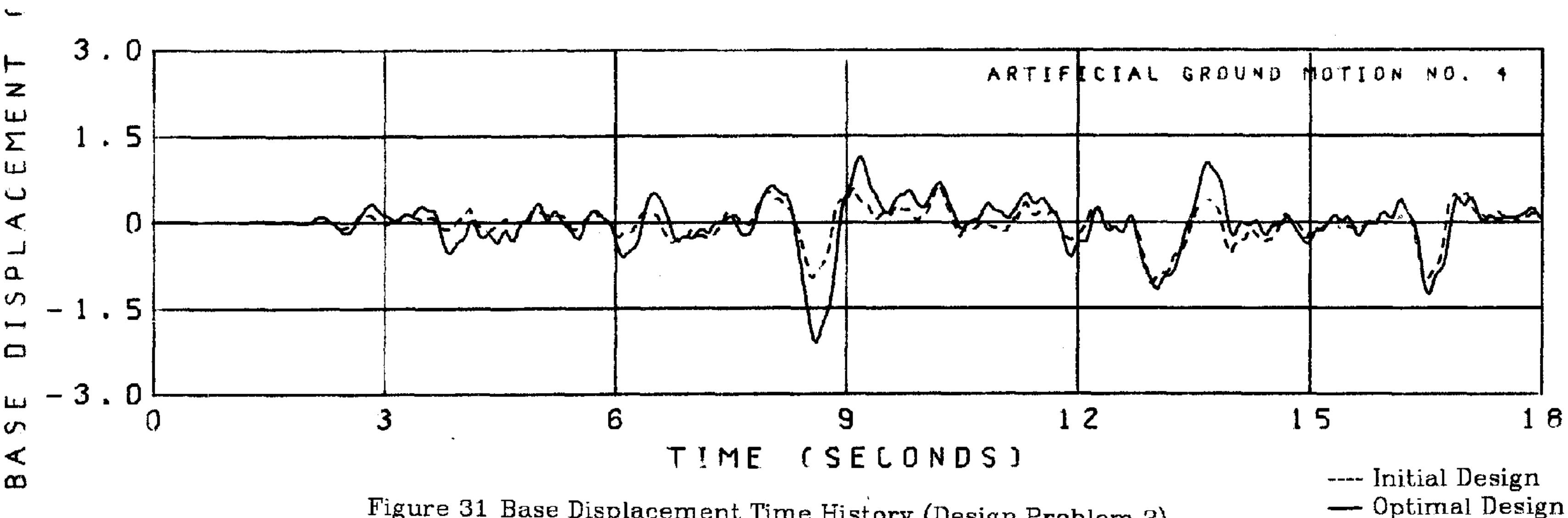

Figure 31 Base Displacement Time History (Design Problem 2)

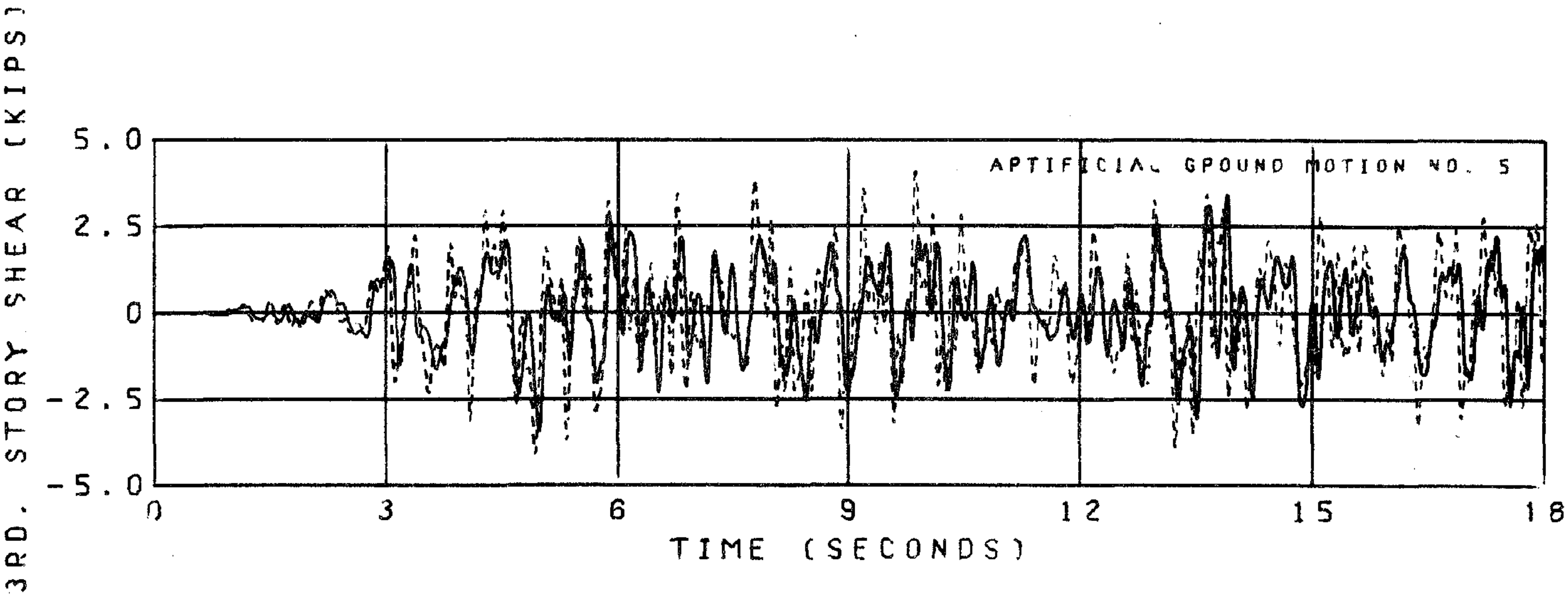

Figure 32 Third Story Shear Time History (Design Problem 2)

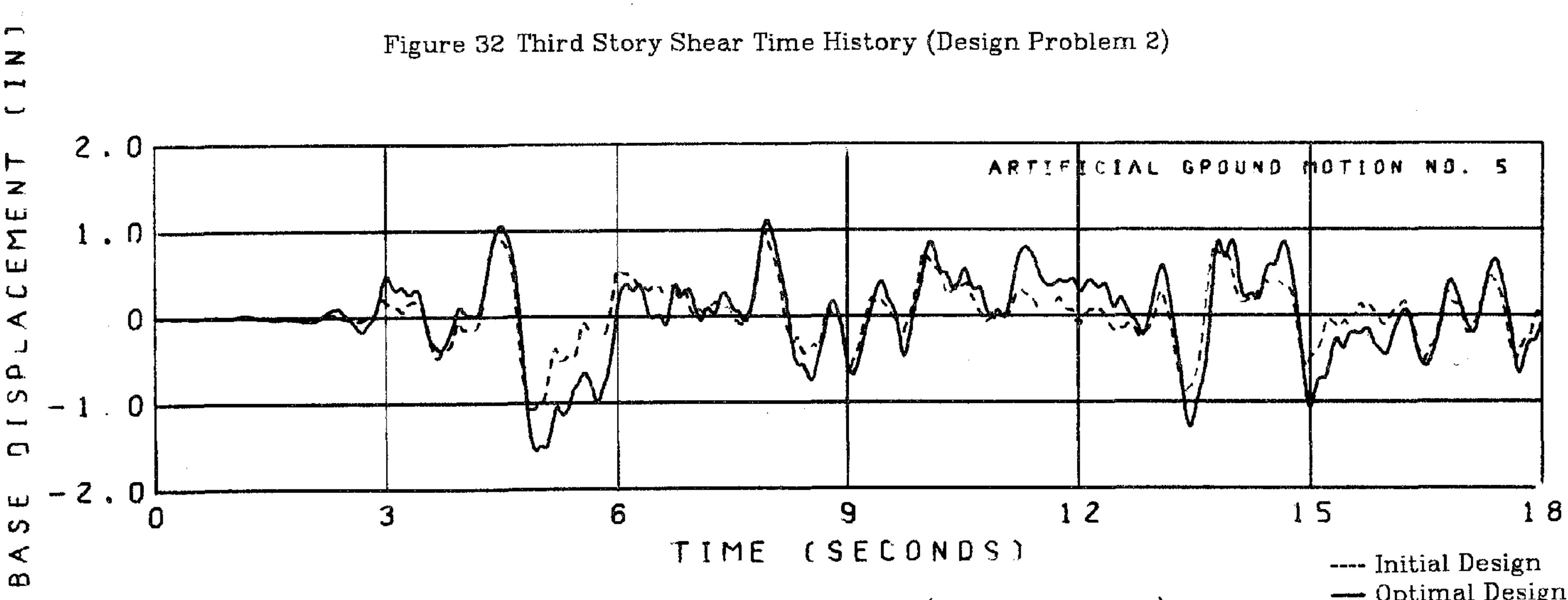

Figure 33 Base Displacement Time History (Design Problem 2)

EARTHQUAKE ENGINEERING RESEARCH CENTER REPORTS

NOTE: Numbers in parenthesis are Accession Numbers assigned by the National Technical Information Service; these are followed by a price code. Copies of the reports may be ordered from the National Technical Information Service, 5285 Port Royal Road, Springfield, Virginia, 22161. Accession Numbers should be quoted on orders for reports (PB --- ---) and remittance must accompany each order. Reports without this information were not available at time of printing. Upon request, EERC will mail inquirers this information when it becomes available.

EERC 67-1 "Feasibility Study Large-Scale Earthquake Simulator Facility," by J. Penzien, J.G. Bouwkamp, R.W. Clough and D. Rea - 1967 (PB 187 905)A07

EERC 68-1 Unassigned

EERC 68-2 "Inelastic Behavior of Beam-to-Column Subassemblages Under Repeated Loading," by V.V. Bertero - 1968 (PB 184 888)A05

EERC 68-3 "A Graphical Method for Solving the Wave Reflection-Refraction Problem," by H.D. McNiven and Y. Mengi - 1968 (PB 187 943)A03

EERC 68-4 "Dynamic Properties of McKinley School Buildings," by D. Rea, J.G. Bouwkamp and R.W. Clough - 1968 (PB 187 902)A07

EERC 68-5 "Characteristics of Rock Motions During Earthquakes," by H.B. Seed, I.M. Idriss and F.W. Kiefer - 1968 (PB 188 338)A03

EERC 69-1 "Earthquake Engineering Research at Berkeley," - 1969 (PB 187 906)A11

EERC 69-2 "Nonlinear Seismic Response of Earth Structures," by M. Dibaj and J. Penzien - 1969 (PB 187 904)A08

EERC 69-3 "Probabilistic Study of the Behavior of Structures During Earthquakes," by R. Ruiz and J. Penzien - 1969 (PB 187 886)A06

EERC 69-4 "Numerical Solution of Boundary Value Problems in Structural Mechanics by Reduction to an Initial Value Formulation," by N. Distefano and J. Schujman - 1969 (PB 187 942)A02

EERC 69-5 "Dynamic Programming and the Solution of the Biharmonic Equation," by N. Distefano - 1969 (PB 187 941)A03

EERC 69-6 "Stochastic Analysis of Offshore Tower Structures," by A.K. Malhotra and J. Penzien - 1969 (PB 187 903)A09

EERC 69-7 "Rock Motion Accelerograms for High Magnitude Earthquakes," by H.B. Seed and I.M. Idriss - 1969 (PB 187 940)A02

EERC 69-8 "Structural Dynamics Testing Facilities at the University of California, Berkeley," by R.M. Stephen, J.G. Bouwkamp, R.W. Clough and J. Penzien - 1969 (PB 189 111)A04

EERC 69-9 "Seismic Response of Soil Deposits Underlain by Sloping Rock Boundaries," by H. Dezfulian and H.B. Seed 1969 (PB 189 114)A03

EERC 69-10 "Dynamic Stress Analysis of Axisymmetric Structures Under Arbitrary Loading," by S. Ghosh and E.L. Wilson 1969 (PB 189 026)A10

EERC 69-11 "Seismic Behavior of Multistory Frames Designed by Different Philosophies," by J.C. Anderson and V. V. Bertero - 1969 (PB 190 662)A10

EERC 69-12 "Stiffness Degradation of Reinforcing Concrete Members Subjected to Cyclic Flexural Moments," by V.V. Bertero, B. Bresler and H. Ming Liao - 1969 (PB 202 942)A07

EERC 69-13 "Response of Non-Uniform Soil Deposits to Travelling Seismic Waves," by H. Dezfulian and H.B. Seed - 1969 (PB 191 023)A03

EERC 69-14 "Damping Capacity of a Model Steel Structure," by D. Rea, R.W. Clough and J.G. Bouwkamp - 1969 (PB 190 663)A06

EERC 69-15 "Influence of Local Soil Conditions on Building Damage Potential during Earthquakes," by H.B. Seed and I.M. Idriss - 1969 (PB 191 036)A03

EERC 69-16 "The Behavior of Sands Under Seismic Loading Conditions," by M.L. Silver and H.B. Seed - 1969 (AD 714 982)A07

EERC 70-1 "Earthquake Response of Gravity Dams," by A.K. Chopra - 1970 (AD 709 640)A03

EERC 70-2 "Relationships between Soil Conditions and Building Damage in the Caracas Earthquake of July 29, 1967," by H.B. Seed, I.M. Idriss and H. Dezfulian - 1970 (PB 195 762)A05

EERC 70-3 "Cyclic Loading of Full Size Steel Connections," by E.P. Popov and R.M. Stephen - 1970 (PB 213 545)A04

EERC 70-4 "Seismic Analysis of the Charaima Building, Caraballeda, Venezuela," by Subcommittee of the SEAONC Research Committee: V.V. Bertero, P.F. Fratessa, S.A. Mahin, J.H. Sexton, A.C. Scordelis, E.L. Wilson, L.A. Wyllie, H.B. Seed and J. Penzien, Chairman - 1970 (PB 201 455)A06

EERC 70-5 "A Computer Program for Earthquake Analysis of Dams," by A.K. Chopra and P. Chakrabarti - 1970 (AD 723 994)A05

EERC 70-6 "The Propagation of Love Waves Across Non-Horizontally Layered Structures," by J. Lysmer and L.A. Drake 1970 (PB 197 896)A03

EERC 70-7 "Influence of Base Rock Characteristics on Ground Response," by J. Lysmer, H.B. Seed and P.B. Schnabel 1970 (PB 197 897)A03

EERC 70-8 "Applicability of Laboratory Test Procedures for Measuring Soil Liquefaction Characteristics under Cyclic Loading," by H.B. Seed and W.H. Peacock - 1970 (PB 198 016)A03

EERC 70-9 "A Simplified Procedure for Evaluating Soil Liquefaction Potential," by H.B. Seed and I.M. Idriss - 1970 (PB 198 009)A03

EERC 70-10 "Soil Moduli and Damping Factors for Dynamic Response Analysis," by H.B. Seed and I.M. Idriss - 1970 (PB 197 869)A03

EERC 71-1 "Koyna Earthquake of December 11, 1967 and the Performance of Koyna Dam," by A.K. Chopra and P. Chakrabarti 1971 (AD 731 496)A06

EERC 71-2 "Preliminary In-Situ Measurements of Anelastic Absorption in Soils Using a Prototype Earthquake Simulator," by R.D. Borcherdt and P.W. Rodgers - 1971 (PB 201 454)A03

EERC 71-3 "Static and Dynamic Analysis of Inelastic Frame Structures," by F.L. Porter and G.H. Powell - 1971 (PB 210 135)A06

EERC 71-4 "Research Needs in Limit Design of Reinforced Concrete Structures," by V.V. Bertero - 1971 (PB 202 943)A04

EERC 71-5 "Dynamic Behavior of a High-Rise Diagonally Braced Steel Building," by D. Rea, A.A. Shah and J.G. Bouwkamp 1971 (PB 203 584)A06

EERC 71-6 "Dynamic Stress Analysis of Porous Elastic Solids Saturated with Compressible Fluids," by J. Ghaboussi and E. L. Wilson - 1971 (PB 211 396)A06

EERC 71-7 "Inelastic Behavior of Steel Beam-to-Column Subassemblages," by H. Krawinkler, V.V. Bertero and E.P. Popov 1971 (PB 211 335)A14

EERC 71-8 "Modification of Seismograph Records for Effects of Local Soil Conditions," by P. Schnabel, H.B. Seed and J. Lysmer - 1971 (PB 214 450)A03

EERC 72-1 "Static and Earthquake Analysis of Three Dimensional Frame and Shear Wall Buildings," by E.L. Wilson and H.H. Dovey - 1972 (PB 212 904)A05

EERC 72-2 "Accelerations in Rock for Earthquakes in the Western United States," by P.B. Schnabel and H.B. Seed - 1972 (PB 213 100)A03

EERC 72-3 "Elastic-Plastic Earthquake Response of Soil-Building Systems," by T. Minami - 1972 (PB 214 868)A08

EERC 72-4 "Stochastic Inelastic Response of Offshore Towers to Strong Motion Earthquakes," by M.K. Kaul - 1972 (PB 215 713)A05

EERC 72-5 "Cyclic Behavior of Three Reinforced Concrete Flexural Members with High Shear," by E.P. Popov, V.V. Bertero and H. Krawinkler - 1972 (PB 214 555)A05

EERC 72-6 "Earthquake Response of Gravity Dams Including Reservoir Interaction Effects," by P. Chakrabarti and A.K. Chopra - 1972 (AD 762 330)A08

EERC 72-7 "Dynamic Properties of Pine Flat Dam," by D. Rea, C.Y. Liaw and A.K. Chopra - 1972 (AD 763 928)A05

EERC 72-8 "Three Dimensional Analysis of Building Systems," by E.L. Wilson and H.H. Dovey - 1972 (PB 222 438)A06

EERC 72-9 "Rate of Loading Effects on Uncracked and Repaired Reinforced Concrete Members," by S. Mahin, V.V. Bertero, D. Rea and M. Atalay - 1972 (PB 224 520)A08

EERC 72-10 "Computer Program for Static and Dynamic Analysis of Linear Structural Systems," by E.L. Wilson, K.-J. Bathe, J.E. Peterson and H.H.Dovey - 1972 (PB 220 437)A04

EERC 72-11 "Literature Survey - Seismic Effects on Highway Bridges," by T. Iwasaki, J. Penzien and R.W. Clough - 1972 (PB 215 613)A19

EERC 72-12 "SHAKE-A Computer Program for Earthquake Response Analysis of Horizontally Layered Sites," by P.B. Schnabel and J. Lysmer - 1972 (PB 220 207)A06

EERC 73-1 "Optimal Seismic Design of Multistory Frames," by V.V. Bertero and H. Kamil - 1973

EERC 73-2 "Analysis of the Slides in the San Fernando Dams During the Earthquake of February 9, 1971," by H.B. Seed, K.L. Lee, I.M. Idriss and F. Makdisi - 1973 (PB 223 402)A14

EERC 73-3 "Computer Aided Ultimate Load Design of Unbraced Multistory Steel Frames," by M.B. El-Hafez and G.H. Powell 1973 (PB 248 315)A09

EERC 73-4 "Experimental Investigation into the Seismic Behavior of Critical Regions of Reinforced Concrete Components as Influenced by Moment and Shear," by M. Celebi and J. Penzien - 1973 (PB 215 884)A09

EERC 73-5 "Hysteretic Behavior of Epoxy-Repaired Reinforced Concrete Beams," by M. Celebi and J. Penzien - 1973 (PB 239 568)A03

EERC 73-6 "General Purpose Computer Program for Inelastic Dynamic Response of Plane Structures," by A. Kanaan and G.H. Powell - 1973 (PB 221 260)A08

EERC 73-7 "A Computer Program for Earthquake Analysis of Gravity Dams Including Reservoir Interaction," by P. Chakrabarti and A.K. Chopra - 1973 (AD 766 271)A04

EERC 73-8 "Behavior of Reinforced Concrete Deep Beam-Column Subassemblages Under Cyclic Loads," by O. Küstü and J.G. Bouwkamp - 1973 (PB 246 117)A12

EERC 73-9 "Earthquake Analysis of Structure-Foundation Systems," by A.K. Vaish and A.K. Chopra - 1973 (AD 766 272)A07

EERC 73-10 "Deconvolution of Seismic Response for Linear Systems," by R.B. Reimer - 1973 (PB 227 179)A08

EERC 73-11 "SAP IV: A Structural Analysis Program for Static and Dynamic Response of Linear Systems," by K.-J. Bathe, E.L. Wilson and F.E. Peterson - 1973 (PB 221 967)A09

EERC 73-12 "Analytical Investigations of the Seismic Response of Long, Multiple Span Highway Bridges," by W.S. Tseng and J. Penzien - 1973 (PB 227 816)A10

EERC 73-13 "Earthquake Analysis of Multi-Story Buildings Including Foundation Interaction," by A.K. Chopra and J.A. Gutierrez - 1973 (PB 222 970)A03

EERC 73-14 "ADAP: A Computer Program for Static and Dynamic Analysis of Arch Dams," by R.W. Clough, J.M. Raphael and S. Mojtahedi - 1973 (PB 223 763)A09

EERC 73-15 "Cyclic Plastic Analysis of Structural Steel Joints," by R.B. Pinkney and R.W. Clough - 1973 (PB 226 843)A08

EERC 73-16 "QUAD-4: A Computer Program for Evaluating the Seismic Response of Soil Structures by Variable Damping Finite Element Procedures," by I.M. Idriss, J. Lysmer, R. Hwang and H.B. Seed - 1973 (PB 229 424)A05

EERC 73-17 "Dynamic Behavior of a Multi-Story Pyramid Shaped Building," by R.M. Stephen, J.P. Hollings and J.G. Bouwkamp - 1973 (PB 240 718)A06

EERC 73-18 "Effect of Different Types of Reinforcing on Seismic Behavior of Short Concrete Columns," by V.V. Bertero, J. Hollings, O. Küstü, R.M. Stephen and J.G. Bouwkamp - 1973

EERC 73-19 "Olive View Medical Center Materials Studies, Phase I," by B. Bresler and V.V. Bertero - 1973 (PB 235 986)A06

EERC 73-20 "Linear and Nonlinear Seismic Analysis Computer Programs for Long Multiple-Span Highway Bridges," by W.S. Tseng and J. Penzien - 1973

EERC 73-21 "Constitutive Models for Cyclic Plastic Deformation of Engineering Materials," by J.M. Kelly and P.P. Gillis 1973 (PB 226 024)A03

EERC 73-22 "DRAIN - 2D User's Guide," by G.H. Powell - 1973 (PB 227 016)A05

EERC 73-23 "Earthquake Engineering at Berkeley - 1973," (PB 226 033)A11

EERC 73-24 Unassigned

EERC 73-25 "Earthquake Response of Axisymmetric Tower Structures Surrounded by Water," by C.Y. Liaw and A.K. Chopra 1973 (AD 773 052)A09

EERC 73-26 "Investigation of the Failures of the Olive View Stairtowers During the San Fernando Earthquake and Their Implications on Seismic Design," by V.V. Bertero and R.G. Collins - 1973 (PB 235 106)A13

EERC 73-27 "Further Studies on Seismic Behavior of Steel Beam-Column Subassemblages," by V.V. Bertero, H. Krawinkler and E.P. Popov - 1973 (PB 234 172)A06

EERC 74-1 "Seismic Risk Analysis," by C.S. Oliveira - 1974 (PB 235 920)A06

EERC 74-2 "Settlement and Liquefaction of Sands Under Multi-Directional Shaking," by R. Pyke, C.K. Chan and H.B. Seed 1974

EERC 74-3 "Optimum Design of Earthquake Resistant Shear Buildings," by D. Ray, K.S. Pister and A.K. Chopra - 1974 (PB 231 172)A06

EERC 74-4 "LUSH - A Computer Program for Complex Response Analysis of Soil-Structure Systems," by J. Lysmer, T. Udaka, H.B. Seed and R. Hwang - 1974 (PB 236 796)A05

EERC 74-5 "Sensitivity Analysis for Hysteretic Dynamic Systems: Applications to Earthquake Engineering," by D. Ray 1974 (PB 233 213)A06

EERC 74-6 "Soil Structure Interaction Analyses for Evaluating Seismic Response," by H.B. Seed, J. Lysmer and R. Hwang 1974 (PB 236 519)A04

EERC 74-7 Unassigned

EERC 74-8 "Shaking Table Tests of a Steel Frame - A Progress Report," by R.W. Clough and D. Tang - 1974 (PB 240 869)A03

EERC 74-9 "Hysteretic Behavior of Reinforced Concrete Flexural Members with Special Web Reinforcement," by V.V. Bertero, E.P. Popov and T.Y. Wang - 1974 (PB 236 797)A07

EERC 74-10 "Applications of Reliability-Based, Global Cost Optimization to Design of Earthquake Resistant Structures," by E. Vitiello and K.S. Pister - 1974 (PB 237 231)A06

EERC 74-11 "Liquefaction of Gravelly Soils Under Cyclic Loading Conditions," by R.T. Wong, H.B. Seed and C.K. Chan 1974 (PB 242 042)A03

EERC 74-12 "Site-Dependent Spectra for Earthquake-Resistant Design," by H.B. Seed, C. Ugas and J. Lysmer - 1974 (PB 240 953)A03

EERC 74-13 "Earthquake Simulator Study of a Reinforced Concrete Frame," by P. Hidalgo and R.W. Clough - 1974 (PB 241 944)A13

EERC 74-14 "Nonlinear Earthquake Response of Concrete Gravity Dams," by N. Pal - 1974 (AD/A 006 583)A06

EERC 74-15 "Modeling and Identification in Nonlinear Structural Dynamics - I. One Degree of Freedom Models," by N. Distefano and A. Rath - 1974 (PB 241 548)A06

EERC 75-1 "Determination of Seismic Design Criteria for the Dumbarton Bridge Replacement Structure, Vol. I: Description, Theory and Analytical Modeling of Bridge and Parameters," by F. Baron and S.-H. Pang - 1975 (PB 259 407)A15

EERC 75-2 "Determination of Seismic Design Criteria for the Dumbarton Bridge Replacement Structure, Vol. II: Numerical Studies and Establishment of Seismic Design Criteria," by F. Baron and S.-H. Pang - 1975 (PB 259 408)A11 (For set of EERC 75-1 and 75-2 (PB 259 406))

EERC 75-3 "Seismic Risk Analysis for a Site and a Metropolitan Area," by C.S. Oliveira - 1975 (PB 248 134)A09

EERC 75-4 "Analytical Investigations of Seismic Response of Short, Single or Multiple-Span Highway Bridges," by M.-C. Chen and J. Penzien - 1975 (PB 241 454)A09

EERC 75-5 "An Evaluation of Some Methods for Predicting Seismic Behavior of Reinforced Concrete Buildings," by S.A. Mahin and V.V. Bertero - 1975 (PB 246 306)A16

EERC 75-6 "Earthquake Simulator Study of a Steel Frame Structure, Vol. I: Experimental Results," by R.W. Clough and D.T. Tang - 1975 (PB 243 981)A13

EERC 75-7 "Dynamic Properties of San Bernardino Intake Tower," by D. Rea, C.-Y. Liaw and A.K. Chopra - 1975 (AD/A008 406) A05

EERC 75-8 "Seismic Studies of the Articulation for the Dumbarton Bridge Replacement Structure, Vol. I: Description, Theory and Analytical Modeling of Bridge Components," by F. Baron and R.E. Hamati - 1975 (PB 251 539)A07

EERC 75-9 "Seismic Studies of the Articulation for the Dumbarton Bridge Replacement Structure, Vol. 2: Numerical Studies of Steel and Concrete Girder Alternates," by F. Baron and R.E. Hamati - 1975 (PB 251 540)A10

EERC 75-10 "Static and Dynamic Analysis of Nonlinear Structures," by D.P. Mondkar and G.H. Powell - 1975 (PB 242 434)A08

EERC 75-11 "Hysteretic Behavior of Steel Columns," by E.P. Popov, V.V. Bertero and S. Chandramouli - 1975 (PB 252 365)A11

EERC 75-12 "Earthquake Engineering Research Center Library Printed Catalog," - 1975 (PB 243 711)A26

EERC 75-13 "Three Dimensional Analysis of Building Systems (Extended Version)," by E.L. Wilson, J.P. Hollings and H.H. Dovey - 1975 (PB 243 989)A07

EERC 75-14 "Determination of Soil Liquefaction Characteristics by Large-Scale Laboratory Tests," by P. De Alba, C.K. Chan and H.B. Seed - 1975 (NUREG 0027)A08

EERC 75-15 "A Literature Survey - Compressive, Tensile, Bond and Shear Strength of Masonry," by R.L. Mayes and R.W. Clough - 1975 (PB 246 292)A10

EERC 75-16 "Hysteretic Behavior of Ductile Moment Resisting Reinforced Concrete Frame Components," by V.V. Bertero and E.P. Popov - 1975 (PB 246 388)A05

EERC 75-17 "Relationships Between Maximum Acceleration, Maximum Velocity, Distance from Source, Local Site Conditions for Moderately Strong Earthquakes," by H.B. Seed, R. Murarka, J. Lysmer and I.M. Idriss - 1975 (PB 248 172)A03

EERC 75-18 "The Effects of Method of Sample Preparation on the Cyclic Stress-Strain Behavior of Sands," by J. Mulilis, C.K. Chan and H.B. Seed - 1975 (Summarized in EERC 75-28)

EERC 75-19 "The Seismic Behavior of Critical Regions of Reinforced Concrete Components as Influenced by Moment, Shear and Axial Force," by M.B. Atalay and J. Penzien - 1975 (PB 258 842)A11

EERC 75-20 "Dynamic Properties of an Eleven Story Masonry Building," by R.M. Stephen, J.P. Hollings, J.G. Bouwkamp and D. Jurukovski - 1975 (PB 246 945)A04

EERC 75-21 "State-of-the-Art in Seismic Strength of Masonry - An Evaluation and Review," by R.L. Mayes and R.W. Clough 1975 (PB 249 040)A07

EERC 75-22 "Frequency Dependent Stiffness Matrices for Viscoelastic Half-Plane Foundations," by A.K. Chopra, P. Chakrabarti and G. Dasgupta - 1975 (PB 248 121)A07

EERC 75-23 "Hysteretic Behavior of Reinforced Concrete Framed Walls," by T.Y. Wong, V.V. Bertero and E.P. Popov - 1975

EERC 75-24 "Testing Facility for Subassemblages of Frame-Wall Structural Systems," by V.V. Bertero, E.P. Popov and T. Endo - 1975

EERC 75-25 "Influence of Seismic History on the Liquefaction Characteristics of Sands," by H.B. Seed, K. Mori and C.K. Chan - 1975 (Summarized in EERC 75-28)

EERC 75-26 "The Generation and Dissipation of Pore Water Pressures during Soil Liquefaction," by H.B. Seed, P.P. Martin and J. Lysmer - 1975 (PB 252 648)A03

EERC 75-27 "Identification of Research Needs for Improving Aseismic Design of Building Structures," by V.V. Bertero 1975 (PB 248 136)A05

EERC 75-28 "Evaluation of Soil Liquefaction Potential during Earthquakes," by H.B. Seed, I. Arango and C.K. Chan - 1975 (NUREG 0026)A13

EERC 75-29 "Representation of Irregular Stress Time Histories by Equivalent Uniform Stress Series in Liquefaction Analyses," by H.B. Seed, I.M. Idriss, F. Makdisi and N. Banerjee - 1975 (PB 252 635)A03

EERC 75-30 "FLUSH - A Computer Program for Approximate 3-D Analysis of Soil-Structure Interaction Problems," by J. Lysmer, T. Udaka, C.-F. Tsai and H.B. Seed - 1975 (PB 259 332)A07

EERC 75-31 "ALUSH - A Computer Program for Seismic Response Analysis of Axisymmetric Soil-Structure Systems," by E. Berger, J. Lysmer and H.B. Seed - 1975

EERC 75-32 "TRIP and TRAVEL - Computer Programs for Soil-Structure Interaction Analysis with Horizontally Travelling Waves," by T. Udaka, J. Lysmer and H.B. Seed - 1975

EERC 75-33 "Predicting the Performance of Structures in Regions of High Seismicity," by J. Penzien - 1975 (PB 248 130)A03

EERC 75-34 "Efficient Finite Element Analysis of Seismic Structure - Soil - Direction," by J. Lysmer, H.B. Seed, T. Udaka, R.N. Hwang and C.-F. Tsai - 1975 (PB 253 570)A03

EERC 75-35 "The Dynamic Behavior of a First Story Girder of a Three-Story Steel Frame Subjected to Earthquake Loading," by R.W. Clough and L.-Y. Li - 1975 (PB 248 841)A05

EERC 75-36 "Earthquake Simulator Study of a Steel Frame Structure, Volume II - Analytical Results," by D.T. Tang - 1975 (PB 252 926)A10

EERC 75-37 "ANSR-I General Purpose Computer Program for Analysis of Non-Linear Structural Response," by D.P. Mondkar and G.H. Powell - 1975 (PB 252 386)A08

EERC 75-38 "Nonlinear Response Spectra for Probabilistic Seismic Design and Damage Assessment of Reinforced Concrete Structures," by M. Murakami and J. Penzien - 1975 (PB 259 530)A05

EERC 75-39 "Study of a Method of Feasible Directions for Optimal Elastic Design of Frame Structures Subjected to Earthquake Loading," by N.D. Walker and K.S. Pister - 1975 (PB 257 781)A06

EERC 75-40 "An Alternative Representation of the Elastic-Viscoelastic Analogy," by G. Dasgupta and J.L. Sackman - 1975 (PB 252 173)A03

EERC 75-41 "Effect of Multi-Directional Shaking on Liquefaction of Sands," by H.B. Seed, R. Pyke and G.R. Martin - 1975 (PB 258 781)A03

EERC 76-1 "Strength and Ductility Evaluation of Existing Low-Rise Reinforced Concrete Buildings - Screening Method," by T. Okada and B. Bresler - 1976 (PB 257 906)A11

EERC 76-2 "Experimental and Analytical Studies on the Hysteretic Behavior of Reinforced Concrete Rectangular and T-Beams," by S.-Y.M. Ma, E.P. Popov and V.V. Bertero - 1976 (PB 260 843)A12

EERC 76-3 "Dynamic Behavior of a Multistory Triangular-Shaped Building," by J. Petrovski, R.M. Stephen, E. Gartenbaum and J.G. Bouwkamp - 1976 (PB 273 279)A07

EERC 76-4 "Earthquake Induced Deformations of Earth Dams," by N. Serff, H.B. Seed, F.I. Makdisi & C.-Y. Chang - 1976 (PB 292 065)A08

EERC 76-5 "Analysis and Design of Tube-Type Tall Building Structures," by H. de Clercq and G.H. Powell - 1976 (PB 252 220) A10

EERC 76-6 "Time and Frequency Domain Analysis of Three-Dimensional Ground Motions, San Fernando Earthquake," by T. Kubo and J. Penzien (PB 260 556)A11

EERC 76-7 "Expected Performance of Uniform Building Code Design Masonry Structures," by R.L. Mayes, Y. Omote, S.W. Chen and R.W. Clough - 1976 (PB 270 098)A05

EERC 76-8 "Cyclic Shear Tests of Masonry Piers, Volume 1 - Test Results," by R.L. Mayes, Y. Omote, R.W. Clough - 1976 (PB 264 424)A06

EERC 76-9 "A Substructure Method for Earthquake Analysis of Structure - Soil Interaction," by J.A. Gutierrez and A.K. Chopra - 1976 (PB 257 783)A08

EERC 76-10 "Stabilization of Potentially Liquefiable Sand Deposits using Gravel Drain Systems," by H.B. Seed and J.R. Booker - 1976 (PB 258 820)A04

EERC 76-11 "Influence of Design and Analysis Assumptions on Computed Inelastic Response of Moderately Tall Frames," by G.H. Powell and D.G. Row - 1976 (PB 271 409)A06

EERC 76-12 "Sensitivity Analysis for Hysteretic Dynamic Systems: Theory and Applications," by D. Ray, K.S. Pister and E. Polak - 1976 (PB 262 859)A04

EERC 76-13 "Coupled Lateral Torsional Response of Buildings to Ground Shaking," by C.L. Kan and A.K. Chopra - 1976 (PB 257 907)A09

EERC 76-14 "Seismic Analyses of the Banco de America," by V.V. Bertero, S.A. Mahin and J.A. Hollings - 1976

EERC 76-15 "Reinforced Concrete Frame 2: Seismic Testing and Analytical Correlation," by R.W. Clough and J. Gidwani - 1976 (PB 261 323)A08

EERC 76-16 "Cyclic Shear Tests of Masonry Piers, Volume 2 - Analysis of Test Results," by R.L. Mayes, Y. Omote and R.W. Clough - 1976

EERC 76-17 "Structural Steel Bracing Systems: Behavior Under Cyclic Loading," by E.P. Popov, K. Takanashi and C.W. Roeder - 1976 (PB 260 715)A05

EERC 76-18 "Experimental Model Studies on Seismic Response of High Curved Overcrossings," by D. Williams and W.G. Godden - 1976 (PB 269 548)A08

EERC 76-19 "Effects of Non-Uniform Seismic Disturbances on the Dumbarton Bridge Replacement Structure," by F. Baron and R.E. Hamati - 1976 (PB 282 981)A16

EERC 76-20 "Investigation of the Inelastic Characteristics of a Single Story Steel Structure Using System Identification and Shaking Table Experiments," by V.C. Matzen and H.D. McNiven - 1976 (PB 258 453)A07

EERC 76-21 "Capacity of Columns with Splice Imperfections," by E.P. Popov, R.M. Stephen and R. Philbrick - 1976 (PB 260 378)A04

EERC 76-22 "Response of the Olive View Hospital Main Building during the San Fernando Earthquake," by S. A. Mahin, V.V. Bertero, A.K. Chopra and R. Collins - 1976 (PB 271 425)A14

EERC 76-23 "A Study on the Major Factors Influencing the Strength of Masonry Prisms," by N.M. Mostaghel, R.L. Mayes, R. W. Clough and S.W. Chen - 1976 (Not published)

EERC 76-24 "GADFLEA - A Computer Program for the Analysis of Pore Pressure Generation and Dissipation during Cyclic or Earthquake Loading," by J.R. Booker, M.S. Rahman and H.B. Seed - 1976 (PB 263 947)A04

EERC 76-25 "Seismic Safety Evaluation of a R/C School Building," by B. Bresler and J. Axley - 1976

EERC 76-26 "Correlative Investigations on Theoretical and Experimental Dynamic Behavior of a Model Bridge Structure," by K. Kawashima and J. Penzien - 1976 (PB 263 388)A11

EERC 76-27 "Earthquake Response of Coupled Shear Wall Buildings," by T. Srichatrapimuk - 1976 (PB 265 157)A07

EERC 76-28 "Tensile Capacity of Partial Penetration Welds," by E.P. Popov and R.M. Stephen - 1976 (PB 262 899)A03

EERC 76-29 "Analysis and Design of Numerical Integration Methods in Structural Dynamics," by H.M. Hilber - 1976 (PB 264 410)A06

EERC 76-30 "Contribution of a Floor System to the Dynamic Characteristics of Reinforced Concrete Buildings," by L.E. Malik and V.V. Bertero - 1976 (PB 272 247)A13

EERC 76-31 "The Effects of Seismic Disturbances on the Golden Gate Bridge," by F. Baron, M. Arikan and R.E. Hamati - 1976 (PB 272 279)A09

EERC 76-32 "Infilled Frames in Earthquake Resistant Construction," by R.E. Klingner and V.V. Bertero - 1976 (PB 265 892)A13

UCB/EERC-77/01 "PLUSH - A Computer Program for Probabilistic Finite Element Analysis of Seismic Soil-Structure Interaction," by M.P. Romo Organista, J. Lysmer and H.B. Seed - 1977

UCB/EERC-77/02 "Soil-Structure Interaction Effects at the Humboldt Bay Power Plant in the Ferndale Earthquake of June 7, 1975," by J.E. Valera, H.B. Seed, C.F. Tsai and J. Lysmer - 1977 (PB 265 795)A04

UCB/EERC-77/03 "Influence of Sample Disturbance on Sand Response to Cyclic Loading," by K. Mori, H.B. Seed and C.K, Chan - 1977 (PB 267 352)A04

UCB/EERC-77/04 "Seismological Studies of Strong Motion Records," by J. Shoja-Taheri - 1977 (PB 269 655)A10

UCB/EERC-77/05 "Testing Facility for Coupled-Shear Walls," by L. Li-Hyung, V.V. Bertero and E.P. Popov - 1977

UCB/EERC-77/06 "Developing Methodologies for Evaluating the Earthquake Safety of Existing Buildings," by No. 1 - B. Bresler; No. 2 - B. Bresler, T. Okada and D. Zisling; No. 3 - T. Okada and B. Bresler; No. 4 - V.V. Bertero and B. Bresler - 1977 (PB 267 354)A08

UCB/EERC-77/07 "A Literature Survey - Transverse Strength of Masonry Walls," by Y. Omote, R.L. Mayes, S.W. Chen and R.W. Clough - 1977 (PB 277 933)A07

UCB/EERC-77/08 "DRAIN-TABS: A Computer Program for Inelastic Earthquake Response of Three Dimensional Buildings," by R. Guendelman-Israel and G.H. Powell - 1977 (PB 270 693)A07

UCB/EERC-77/09 "SUBWALL: A Special Purpose Finite Element Computer Program for Practical Elastic Analysis and Design of Structural Walls with Substructure Option," by D.Q. Le, H. Peterson and E.P. Popov - 1977 (PB 270 567)A05

UCB/EERC-77/10 "Experimental Evaluation of Seismic Design Methods for Broad Cylindrical Tanks," by D.P. Clough (PB 272 280)A13

UCB/EERC-77/11 "Earthquake Engineering Research at Berkeley - 1976," - 1977 (PB 273 507)A09

UCB/EERC-77/12 "Automated Design of Earthquake Resistant Multistory Steel Building Frames," by N.D. Walker, Jr. - 1977 (PB 276 526)A09

UCB/EERC-77/13 "Concrete Confined by Rectangular Hoops Subjected to Axial Loads," by J. Vallenas, V.V. Bertero and E.P. Popov - 1977 (PB 275 165)A06

UCB/EERC-77/14 "Seismic Strain Induced in the Ground During Earthquakes," by Y. Sugimura - 1977 (PB 284 201)A04

UCB/EERC-77/15 "Bond Deterioration under Generalized Loading," by V.V. Bertero, E.P. Popov and S. Viwathanatepa - 1977

UCB/EERC-77/16 "Computer Aided Optimum Design of Ductile Reinforced Concrete Moment Resisting Frames," by S.W. Zagajeski and V.V. Bertero - 1977 (PB 280 137)A07

UCB/EERC-77/17 "Earthquake Simulation Testing of a Stepping Frame with Energy-Absorbing Devices," by J.M. Kelly and D.F. Tsztoo - 1977 (PB 273 506)A04

UCB/EERC-77/18 "Inelastic Behavior of Eccentrically Braced Steel Frames under Cyclic Loadings," by C.W. Roeder and E.P. Popov - 1977 (PB 275 526)A15

UCB/EERC-77/19 "A Simplified Procedure for Estimating Earthquake-Induced Deformations in Dams and Embankments," by F.I. Makdisi and H.B. Seed - 1977 (PB 276 820)A04

UCB/EERC-77/20 "The Performance of Earth Dams during Earthquakes," by H.B. Seed, F.I. Makdisi and P. de Alba - 1977 (PB 276 821)A04

UCB/EERC-77/21 "Dynamic Plastic Analysis Using Stress Resultant Finite Element Formulation," by P. Lukkunapvasit and J.M. Kelly - 1977 (PB 275 453)A04

UCB/EERC-77/22 "Preliminary Experimental Study of Seismic Uplift of a Steel Frame," by R.W. Clough and A.A. Huckelbridge 1977 (PB 278 769)A08

UCB/EERC-77/23 "Earthquake Simulator Tests of a Nine-Story Steel Frame with Columns Allowed to Uplift," by A.A. Huckelbridge - 1977 (PB 277 944)A09

UCB/EERC-77/24 "Nonlinear Soil-Structure Interaction of Skew Highway Bridges," by M.-C. Chen and J. Penzien - 1977 (PB 276 176)A07

UCB/EERC-77/25 "Seismic Analysis of an Offshore Structure Supported on Pile Foundations," by D.D.-N. Liou and J. Penzien 1977 (PB 283 180)A06

UCB/EERC-77/26 "Dynamic Stiffness Matrices for Homogeneous Viscoelastic Half-Planes," by G. Dasgupta and A.K. Chopra - 1977 (PB 279 654)A06

UCB/EERC-77/27 "A Practical Soft Story Earthquake Isolation System," by J.M. Kelly, J.M. Eidinger and C.J. Derham - 1977 (PB 276 814)A07

UCB/EERC-77/28 "Seismic Safety of Existing Buildings and Incentives for Hazard Mitigation in San Francisco: An Exploratory Study," by A.J. Meltsner - 1977 (PB 281 970)A05

UCB/EERC-77/29 "Dynamic Analysis of Electrohydraulic Shaking Tables," by D. Rea, S. Abedi-Hayati and Y. Takahashi 1977 (PB 282 569)A04

UCB/EERC-77/30 "An Approach for Improving Seismic - Resistant Behavior of Reinforced Concrete Interior Joints," by B. Galunic, V.V. Bertero and E.P. Popov - 1977 (PB 290 870)A06

UCB/EERC-78/01 "The Development of Energy-Absorbing Devices for Aseismic Base Isolation Systems," by J.M. Kelly and D.F. Tsztoo - 1978 (PB 284 978)A04

UCB/EERC-78/02 "Effect of Tensile Prestrain on the Cyclic Response of Structural Steel Connections, by J.G. Bouwkamp and A. Mukhopadhyay - 1978

UCB/EERC-78/03 "Experimental Results of an Earthquake Isolation System using Natural Rubber Bearings," by J.M. Eidinger and J.M. Kelly - 1978 (PB 281 686)A04

UCB/EERC-78/04 "Seismic Behavior of Tall Liquid Storage Tanks," by A. Niwa - 1978 (PB 284 017)A14

UCB/EERC-78/05 "Hysteretic Behavior of Reinforced Concrete Columns Subjected to High Axial and Cyclic Shear Forces," by S.W. Zagajeski, V.V. Bertero and J.G. Bouwkamp - 1978 (PB 283 858)A13

UCB/EERC-78/06 "Inelastic Beam-Column Elements for the ANSR-I Program," by A. Riahi, D.G. Row and G.H. Powell - 1978

UCB/EERC-78/07 "Studies of Structural Response to Earthquake Ground Motion," by O.A. Lopez and A.K. Chopra - 1978 (PB 282 790)A05

UCB/EERC-78/08 "A Laboratory Study of the Fluid-Structure Interaction of Submerged Tanks and Caissons in Earthquakes," by R.C. Byrd - 1978 (PB 284 957)A08

UCB/EERC-78/09 "Model for Evaluating Damageability of Structures," by I. Sakamoto and B. Bresler - 1978

UCB/EERC-78/10 "Seismic Performance of Nonstructural and Secondary Structural Elements," by I. Sakamoto - 1978

UCB/EERC-78/11 "Mathematical Modelling of Hysteresis Loops for Reinforced Concrete Columns," by S. Nakata, T. Sproul and J. Penzien - 1978

UCB/EERC-78/12 "Damageability in Existing Buildings," by T. Blejwas and B. Bresler - 1978

UCB/EERC-78/13 "Dynamic Behavior of a Pedestal Base Multistory Building," by R.M. Stephen, E.L. Wilson, J.G. Bouwkamp and M. Button - 1978 (PB 286 650)A08

UCB/EERC-78/14 "Seismic Response of Bridges - Case Studies," by R.A. Imbsen, V. Nutt and J. Penzien - 1978 (PB 286 503)A10

UCB/EERC-78/15 "A Substructure Technique for Nonlinear Static and Dynamic Analysis," by D.G. Row and G.H. Powell - 1978 (PB 288 077)A10

UCB/EERC-78/16 "Seismic Risk Studies for San Francisco and for the Greater San Francisco Bay Area," by C.S. Oliveira - 1978

UCB/EERC-78/17 "Strength of Timber Roof Connections Subjected to Cyclic Loads," by P. Gülkan, R.L. Mayes and R.W. Clough - 1978

UCB/EERC-78/18 "Response of K-Braced Steel Frame Models to Lateral Loads," by J.G. Bouwkamp, R.M. Stephen and E.P. Popov - 1978

UCB/EERC-78/19 "Rational Design Methods for Light Equipment in Structures Subjected to Ground Motion," by J.L. Sackman and J.M. Kelly - 1978 (PB 292 357)A04

UCB/EERC-78/20 "Testing of a Wind Restraint for Aseismic Base Isolation," by J.M. Kelly and D.E. Chitty - 1978 (PB 292 833)A03

UCB/EERC-78/21 "APOLLO - A Computer Program for the Analysis of Pore Pressure Generation and Dissipation in Horizontal Sand Layers During Cyclic or Earthquake Loading," by P.P. Martin and H.B. Seed - 1978 (PB 292 835)A04

UCB/EERC-78/22 "Optimal Design of an Earthquake Isolation System," by M.A. Bhatti, K.S. Pister and E. Polak - 1978 (PB 294 735)A06

UCB/EERC-78/23 "MASH - A Computer Program for the Non-Linear Analysis of Vertically Propagating Shear Waves in Horizontally Layered Deposits," by P.P. Martin and H.B. Seed - 1978 (PB 293 101)A05

UCB/EERC-78/24 "Investigation of the Elastic Characteristics of a Three Story Steel Frame Using System Identification," by I. Kaya and H.D. McNiven - 1978

UCB/EERC-78/25 "Investigation of the Nonlinear Characteristics of a Three-Story Steel Frame Using System Identification," by I. Kaya and H.D. McNiven - 1978

UCB/EERC-78/26 "Studies of Strong Ground Motion in Taiwan," by Y.M. Hsiung, B.A. Bolt and J. Penzien - 1978

UCB/EERC-78/27 "Cyclic Loading Tests of Masonry Single Piers: Volume 1 - Height to Width Ratio of 2," by P.A. Hidalgo, R.L. Mayes, H.D. McNiven and R.W. Clough - 1978

UCB/EERC-78/28 "Cyclic Loading Tests of Masonry Single Piers: Volume 2 - Height to Width Ratio of 1," by S.-W.J. Chen, P.A. Hidalgo, R.L. Mayes, R.W. Clough and H.D. McNiven - 1978

UCB/EERC-78/29 "Analytical Procedures in Soil Dynamics," by J. Lysmer - 1978

UCB/EERC-79/01 "Hysteretic Behavior of Lightweight Reinforced Concrete Beam-Column Subassemblages," by B. Forzani, E.P. Popov, and V.V. Bertero - 1979

UCB/EERC-79/02 "The Development of a Mathematical Model to Predict the Flexural Response of Reinforced Concrete Beams to Cyclic Loads, Using System Identification," by J.F. Stanton and H.D. McNiven - 1979

UCB/EERC-79/03 "Linear and Nonlinear Earthquake Response of Simple Torsionally Coupled Systems," by C.L. Kan and A.K. Chopra - 1979

UCB/EERC-79/04 "A Mathematical Model of Masonry for Predicting Its Linear Seismic Response Characteristics," by Y. Mengi and H.D. McNiven - 1979

UCB/EERC-79/05 "Mechanical Behavior of Light Weight Concrete Confined by Different Types of Lateral Reinforcement," by M.A. Manrique, V.V. Bertero and E.P. Popov - 1979

UCB/EERC-79/06 "Static Tilt Tests of a Tall Cylindrical Liquid Storage Tank," by R.W. Clough and A. Niwa - 1979

UCB/EERC-79/07 "The Design of Steel Energy Absorbing Restrainers and Their Incorporation Into Nuclear Power Plants for Enhanced Safety: Volume 1 - Summary Report," by P.N. Spencer, V.F. Zackay, and E.R. Parker - 1979

UCB/EERC-79/08 "The Design of Steel Energy Absorbing Restrainers and Their Incorporation Into Nuclear Power Plants for Enhanced Safety: Volume 2 - The Development of Analyses for Reactor System Piping," "Simple Systems" by M.C. Lee, J. Penzien, A.K. Chopra, and K. Suzuki "Complex Systems" by G.H. Powell, E.L. Wilson, R.W. Clough and D.G. Row - 1979

UCB/EERC-79/09 "The Design of Steel Energy Absorbing Restrainers and Their Incorporation Into Nuclear Power Plants for Enhanced Safety: Volume 3 - Evaluation of Commerical Steels," by W.S. Owen, R.M.N. Pelloux, R.O. Ritchie, M. Faral, T. Ohhashi, J. Toplosky, S.J. Hartman, V.F. Zackay, and E.R. Parker - 1979

UCB/EERC-79/10 "The Design of Steel Energy Absorbing Restrainers and Their Incorporation Into Nuclear Power Plants for Enhanced Safety: Volume 4 - A Review of Energy-Absorbing Devices," by J.M. Kelly and M.S. Skinner - 1979

UCB/EERC-79/11 "Conservatism In Summation Rules for Closely Spaced Modes," by J.M. Kelly and J.L. Sackman - 1979

UCB/EERC-79/12 "Cyclic Loading Tests of Masonry Single Piers Volume 3 - Height to Width Ratio of 0.5," by P.A. Hidalgo, R.L. Mayes, H.D. McNiven and R.W. Clough - 1979

UCB/EERC-79/13 "Cyclic Behavior of Dense Coarse-Grain Materials in Relation to the Seismic Stability of Dams," by N.G. Banerjee, H.B. Seed and C.K. Chan - 1979

UCB/EERC-79/14 "Seismic Behavior of R/C Interior Beam Column Subassemblages," by S. Viwathanatepa, E.P. Popov and V.V. Bertero - 1979

UCB/EERC-79/15 "Optimal Design of Localized Nonlinear Systems with Dual Performance Criteria Under Earthquake Excitations," by M.A. Bhatti - 1979